EFFECT OF NANOCLAY FILLERS ON WOOD ADHESIVES AND PARTICLE BOARD PROPERTIES

by

Diyan Xian

B.Eng., South China Agriculture University, 2009

A THESIS SUBMITTED IN PARTIAL FULFILMENT OF
THE REQUIREMENTS FOR THE DEGREE OF

MASTER OF APPLIED SCIENCE

in

The Faculty of Graduate Studies

(Forestry)

THE UNIVERSITY OF BRITISH COLUMBIA
(Vancouver)

April 2012

Abstract

The objective of this research is to investigate the effect of nanoclay additions to particleboard resins on the properties of particleboard made with those resins. Two nanoclays, Cloisite30B, a modified nanoclay and Nanofil16, an unmodified clay, were blended with the two resins used to produce particleboard: Urea Formaldehyde (UF) and Melamine Formaldehyde (MF). Coupling agent was added to nanoclays to facilitate clay dispersion into the resin. X-ray diffraction tests showed that mechanical mixing was sufficient to exfoliate Closite30B into both resin types and enable the intercalation of Nanofil116/resin mixtures.

Addition of nanoclays and coupling agents had small to severe adverse effects on resin curing: Cloisite30B slightly delayed the curing process of both UF and MF resin and reduced the reaction heat of curing, and the addition of coupling agent together with Closite30B further compounded this effect. Nanofil116 significantly delayed the curing reaction of both resins and decreased the heat of reaction. The coupling agent had a significant further detrimental effect on the resin cure.

In order to test whether nanoclays had a positive or negative effect on the adhesive strength of UF and MF resins, the shear strength of clay-modified resin were tested and compared with that of unadulterated resin. Regardless of whether coupling agent was used, the clay-modified UF resin had lower bonding strength than pure UF resin. In contrast, three kind of clay-modified MF resin had higher bonding strength then pure MF resin.

Based on these findings those MF resins which have higher shear strength were blended with furnish to fabricate particle board using different clay loading rates. Most clay treatments had no significant effect on particleboard physical or mechanical properties. The only significant

improvement was for internal bond strength which increased when using either 2% Closite30B or Nanofil116 with or without coupling agent. Higher clay loading rates tended to decrease board strength properties. In conclusion, the modified Closite30B nanoclay and the unmodified Nanofil116 nanoclay had only a minor effect on improving UF and MF resin strength and the particle board properties.

Tables of contents

List of tables

List of figures

Acknowledgements

I owe a lot of thanks to many people who accompanied me through this journey. First and foremost, I would like to express my sincere appreciation to my supervisor Dr. Gregory D. Smith for his remarkable support, advice, understanding, and encouragement during the research, especially when failures and frustration came. Without that I would have been lost. I would also like to acknowledge the helpful advice from my committee members, Dr. John Kadla and Dr. Taraneh Sowlati.

My heartfelt thanks to the current and former members of the wood composite group: Chao Zhang, Emanuel Sackey, Jorn Dettmer, Kate Semple, Solace Sam-Brew, Shayesteh Haghdan, Ying-Li Tasi and Xuelian Zhang for their teaching of operating laboratory equipment, their help in the preparation of sample and thesis and sharing their useful experience with me.

Appreciation is also extended to Jennifer Braun, Feng-Cheng (Aries) Chang of BioMaterials Chemistry group , George Lee of the Timber Engineering Group, Vincent Leung and Lawrence Gunther from Advanced Wood Processing Center for their help in running samples and setting up the equipment.

I owe a special thanks to all my friends in Faculty of Forestry for their advice and dedication to my study and life. Finally, I would like to express my sincerest gratitude and appreciation to my parents for their constant encouragement, patience, and support in both good and difficult times.

1 Introduction

1.1 Background

Particleboard (PB) is a commonly used panel product made from hammer-milled wood particles that has a relatively low cost of production compared with Medium fiber board (MDF). It has a smooth surface that can be easily laminated or painted. As a result, it is widely used in furniture applications such as desks, shelves, and cabinets (Wong, 2008).

The price of PB has declined slightly over the past 5 years(Douglas Clark, 2011). However, the production cost per cubic meter of PB has been increasing since 2008 and is expected to increase further in 2011and 2012 (RISI, 2011). Since the price of PB has not changed greatly and production costs continue to increase, this places significant pressure on PB manufacturers to remain profitable and as a result several plants have closed over the past few years (Pepke, 2010).

The objective of this research is to investigate whether using nanoclays as fillers in PB resins can improve the panel properties, and if so, can the amount of resin used to make the PB be decreased while maintaining board properties. The raw material costs for manufacturing PB include wood furnish, resin, and wax, and resin is the most costly. Thus it is necessary to find ways of reducing resin costs while maintaining adequate board properties. Usually, increasing the resin content of the board will result in improved panel properties. One possibility for reducing resin costs is to add a low-cost filler to the resin thereby reducing the total amount of resin required for board production (Shi, Qiu, and Zheng, 2004). Additives such as fillers, curing agents, and coupling agents, could reinforce the resin and improve composite properties (Giannelis, Krishnamoorti, and Manias, 1999). Powdered fillers such as finely ground wood flour, nut shells, and rice hulls have been mixed with wood adhesives in an attempt to reduce over penetration of adhesive into wood or better reinforced panels (Nishizawa *et al* , 1982). Mineral fillers are also low cost additives and have been shown to be able to reduce resin usage while maintaining board properties (Shi *et al*., 2004).

Nanomaterials have least one dimension in the nanometer (10^{-9} m) range, and have been proven to be excellent fillers for wood resins and other polymers (Pavlidou and Papaspyrides, 2008). Montmorillonite (MMT) clays are naturally nanomaterials silicate minerals when it dispersed in various polymer matrices (Alexandre and Dubois, 2000). MMT is more widely available and significantly lower in cost than other nanomaterials such as carbon nanotubes or nanoaluminum particles. The price of MMTs typically is ranging from $US2.0 to $3.50 per pound.

The surface area of MMT platelets becomes very large once the clay stacks are dispersed and can interact with the resin and improve its mechanical properties (Giannelis, *et al.*, 1999; Hetzer and Dekee, 2008). MMT has shown some promise in improving the strength and mechanical properties of various resin matrices. Most research to date has focused on blending processes and clay dispersion in thermoplastic resins and wood plastic composites (WPC). For example, Hetzer and De Kee (2008) reported that adding 2-10% MMT to polyamide-6, polypropylene, and polyethylene high polymers improved their strength, elastic modulus, flame and heat resistance, and water resistance. Zerda *et al.,* (2001) found that small amounts of modified MMT can improve the mechanical strength of the epoxy resin when using a MMT content of 3-12 %.

Only a small amount of work had been done on using nanoclay-filled adhesives to make wood panels. Ashori and Nourbakhsh (2009), found that the mechanical properties (MOR and MOE) of MDF increased with clay content over the 2 to 6% range. Wang, *et al.* (2008) used nanoclay-filled adhesives to fabricate experimental OSB, MDF, plywood and PB but found no beneficial effects of using nanoclay-modified resins. Further studies are needed in in this area, i.e. the application of MMT nanoclays to fabricated wood adhesive and wood composites, in particular, particleboard.

1.2 Rationale

Based on the literature review, it was concluded that the addition of MMT to particleboard resin has the potential to improve its properties. The phyllosilicates structure of montmorillonite should facilitate the platelet separation process and make it easier to exfoliate the nano-sized clay layers to reinforce resins used in wood panels (Wang *et al*., 2008).

The potential for cost savings if resin can be partially substituted with nano-clay, even to a small extent, are substantial. At current resin prices if 0.5% MMT clay was added to a binder system permitted the resin content to be reduced by 1%, say from 8% to 7%, then for a plant with an annual production capacity 200,000 m^3 the approximate savings in resin cost alone would be $660,000 CAD per plant per year.

1.3 Hypothesis

The hypothesis for this study is: the addition of small amounts of MMT nanoclay to the resin used to make PB will improve the physical and mechanical properties of PB.

The goal of this work is to determine if MMTs are compatible with UF and MF resins and whether resin-clay mixtures can improve the adhesive strength of these resins, and in doing so, improve the properties of PB made from the same amount of MMT-fortified resins or maintain the PB properties using less modified resin.

1.4 Approach

The aim of this study is to reduce the amount of wood adhesive, and by extension PB production cost, to meet minimum property requirements through the addition of MMT nanoclays to the resin before blending with wood furnish. At the very least, replacing a portion of the resin with nanoclay should not reduce board properties.

The first phase of the work is a preliminary study to determine the effect of adding different types and amounts of nanoclay to several candidate resins and to characterize the ability of the clay to disperse in those resins.

In the second phase of the work, thermomechanical properties of the resin are assessed using Dynamic Mechanical Analysis and the lap shear strength testing of bonded wooden veneers is used as a screening test for determining which clay resin combinations are likely to lead to properties improvement in PB.

The final phase will examine the effect of selected clay-resin mixes (determined from the wood veneer lap shear tests) on the physical and mechanical properties of laboratory-fabricated PB.

1.5 Structure of thesis

The structure of this work is presented in the following:

Chapter 1. Introduction: This chapter introduces basic information on PB and discusses how board properties are affected by board resin content and possible solutions for reduce production cost while maintaining or improving panel properties.

Chapter 2. Literature review: This chapter was the review of pervious work of nanoclay, resins, processing method of nanoclay-resin wood composite. The techniques for evaluate the clay dispersion, clay reinforced mechanism, and the effect of the nanoclay on wood composite are covered.

Chapter 3. Materials and methods: Introduction of the raw materials including adhesives, wood furnish, coupling agent and nanoclay. The processing method for each tests were also detailed in this chapter.

Chapter 4. Results and discussion: In this chapter the results from the various tests and the effect of each treatment on resin and panel properties are identified and discussed.

Chapter 5. Comments and future work: The final conclusions are summarized and a few possible directions for further investigation described.

2 Literature review

2.1 Overview

This review examines the enhancement of the physical and mechanical properties the addition of thermoplastic and thermosetting resins when they are mixed with nanoclays. The review focusses mainly on phyllosilicates nanoclays, specifically modified montmorillonite (MMT). The following topics are reviewed:

1. The structure of nanoclay fillers and resin matrices;
2. Methods for incorporating nanoclay into thermoplastic and thermosetting resins for properties enhancement;
3. Characterization of the resin- nanoclay hybrid structure;
4. Nanoclay reinforcement mechanism;
5. Instances of nanoclays used in wood composite and their properties.

The structure of nanoclay and the morphology of clays dispersed in the resin matrix are introduced first since the properties of nanoclay-reinforced material depends on the clay platelet size, aspect ratio, processing method and other factors such as clay distribution quality. Analytical methods used to characterize clay morphology and clay dispersion in polymer matrices include X-ray Diffraction (XRD), Transmission Electron Microscopy (TEM) and Scanning Electron Microscopy (SEM). These can determine whether a nanoclay hybrid structure has been obtained. If so then further thermo analysis of the mixtures can be made to determine how the clay interacts with the polymer to affect the chain structure, crystallize rate, curing process and thermo mechanical properties(Pavlidou and Papaspyrides, 2008). Clay effects on polymer structure and curing can be quantified using Differential Scanning Calorimetry (DSC) and Dynamic Mechanical Analysis (DMA).

The effects of a nanoclay on the physical and mechanical properties of nanoclay-resin composites and nanoclay-resin-wood composites are also covered. Most of the applications of nanoclay have been in the field of wood plastic composites and so these are also included in this review.

2.2 Nanoclay fillers and resins

2.2.1 Structure of nanoclay

Any particle that has at least one dimension in the nanometer size range (1-100 nm) is deemed to be a nanoparticle. Such particles can be divided into three different categories according to the number of nano-scale dimensions. Iso-dimensional nanoparticles, such as spherical silica, have three dimensions in nanometers. Carbon nanotubes or cellulose whiskers are two dimensional nanoparticles, whereby the cross section is in nano-scale and the third dimension (length) can extend to micrometer or even millimeter size ranges. The third kind of nanoparticle has only one dimension in the nano-scale. These usually take the form of thin sheets that are several nanometers thick. Some synthetic and natural crystals, and layered silicate clays can be classified into the third kind of nano-particle (Sinha Ray and Okamoto, 2003; Lebaron, *et al*., 1999)

This review is mainly focused on phyllosilicates clays, of which the clay layer thickness is in the nano range. The structure of montmorillonite and hectorite and spaonite place them among the common types of phyllosilicates. As shown in Figure 2.1, the structure consists of 1 nm thick, two-dimensional negatively charged silicate layers with exchangeable cations between the layers

(Alexandre and Dubois, 2000). Phyllosilicate clays contain cations such as Li, Na, Rb, Cs, which make them strongly hydrophilic. These exchangeable cations facilitate the modification of phyllosilicate because they can be easily replaced by other cations. In order to make the phyllosilicates more compatible with polymers, the hydrated cations are exchanged with organic cations or cationic surfactants such as alkylammonium (Giannelis, *et al*., 1999). Organic-modified phyllosilicates have a lower surface energy and allow the silicate layers to interact with the polymers. Usually, the organic modifiers with longer molecule chains are more effective at expanding the interlayer space and separating layers into single sheets (Lebaron et al., 1999).

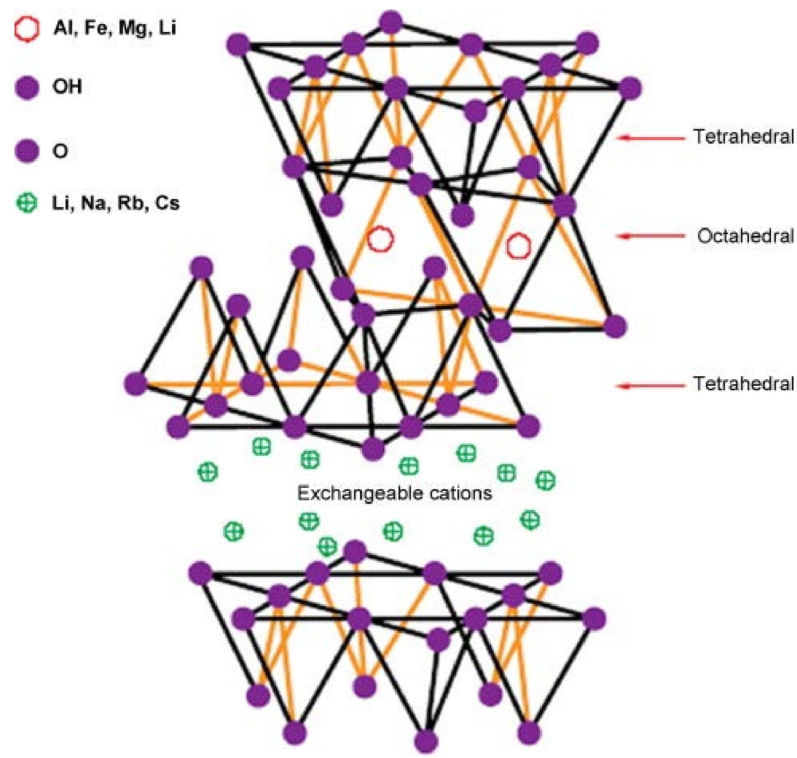

Figure 2.1: Structure of layer montmorillonite (Adapted from Pavlidou and Papaspyrides, 2008 used with permission from Elsevier)

2.2.2 Thermoplastic resin and thermosetting resin

Nanoclay as a filler or additive is usually added in to a polymer (referred to as the matrix) in order to enhance the properties of the polymer. A polymer is a very large molecule which is comprised of repeating units and those units connected with each other to form long chains which can be linear, branching or cross-linked (Edwards, 2004). There are two main types of polymers used in wood composite industry: thermoplastics and thermosetting resins.

Thermoplastics are usually linear polymers which may change in structure as temperature changes, such as glass transition, crystallization and melting (Kulshreshtha, and Vasile, 2002). Polylactic acid (PLA), Polyvinyl chloride (PVC) are the most commonly used thermoplastic resins for fabricating wood plastic composites(Pavlidou and Papaspyrides, 2008).

Thermosetting resins are three-dimensional cross-linked networks which are hard, infusible and insoluble after curing. Thermosetting resin is more difficult to characterize than a thermoplastic resin because it remains stable after curing (Hon, 2003). Polypropylene (PP), Polyethylene (PE), Urea formaldehyde (UF), melamine formaldehyde (MF), phenol formaldehyde (PF) resins are the predominant thermosetting resins used as wood adhesives in the production of hot pressed wood composites.

Thermosetting resins are usually a mixture of low molecular weight condensates, intermediates generated by primary addition reactions, and monomers which are all soluble in water. These low molecular weight condensates will further react at higher temperatures and form the final cross-linked, rigid network (Pizzi & Mittal, 1994). The condensation process of UF resin and MF resin synthesis process are shown in Figure 2. 3.

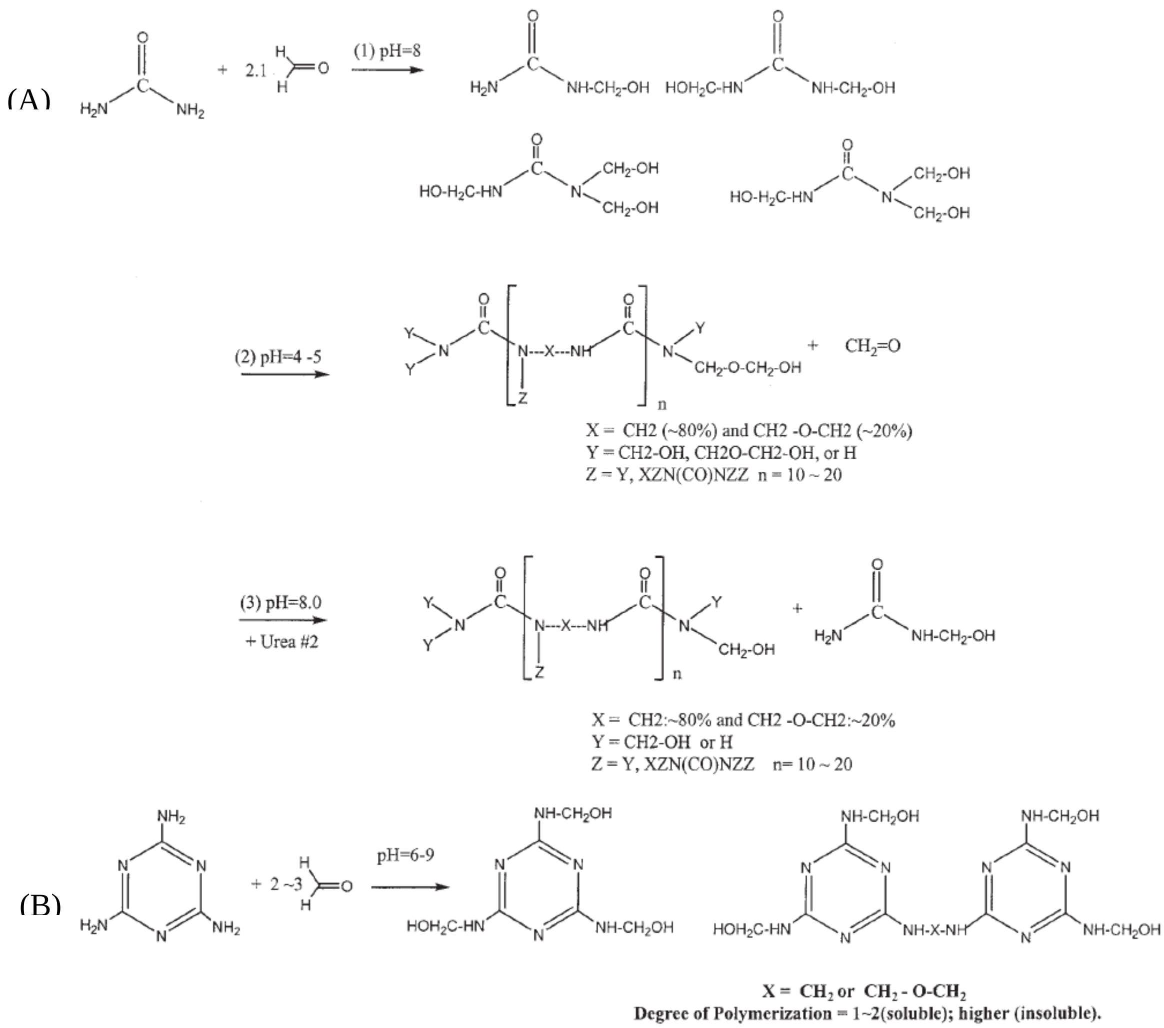

Figure 2.2: Schematic representation of (A) urea-formaldehyde (UF) and (B) melamine-formaldehyde (MF) resin systems (Adapted fromYoung No and Kim, 2005 with permisstion).

The condensation process of MF resin is similar to that of UF, however its network is denser and more cross-linked that the UF network. The stiffness and hardness of MF resin is highest among the know polymers (Doyle, Hagstrand, and Manson, 2003). MF resin is more expensive compared to UF resin and it is often used in conjunction with cheaper UF resin and other modifiers to reduce cost, and reduce the rigidity of the MF resin network. Approaches include incorporating urea and other substituted modifiers to reduce the crosslinking density.

2.2.3 Hybrid morphology of nanoclay-resin composites

There are three main types of nanoclay dispersions in a resin matrix that affect its properties and by extension, the bulk properties of clay modified wood composites (Alexandre and Dubois, 2000):

1. Phase separated: The nanoclay particles mix with the resin uniformly throughout the resin matrix as shown in Figure 2.4a. The clay platelets do not separate and the structure is still classified as a micro-composite or aggregate.

2. Interlayer structure: This involves more intimate mixing whereby the polymer is able to penetrate between the clay layers but not fully separate them (Figure 2.4b). The thickness of the resin between the clay layers ranges from a few nm to a few microns. This state is known as intercalation, an important feature being that the thickness of the polymer layer between clay platelets is relatively uniform and the plates remain parallel to each other, and the polymer chains are able to enter the interlayers of the clay and interact with the clay sheets. Nano size silicate clay layers remain distributed almost in parallel direction and the gaps between clay layers are increase from a few nm to µm (Figure 2.3 b).

3. Exfoliated structure (sometimes referred to as a delaminated structure). In this state the clay platelets fully separate and disperse evenly at random angles throughout the polymer matrix (Figure 2.4 c). The distances between the clay platelets become so large that they are no longer aligned together.

When the nano-thickness clay platelets fully disperse into the polymer matrix a true nanocomposite is obtained (Giannelis, *et al.*, 1999b,Hetzer and Dekee, 2008, Lü and Zhao, 2004). When nanoclay in a resin is either intercalated or exfoliated, it can significantly enhance the mechanical properties of the clay-filled matrix(Sinha Ray & Okamoto, 2003). This is because in these two hybrid structures the thin layers of nanoclay separate in to the polymer with a high aspect ratio which is between 10:1 and 1000: 1.

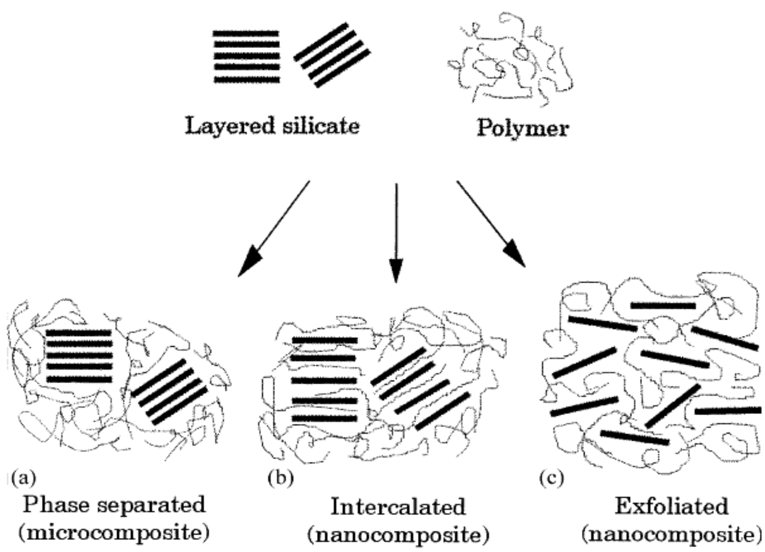

Figure 2.3: Scheme of different types of composite arising from the interaction of layered silicates and polymers: (a) phase separated microcomposite; (b) intercalated nanocomposite, and (c) exfoliated nanocomposite (Adapted from Alexandre and Dubois, 2000 with permission).

2.3 Nanoclay dispersion methods

The method used to disperse nanoclay into resin will greatly affected by the clay hybrid structure and the properties of clay-filled resin. In order to obtain the desired intercalated or exfoliated hybrid structure, various mixing methods had been developed to separate and disperse the clay into the resin. Ribbon mixing, tumbler mixing, high shear mixing, and even manual shaking have been used to disperse clay into resin (Wang, *et al*., 2008). Mechanical mixing method is the simplest method for blending the clay and liquid resin together.

Some grinding instruments have also been developed for the purpose of shear mixing silicate nanoclay into resin. A comparative analysis of the effect of different milling and grinding such as bread mill, ball mill, three roll mill, and high speed mixing on nanoclay dispersion into a UV coating was carried out by Landry *et al*., (2008). TEM results showed that three roll milling and bread mill treatments achieved better clay distribution and clay exfoliation. However, milling and grinding methods can have a negative effect on organic modified clays in that the shearing force scan damage the organic modified group on the clay sheet surface during grinding, resulting in reduced mechanical properties in wood composites made with clay- resin mixtures (Cai *et al*., 2010; Landry, *et al*., 2008).

Ultrasonic homogenization has also been employed to obtain an even clay dispersion in liquid resin. In a study by Dean *et al*. (2007), high shear mixing, ultrasonic bath techniques, and cell disruptor horn sonication were compared. Better clay dispersion was observed in the horn sonication and bath sonication treatment than for the high shear mixing method. However, the heat produced by continued ultrasonic vibration can lead to clay aggregation (Lin *et al.*, 2005). Therefore, careful attention to the mixing temperature and mixing time is necessary to avoid overheating. To get a better mixing result, Chowdhury *et al*. (2006) used a pulse cycle and water bath to control the mix temperature at around 40˚C to 50˚C when applying the ultrasonic technique. Discontinuous ultrasonic vibration is another alternative processing technique for distributing nanoclay into liquid resin as it reduces overheating and clay aggregation (Lin, *et al*., 2005).

Compared to all the other clay mixing methods, mechanical mixing has been shown to be the simplest and lowest cost method for blending nanoclay and liquid resin. According to Wang *et al*. (2008), the mixing method used needs only to result in uniform dispersion of phyllosilicate clay into the resin. It is reported that simple mechanical mixing was sufficient to completely exfoliate nanoclay into UF resin (Lei *et al.*, 2008) and produce intercalation with epoxy resin (Adam *et al.*, 2001) and even exfoliation in epoxy resin (Lan and Pinnavaia, 1994).

The ideal mixing temperature for thermosetting resin should be around room temperature (around 20˚C), because thermosetting resins will start curing or setting at higher temperatures. There is no fixed blending time for mechanical mixing; blending time can vary from 5 min to more than 60 min, as long as the clay is dispersed into the resin uniformly (Lei *et al*., 2008). Blending speed usually ranges from 500 rpm to as high as 3050 rpm (Cai *et al*., 2007), a medium mixing speed, 800 or 1000 rpm, is preferred (Wang *et al*., 2008).

When separating nanoclay into thermoplastic resin, a higher blending temperature is preferred. Melt blending is the most common method used to mix nanoclay with thermoplastic resin, at a temperature that is high enough to give the resin adequate viscosity for further processing, such as exfoliation (Lee *et al*., 2005 , Lei *et al*., 2007). An analysis comparing different processing parameters on nanoclay dispersion in polyolefin was carried out by optimizing the mixing parameters. Up to 30 to 40 min mixing time was required for clay delamination. A higher mixing speed, 110 rpm, was significantly better than the low speed, 35 rpm. However, higher concentration of clay made it more difficult for the clay to become completely exfoliated in the polymer (Lee, 2008). In summary, higher mixing speeds and longer blending times can greatly improve clay dispersion.

In addition to the optimization of mixing parameters, the use of compatibilizers, such as coupling agents, can also aid in exfoliating the silicate clay (Kim *et al.*, 2003). It is known that long chain organic modifiers, such as alkyl ammonium, will enlarge the interlayer distance of nanoclay therefore facilitating the exfoliation of clay (Labidi *et al.*, 2010). Coupling agents together with organic modifiers also help the clay platelets exfoliate because the coupling agent has the similar effect on hydrophilic nanoclay (Han *et al.*, 2008). Commonly used coupling agents are maleated polypropylene (MAPP) , silane coupling agent, and are usually used at less than 10% of the matrix mass or based on the amount of clay additive (Zhao *et al.*, 2006, Nourbakhsh and Ashori, 2009).

2.4 Wood nanoclay composites processing

As illustrated in Figure 2. 3, there are two different methods for producing wood nanoclay composites (Lü and Zhao, 2004). In the case of wood-plastic composites wood furnish can be compounded with polymer, nanoclay and other additives in one step. The two steps method is to prepare the nanoclay and polymer mixture then incorporated the mixture with wood furniture or solid wood to form the wood nanoclay composite. In the case of hot pressed wood panels where resin is used as a binder in small quantities and the resin is pre-mixed with nanoclay and then blended with wood furnish in a secondary step (Lü *et al.*, 2006).

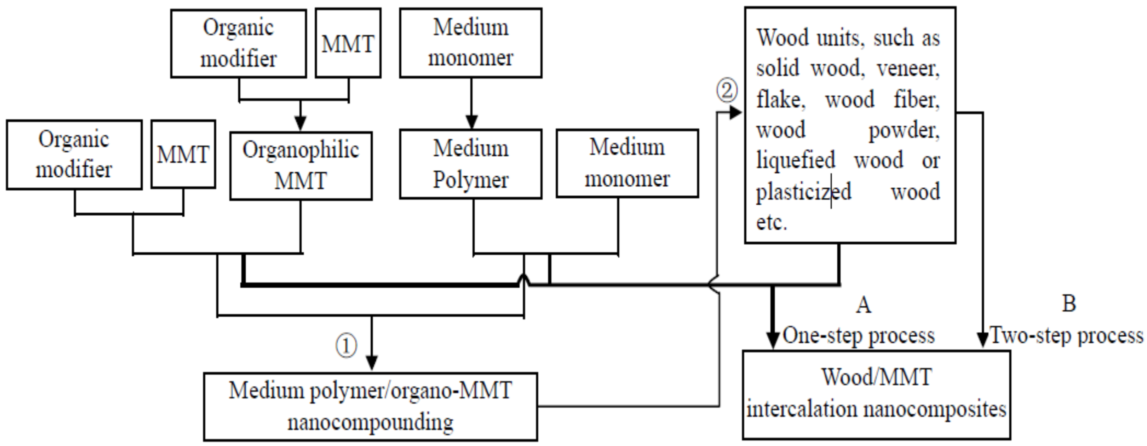

Figure 2.4: Flow chart of wood nanoclay polymer composite process (Adapted from Lü and Zhao, 2004 with permission)

The process for fabricating nanoclay- reinforced wood plastic composites (WPC) is similar to conventional WPC or other thermoplastic polymers. Compounding thermoplastic resin and nanoclay is a one-step melt blending process and the mix is extruded and cooled in the designed shape of the end product. In the two step process, nanoclay is first dispersed into the resin or molten polymer matrix and wood flour is then melt blended into the clay resin mixture. An alternative one step process for fabricating wood-plastic composites is to blend nanoclay with the polymer and wood flour or wood fiber simultaneously during grinding, batch mixing, or compounding using a twin-screw or single-screw compounder. The mixture is then consolidated into a nano-composite by hot injection modeling, extrusion, or pressing (Faruk and Matuana, 2008).

For wood composite panels that are bonded with thermosetting resin using veneer, particles, strands, or fibers, the processing methods are similar to those for conventional board manufacturing whereby the binder is the nanoclay-resin mixture. The only requirement for the mixing method is that it is sufficient to intercalate or exfoliate the clay into the resin (Wang *et al.*, 2008).

Blending the nanoclay and adhesive is the first step in producing nanoclay-modified wood composites, whereby the blend of adhesive and clay is further mixed with wood furnish. After applying the resin, the furnish is form into a mat then hot pressed into wood panels during hot pressing process (Lei *et al*., 2008, Wang, *et al.*, 2008).

Other studies have investigated incorporating nanoclays into solid wood. A common approach for fabricating solid wood-nanoclay-polymer composites is to fill the cell lumens of solid wood with a clay resin mixture (Lü *et al.*, 2006). In this case the oven dried solid wood was placed under vacuum to remove air, then dipped into liquid resin-clay mix under atmospheric pressure (or higher pressure) and evacuated again after absorption. The wood pieces which impregnated with resin were then air dried in fume hood for one day (Cai *et al.*, 2008).

2.5 Characterization nanoclay-resin hybrid structure

There are several techniques used to investigate the distribution of nanoclay resin mixtures and the effect of the nanoclay on resin properties. X-ray diffraction (XRD) is the main technique used to provide information on the degree of clay agglomeration and exfoliation. Transmission electron microscopy (TEM) and scanning electron microscopy (SEM) are also useful for visualizing the homogeneity of clay distribution in the matrix by providing direct observation of clay platelets or agglomerates in the hybrid structure.

The addition of nanoclay into thermoplastic resin will affect the chain mobility of polymer and the fillers share the stress with polymer matrix (Sui *et al*., 2007). The presence of a nanoclay will reduce the crystallinity of thermoplastic resin, increase the free volume and therefore change the glass transition temperature. The change in degree of crystallinity can be detected by XRD and DSC, and glass transition temperature can also tested using DSC and Dynamic mechanical analysis (DMA).

2.5.1 X-ray diffraction

X-ray diffraction (XRD) has been extensively used for characterizing the microstructure of polymer/layer silicate nanocomposites. XRD is traditionally used to identify and analyze the crystal structure of solid materials. In the silicate layer arrangement of montmorillonite the interlayer distance of the pristine clay and the modified clay is in the range of 1-4 nm (Giannelis, *et al.*, 1999b). The interlayer space between clay layers can be detected by XRD by a peak in the x-ray intensity at a characteristic angle and the inter-platelet distance calculated (Bragg and Bragg, 1913). According to Bragg's law, the interlayer spacing (*d*) in nanoclays and the relative intercalation (*RI*) of the polymer in nanoclays can be determined using the following equations (Pegoretti, 2007):

$$n\lambda = 2d \sin\theta \qquad (2.\ 1)$$

$$RI = \frac{(d - d_o)}{d_o} \times 100 \qquad (2.\ 2)$$

where n is the integer number of wavelength ($n = 1$); λ is the wavelength of X-ray; d is the actual interlayer or d-spacing of the clay in the matrix; θ is the diffraction angle corresponding to a specific intensity peak, and d_0 is the d-spacing of the sheets in the pristine clay or organic modified clay. Usually, the results of XRD analysis are 2-dimensinal XRD patterns showing the 2θ angle (twice the diffraction angle) on the horizontal axis and the vertical axis representing the intensity of the X rays. The distance between clay lattices will result in an intensity peak which appears at a specified angle.

From the Bragg Law, the lower peak diffraction angles indicate larger distances between the interlayers of nanoclay. If the nanoclay is totally exfoliated in the resin none of the clay platelets are aligned with each other and the diffraction angle may be too small to be detected. If the nanoclay is intercalated with the resin, the clay platelets are still parallel to each other and just further apart than in the pristine clay, the intensity peaks will shift to a lower angle.

In addition to characterizing the clay dispersion, XRD can also provide other information about the hybrid resin such as crystallite size of thermoplastic resin (Vaia and Liu, 2002). The crystallinity of thermoplastic resin shows up as intensity peaks in XRD patterns. In the case of thermosetting resins, which are generally amorphous, non-crystalline solids there are no sharp intensity peaks in the XRD pattern, instead, it shows up as smooth, rounded wide peaks.

The degree of clay intercalation is quantified at the lower X-ray angles while information on the crystalline phases in the polymer usually appears in the higher range of diffraction angles (Sarrazin *et al.*, 2005). For the range 18˚-30˚, the X-ray intensity peak of clay-added HDPE and clay and wood flour reinforced HDPE were lower than that of pure HDPE, suggesting that the addition of clay and wood flour decreased the crystallite of HDPE in the clay hybrid (Lei *et al.*, 2007).

2.5.2 Microscopy techniques

Transmission Electron Microscopy (TEM) can provide direct visual evidence of clay dispersion (Morgan and Gilman, 2002). The silicate layers in thin sliced sections show-up as dark lines in

TEM images, while the light areas correspond to resin (Deka and Maji, 2010). When the clay is totally exfoliated, the platelets are visible as dark lines in different orientations. Intercalated clay shows up as parallel layers of alternating dark and light bars (Giannelis *et al.*, 1999a). Clay aggregation can also be easily observed in TEM images. TEM was used by Landry *et al.*, (2008) to evaluate which clay dispersion process (bead milling, ball milling, three roll milling, and high speed mixing) achieved better clay distribution, showing that three-roll milling and bead milling lead to better dispersion than bead milling and high shear mixing treatment.

Vermogen *et al*., (2005) used statistical analysis of TEM images to evaluate the clay dispersion in clay-plastic composites which were prepared using different screws in a twin screw extruder. The clay platelet length, thickness and aspect ratio, inter-platelet distance and the amount of clay aggregation were quantified and statistically analyzed. Based on these results the effect of screw profile on the final clay morphology was assessed.

The main issue with TEM and SEM techniques is the very small volumes of materials examined may not be representative of the whole volume, and many different samples are required in order to develop a more comprehensive view of the bulk of the material. A solution to examining a large number of samples is to use microscopy techniques in conjunction with XRD.

Microscopy is not only useful for direct observation of the clay dispersion, it can also examine the effect of clay on the crystallization and the facture toughness of the resin. Using SEM examination, nano-sized spherulite crystals were easily observed in pure PP, but the size of spherulites was reduced with the addition of nanoclay, suggesting that the presence of the clay interfered with the growth of spherulites (Perrin-Sarazin *et al.*, 2005). This effect was even more pronounced when a coupling agent was added (MA330k).

The facture behavior of clay reinforced resin has also been examined by SEM. Typically, the fracture surface of neat resin is smooth with very few cracks are appearing on the surface indicating a typical brittle facture. A cracking trail is formed when two secondary crack fronts come together (Wang *et al.*, 2005). The micro cracks start between the between clay particles and weakly bonded layers then grow and extend further into the matrix when further load is applied. The path taken by the crack can be quite tortuous with the presence of clay, as shown in Figure 2.6. The crack will absorb more energy during growth than the more brittle, smoother cracks. Therefore the sub fracture surface area will increase and share more stress. At low clay content, sample showed minimal fracture surface roughness which isolated to small regions because the clay plays a part in reducing the stress concentration and therefore makes the matrix more resistant to the crack growth (Chen *et al.*, 2003). At a higher clay concentration, this mechanism works on a smaller scale because the distance between clay platelets is decreased. Similar behavior in unsaturated polyester-clay nanocomposites is also reported (Adam, 2001).

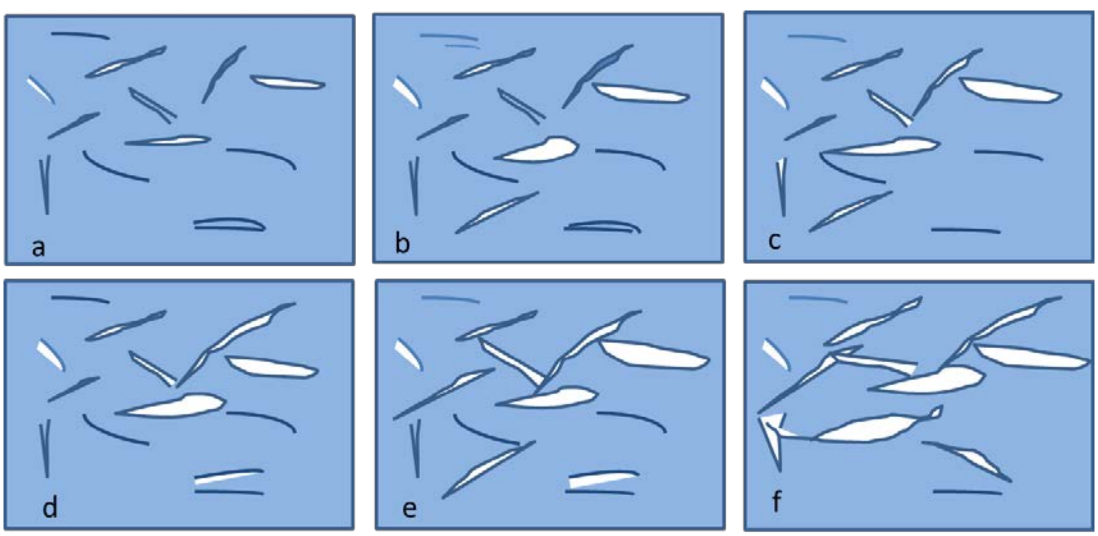

Figure 2.5: Crack initiation process of clay-filled epoxy resin (Adapted fromWang *et al.*, 2005 with permission).

One possible reason for clay reinforcement is that the clays share the stress with the resin matrix and prevent the crack to growth. However, this mechanism is as not as effective to gain strong improvement in fracture toughness.

2.5.3 Thermo analysis

As was alluded to earlier, once nanoclay is added to the resin matrix the polymer's crystallization and chain mobility can change. Thermoanalysis instruments such as Differential scanning calorimeter (DSC) and Dynamic mechanical analysis (DMA) can be used to detect these changes and characterize the clay's effect on resin on several parameters: i.e., glass transition temperature (T_g), crystallization temperatures (T_c), heat of fusion, and entropy of fusion(ΔH) (Menczel and Prime, 2008).

The result of a DSC experiment is a plot of heat flow versus temperature or time. Examples of exothermic peaks (a heat producing event) on the curve, an example of which is shown in Figure 2.7, include crystallization and oxidation reactions, while an endothermic event (heat absorbing) includes phenomena such as melting and decomposition (Hon, 2003).

Figure 2.6 was the schematic of DSC curve of transition enthalpy as the temperature changes. The image is not given here according to the Canadian copyright law. Please find the original image in the following reference:

Hon, D. . (2003). Analysis of Adhesives. In K. L. Pizzi, Antonio; Mittal (Ed.), *Hand book of wood Adhesive technology* (2nd ed.). (pp. 129-150).M. Dekker.

Figure 2.6: Schematic of DSC curve (Hon, 2000).

The enthalpy of transition, *ΔH*, can be expressed using the following equation:

$$\Delta H = KA \qquad (2.\ 3)$$

where *K* is the calorimetric constant and *A* is the area under the curve.

The degree of crystallinity, χ_c, of a thermoplastic polymer composite can be computed using the following equation:

$$\boldsymbol{\chi_c = \frac{\Delta H_{exp}}{\Delta H} \times \frac{1}{W_f} \times 100\%} \quad (2.\ 4)$$

where ΔH_{exp} is the measured heat of crystallization, ΔH is the heat of crystallization for a 100% crystalline polymer (e.g. ΔH for pure HDPE is 293 J/g), and W_f is the weight fraction of thermoplastic resin in the composite.

Lei *et al*., (2007) found that the addition of pine flour or clay will lower the crystallization rate of HDPE. However, the use of a compatibilizer, maleated polyethylene (MAPE), increased the crystallization of the HDPE in the HDPE -clay-pine composite. The nanoclay acted as an nucleating agent for PP and reducing the crystallization rate provided sufficient time for clay diffusion and produced a more intercalated arrangement (Maiti, Nam, and Okamoto, 2002).

In most cases, the curing peak temperature and heat of reaction are used to quantify uncured thermosetting resins. Liquid samples are usually sealed in high volume pans or tested in pressure DSC to minimize the confounding effect of water evaporation. The cure peak temperature indicates the maximum curing rate (Sichina and Manager, 2000). Becker et al., (2003) found that the presence of nanoclay reduced the resin curing rate as evidenced by a broadening of the exothermic peak and the peak shift to a lower temperature. Other studies suggest that nanoclay does not strongly affect the onset temperature and the peak temperature of the cure reaction (Hussain *et al.*, 2007) (Ton-That *et al*., 2004).

MMT-modified UF resin cures faster than pure UF resin with hardener, as evidenced by earlier onset and higher exothermic peak temperature of than UF resin (Lei *et al*., 2008). The DSC curve of nanoclay and hardener-added UF resin also displayed a wider and lower exothermic peak than that of pure UF with hardener.

Nanoclays may also influence the resin at the molecular level by changing the molecular motion and chain flexibility. Such changes are difficult to detect using DSC but can be measured using DMA (Hatakeyama and Quinn, 1999). A typical DMA scan for a thermoplastic resin is shown in Figure 2.8.

Figure 2.7 was not given here according to the Canadian copyright law. It was the curves of tan δ, storage (E') and loss (E") modulus for a sample of PVA in DMA test. Please find the original image in the following reference:

Hatakeyama, T., & Quinn, F. X. (1999). Thermal Analysis Fundamentals and Applications to Polymer Science. (T. Hatakeyama & F.X. Quinn, Eds.)Recherche (2nd ed., p. 131). Toko,Japan: John wiley& sons.

Figure 2.7: Tan δ, storage (E') and loss (E") modulus for a sample of PVA (Hatakeyama and Quinn, 1999).

For thermoplastic resins the storage modulus, E', is the dynamic elastic response of the sample. The loss modulus, E", is the dynamic plastic response of samples, and tan δ is the ratio of loss modulus/storage modulus. Usually, the peak of tan δ or E" are defined as T_g . As can be seen from Figure 2.8, E' is approximately constant from before T_g , after which point it abruptly decreases. Below T_g there is no slippage between adjacent molecules because energy is much less as chain movement cannot occur whereas above T_g slippage occurs and the ability of the sample to store elastic. The peak of loss modulus or the tan δ shows that the sample passed through the glass transition temperature (Groenewoud, 2001).

Most studies have found enhancement of storage modulus with the addition of nanoclay. Different studies have found various different clay loadings whereby there is maximum improvement in storage modulus. Nanoclay-reinforced polyethylene (PE) had a higher storage modulus than neat PE, and the storage modulus and loss modulus increase with clay content (Lee *et al.*, 2005). Similar results were obtained for HDPE-clay mixtures, indicating higher stiffness of clay-reinforced polymer and reduced mobility of the polymer chains between the nanoclay layers.

Chowdhury *et al.*, (2006) used pre-cured epoxy resin to impregnate a woven carbon fabric which was tested using a DMA single cantilever beam mode. Storage modulus reached the highest value at the 2% nanoclay (in this case Nanomer® I-28E) loading rate while at 3% clay loading storage modulus was lower than that of the neat resin. Miyagawa, *et al.* (2004) found that the storage modulus of anhydride cured epoxy/clay composite increased with increasing clay content. A 13% increase in storage modulus was obtained with only 2.5 wt% clay addition. These improvements may have resulted from the high aspect ratio and the interfacial adhesion between epoxy resin and nanoclay (Kotsilkova and Pissis, 2007).

Glass transition temperature (T_g) can be related to molecular weight, cross-linking density, free volume density, and strength of the interface layer between the nanoclay platelets (Hussain *et al.*, 2007). If the T_g of a nanoclay-filled resin increases to a higher temperature, then the clay has improved the resin's thermomechanical properties. However, Awad (2009) found the nanocomposite's T_g was not significantly different from the pure polymer. The T_g of a thermosetting adhesive is dependent on the degree of cure and water content (Lapique, 2002) and therefore T_g is not as reliable for characterizing thermosetting adhesives.

Mostly, DMA is applied in detecting the curing process of thermosetting resin. In contrast to thermoplastic resin the storage modulus increases as the temperature increases and reaches the peak temperature when the resin was completely cured and forms a highly cross-linked network (Figure 2.9) (Pilato *et al.*, 2010). The onset of curing and end of curing is determined by the storage modulus, the different of the maximum and minimum E′ (ΔE′) represent the rigidity of the resin network (Park and Kim, 2008).

Figure 2.8 was not given here according to the Canadian copyright law. It was the storage (E') and loss (E") modulus curve of resole resin in DMA test. The storage modulus increased as the temperature increased. Please find the original images in the following reference:

Pilato David Nagy, Ellen, L. V. (2010). Phenolic Resins: A Century of Progress Analyses/Testing (pp. 93-135).

Figure 2.8: DMA result of a resole resin. (Pilato, *et al*., 2010)

Preparation of DMA samples for thermosetting resin's is different from that of a thermoplastic resin, especially for studying the curing process of thermosetting resin (ASTM, 2008). Various methods had been developed for preparing thermosetting resin DMA samples. One involves placing resin between two plywood pieces as a sandwich sample (Lei *et al.*, 2008), another is to impregnate glass fiber (Mequanint and Sanderson, 2003), carbon fiber (Mequanint and Sanderson, 2003 Kim *et al.,* 1991) or other supporting materials with resin to form a thin film.

The storage modulus of nanoclay-filled MUF resin first decreased with the temperature from 30°C to around 80°C, but increased as heating process continued and reached a plateau. With the presence of nanoclay filler, MUF increased in both the storage modulus and tan δ (Cai *et al.,* 2010). In general, the storage modulus of thermosetting resin (derived from E′ in the rubbery plateau) represents the rigidity of the resin network (density of crosslinking) and increases with nanoclay loading (Park and Kim, 2008, He and Riedl, 2003).

2.6 Nanoclay reinforcement mechanism

It is believed that some chemical bonding between the resin polymers with and nanoclay platelet surfaces may occur. Fourier transform spectroscopy (FTIR) and Nuclear magnetic resonance **(**NMR**)** have been employed to investigate the chemical interaction between the nanoclay and resin. Lü *et al,* (2006) modified PF resin with organic MMT and then impregnated the mixture into solid wood to produce a wood-MMT nanocomposite. The FTIR spectrum of this composite showed −OH vibrating adsorption, which indicates strong linking between PF and MMT had generated by their oxygen atoms. Stronger −C−O vibrating adsorption indicated that more chemical combinations had been built-up between organic clay and the wood (Lü *et al.,* 2006). Han, *et al.,* (2008) has also verified enhanced chemical bonding between organic clay, coupling agent and pMDI resin using both FTIR and NMR.

The large aspect ratio (the ratio of length and width) and large specific surface area of nanoclay platelets is a major contributor to reinforce the polymer matrix. The addition of larger aspect ratio platelets results in a greater increase in the elastic modulus (stiffness) for clay-reinforced resins (Miyagawa et al., 2004). The intercalated or exfoliated hybrid structure of nanoclay-filled resins also improves the fracture toughness of resin. Nanoclay was shown to have larger interfacial adherent surface to the resin (Siddiqui *et al.,* 2007).

The nanoclay platelets hamper the propagation of cracks in a hybrid resin as evidenced by the rough fracture surface of nanoclay-resin composites compared with fracture surface of the same resin containing no nanoclay. As the crack pass through the clay region they impinge on the platelets and later branches. As the clay content increase, the distance between clay platelets decrease creating a more tortuous route for crack propagation (Adam *et al.*, 2001). The major toughening mechanism of nanoclay in resin matrices is that cracks branch into more micro-cracks to yield more fracture surface areas (Wang *et al.*, 2005). At low clay loading, from 2 to 5%, fracture toughness increased with clay content (Siddiqui *et al.*, 2007).

2.7 Characterization of properties of polymer-nanoclay-wood composites

There are more reports in the literature on the effectiveness of various nanoclays to improve the properties of wood-plastic composites than there are for conventional wood composites such as particleboard. This section briefly covers the studies for these two types of composites.

2.7.1 Dimensional stability of clay-reinforced nanocomposites (thickness swell and water absorption)

The dimensional stability of wood-nanocomposites or nanoclay-polymer mixes are reported to be significantly improved with the incorporation of nanoclays. One property that was unaffected by the presence of the nanoclay was the fire retardant of polymers (Zhang *et al.*, 2009, Wang *et al.*, 2007).

Most of studies of nanoclay-added -wood composites found that thickness swelling decreased. Deka and Maji (2010) reported that for clay contents up to 10% in wood flour/ HDPE composites, thickness swell decreased with increasing clay content. For example, adding 2% nanoclay into HDPE-wood flour composites reduced thickness swelling by 41%; higher clay contents further reduced swelling. This may be because the exfoliated clay produces a longer moisture diffusion path. In terms of water absorption Yeh (2007) found that water absorption decreased between 10% to 40% (Yeh, 2007) . The addition of the coupling agent, maleic anhydride grafted polyethylene (MAPE), into PP/wood flour composites further improved the dimensional stability as the coupling agent reduced the chain movement by increasing chain cross linking in the polymer (Sheshmani, Ashori, and Hamzeh, 2010). The thickness swelling rate of PP/bagasse composites decreased with increasing nanoclay content up to 8% (Amir Nourbakhsh and Ashori, 2009).

Cai *et al.,* (2007) studied the water absorption and thickness swelling of clay-resin impregnated solid wood. MUF treated wood showed lower water absorption and thickness values than solid wood, MUF/nanoclay treated wood had significantly lower values than MUF treated wood and solid wood. The nanofiller, Claytone®APA, turned out to be more effective than Cloisite® 30B and Cloisite® Na^{+}.

Thickness swelling of nanoclay-reinforced MDF (Medium Density Fiberboard) has also been investigated. The thickness swelling decreased significantly as the clay content increased. It is believed that voids in the composite and the lumens of fibers were filled with nanoclay which prevented the penetration of water by capillary action into the deeper parts of composite .

2.7.2 Mechanical properties of polymer-nanoclay and wood -nanoclay composite

Flexural strength and tensile strength are key properties used to evaluate the performance of wood-based nanocomposites. Studies have shown that the addition of nanoclay influences the flexural properties of both polymer and wood based composites. Clay loading rate has the stronger effect on strength properties, but other factors such as clay type, blending method and coupling agent also play a role.

Faruk and Matuana, (2008) tested five types of Cloisite nanoclays in modified HDPE wood flour composites. They were able to enhance polymer properties using the melt blending process whereas dry blending of ingredients was not effective and that the Closite10A was more effective than other clays. The addition of a coupling agent resulted in higher MOR, MOE and tensile strengths compared with Cloisite10A alone. Lei *et al*., (2008) found that 1% clay addition to HDPE improved its tensile and flexural strength by 24.2% and 19.6% respectively. Higher clay content reduced the extent of strength increase. The flexural and tensile modulus of PP-wood flour- nanoclay composite were increased at 3% loading of organic-modified montmorillonite (OMMT) but were reduced at a higher 6% loading rate. Both of the clay loading rates, 3% and 6%, decreased the impact strength of the composite (Kord, Hemmasi, and Ghasemi, 2010).

Nanoclay has been shown to influence the mechanical properties of wood-based panels. In a study by Ashori (2009), Cloisite Na^{+} was mixed with dried UF-resinated MDF wood fiber. In the 2% to 6% clay content range, MOR and MOE increased as the clay content increased, but the effect was reduced at 8% clay loading. Higher clay concentration can lead to clay aggregation, reduced bonding strength of the adhesive and reduced board properties (Ashori and Nourbakhsh, 2009).

Internal bond, IB, strength refers to the tensile strength perpendicular to the surface of the panel. According to Ashori and Nourbakhsh (2009), IB strength of MDF increased for clay contents from 2 to 8% and reached a maximum value of 0.6 MPa at 4%. Lei *et al.* (2008) exfoliated different percentages of nanoclay into UF resin by mechanical stirring and made particle board bonded with the clay-resin mix. They found that in 2-8% range, higher clay loading rate improved the IB strength more evidently.

Wang et al. (2008) used UF resin containing 1 or 2% nanoclay to produce Oriented Strand Board (OSB). They found that IB strength increased by 28% for a 1% clay addition while the IB strength of the samples made with a 2% addition only increased by 11%. However there were no significant changes in the other board properties and in some cases decreased slightly. It was shown that substituting 1% clay in liquid PF resin resulted in the same board properties as pure PF resin (Wang *et al.,* 2008).

In conclusion, the addition of nanoclay can enhance the mechanical properties of nanoclay -polymer composites and nanoclay-reinforced wood composite up to a point and then tended to decrease at higher clay contents. Thickness swelling also benefitted from the addition of a small amount of nanoclay to the resin and it is postulated that it filled voids in the furnish and blocked water ingress.

2.8 Summary

Nanoclay-polymer composites, especially platelet nanoclay- reinforced polymers have been extensively studied. There are three types of nanoclay distribution arrangements in the polymer matrix: phase separated, intercalated and exfoliated. Various methods have been used to distribute clay to achieve an intercalated or exfoliated state which is ideal for polymer reinforcement. The methods include, but are not limited to, mechanical mixing, high shear mixing, melt blending (for thermoplastic polymers only), ultrasonic dispersion, and even

grinding methods such as ball mill mixing and bead mill mixing. Each mixing method has its advantages and disadvantages. To get uniform clay distribution the appropriate method should be selected according to the material properties. The mixture of clay and resin can be further processed to form a nanoclay-polymer composite or wood-nanoclay-polymer composite.
TEM, SEM and XRD have been used to examine the clay dispersion in the polymer or resin matrix. The distance between the phyllosilicate layers can be determined by the X-ray diffraction angle. When clay is intercalated or exfoliated the distances between sheets is greater, it shows in the XRD pattern as the peak of diffraction angle shifting to a lower value. SEM or TEM can further elucidate the clay distribution and is useful for analyzing fracture surfaces and cracking behavior of the nanocomposites.

DSC and DMA tests measure the effect of nanoclay on the thermal behavior of polymers and resins. DSC curves have shown that the clay decreases the degree of crystallinity of thermoplastic polymers and wood plastic composites, making them less brittle. The addition of nanoclay improves the thermo-mechanical properties of thermoplastic resin and influences the curing process of thermosetting resin by altering the cross linking of resin.

Some studies have concluded that nanoclays with high aspect ratio and specific size can be used as fillers to improve the mechanical properties of the polymer matrix. FTIR and NMR analyses show there are extra chemical bonds formed between organic-modified clay and resin which may also contribute to the clay reinforcing mechanism. Organic modifier and coupling agents help separate the clay into resin and facilitate the interaction between clay and resin.

Phyllosilicate nanoclay has been shown to significantly improve the water resistance of nanoclay-wood composites, higher clay content results in reduced water absorption. This is especially so for MDF and wood plastic composites. Most studies that have added nanoclay to conventional wood composites have found that the mechanical properties including bond strength and bending strength are unaffected or improved. The most significant enhancement of properties are for dimensional stability, i.e., reduced thickness swell and water absorption. There are fewer studies on, and less success with adding nanoclays to solid wood.

3 Materials and methods

3.1 Materials

PB Furnish: The particleboard furnish used in this work was provided by the NewPro Particleboard plant located in Smithers BC. The furnish consisted of spruce (*Picea glauca*) and pine residues from saw-mills and other facilities in that region.

The particles are produced from saw mill residues, such as hogged mill waste, sawdust, planer shavings, and are distinguished by size: coarse, medium and fine furnish by screening. In this work, the coarse furnish can pass through the 9-mesh screen (mesh opening size is 2.0mm), and the fine furnish can pass through a 32-mesh (mesh opening size is 0.5mm) (Sackey, *et al.*, 2008). Three layered particleboards were made with coarse furnish in the core layer and fine particle in the face layers. The moisture content of the furnish was approximately 7%.

Veneer: Sliced aspen (*Populus tremuloides*) veneer, 0.027-inch or 0.7 mm thick was used for lap-shear tests. The moisture content of this veneer was measured to be 8%.

Resins: The resins used in this study were urea formaldehyde (UF) and melamine formaldehyde (MF) resins provided by Momentive Ltd. (previously Hexion Ltd.) (Table 3.1). For some of the experiments a coupling agent, 3-Aminopropyltriethoxysilane (purchased from Alf Aescer) was added to the resins and that mixture used to make PB and the lap-shear specimens.

Table 3.1: Nominal properties of the UF and MF resins.

Resin	Name	pH	Solid content (wt. %)
UF	Casco-resin C04SS	8.1-8.4	62
MF	Casco-Resin HM707	9.1-9.5	57

Nanoclays: The nanoclays used in this study were all platelet-based montmorillonite (MMT) clays provided by Southern Clay Ltd. (Austin TX, USA) and are listed in Table 3.2. These clays modified with different quaternary ammonium chlorides. The selected organic modified nanoclay, Cloisite®30B is considered to be organophilic while the pristine montmorillonite Nanofil®116 is hydrophilic. The median particle size of each of these clays was reported to be 13 μm.

Table 3.2: Nanoclays supplied by Southern Clay Ltd.

Nanoclay	Organic modifier (exchange cation)
Cloisite®30B	Methyl, tallow, bis-2-hydroxyethyl, quaternary ammonium
Nanofil®116	None

3.2 Preparation of resin and nanoclay mixtures

Mixtures of each resin and nanoclay were prepared by measuring out 200 g of resin and the appropriate mass, 4, 8 or 12 g of nanoclay added to the resins and the mixture stirred using a high-shear mechanical stirrer (Lightning Labmaster Model TS-2010, Figure 3.1 a) using a rotation speed of 1000 rpm for 30 min. The 33.2 mm diameter impeller agitator of stirrer is showed in Figure 3.1 b. The actual concentrations of the clays in the resin were 1.96, 3.84, and 5.66 wt/% for the 4, 8, and 12 g clay additions, respectively.

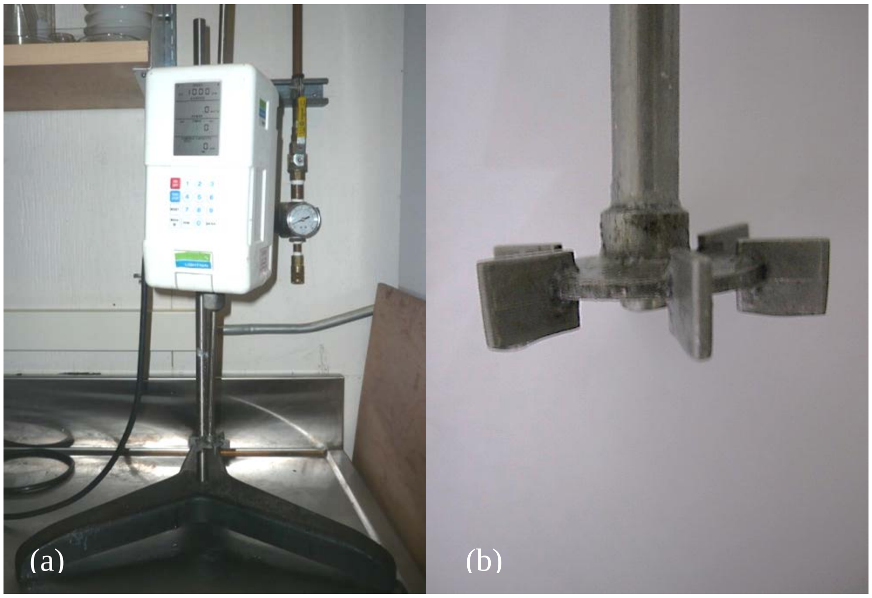

Figure 3.1: The Labmaster TS-2010 mechanical mixer: *(a)* the mixing head and *(b)* the impellor agitator.

Batches of 200g liquid resin and clay combination were blended using the mechanical stirrer shown in section 3.2 at a speed of 1000 rpm for 30 min. For the treatments where coupling agent was used, the coupling agent 10% of the clay mass was added into the resin before the clay, mixed for 5 min to allow its hydrolysis. Clay was then added into the resin for further 30 min mixing time.

3.3 Evaluation of bulk resin properties

For XRD and DSC tests, two types of platelet nanoclay, Cloisite30B, Nanofil116, were added into UF resin respectively, at a loading of 2%, 4% and 6%, with and without a coupling agent. When coupling agent was used it was added at 10% of the clay mass. Another 4 batches of MF resin containing nanoclays were also prepared with and without coupling agent. DMA and Lap-shear test were made only for the 2% clay loading.

3.3.1 X-ray diffraction test

After mixing using the mechanical stirrer, clay/resin mixtures were cured in a drying oven at 103°C for 24 hours, removed from the oven and cooled. The samples were ground down to powder and mounted in the sample holders of a D8 Focus (Bruker) X-ray diffractometer, and scanned from 3° to15° with a step size of 0.04°, and 0.8 s/step. X-ray radiation was generated by using a 35KV, 40mA Cobalt radiation source.

3.3.2 DSC test of resin and clay mixture

Since the curing of the resins may be affected by the clay in the mixtures, the curing of these mixtures was examined using a TA Q1000 Dynamic Scanning Calorimeter (DSC). A high volume pan was placed on an analytical balance and a 10±5 mg sample of either pure resin or the resin-clay mixtures pipetted into the pan and the actual mass of the sample recorded. The O-ring and lid were then placed to cover the pan and the sample then crimped shut using the sample encapsulating press provided with the DSC pan kit. A second reference pan containing no resin was also crimped closed and these pans then placed in the DSC, and calibration was performed using indium standards. Prior to performing a DSC scan, the cell temperature was equilibrated at 20°C and the samples and reference pans heated from 20°C to 200°C at a constant rate of 10°C/min using nitrogen as a purge as at a 50 ml/min flow rate.

3.3.3 Dynamic mechanical analysis (DMA) test

For each resin, four treatments were applied for each resin: 2% Cloisite30B addition with or without coupling agent (0.2% based on resin weight or 10% of clay weight), 2% Nanofil116 with and without coupling agent. To detect the curing process, samples were pre-cured by first impregnating resins into filter paper which supports the resins film then heat drying. Filter papers were cut into strips 60 mm long by 12 mm and soaked in the resin mixture for 24 hours to absorb sufficient resin then dried at 80°C for 24 hours to form a thin solid film. Samples were examined using a DMA TA Q800 with a 3-point bending clamp type, scanned from 60°C to 200°C, at a frequency of 1Hz. 0.01% and 0.05% stress applied to the samples respectively.

3.3.4 Lap-Shear test - automatic bonding evaluation system (ABES)

DMA tests relevant to the resin's cohesion strength (Park and Kim, 2008), which evaluate the bulk resin properties. Lap-shear strength can determine the resin's bonding strength with wood and shear strength of resin. So the resins with the same treatment in DMA were also test in this experiment to further evaluate the effect of clay on resins.

Aspen veneers were cut into pieces 120 mm long by 20 mm wide using a pneumatic clipper (Figure 3.4 a), the veneers that had straight grain and without defects were selected. The overlap length was 5 mm providing an overlap area of 5 mm by 20 mm (The overlap area is 100mm^2, 1Mpa =1N/mm^2, therefore the strength unit is MPa).

Mixtures of resin and clay were prepared as described previously. The resins were applied to the veneer samples using a small paint brush and the veneer was weighed (Figure 3.2 b). The mass of resin applied to the veneer was in the range of 0.009g-0.01g. The open assembly time for all samples was approximately 1 minute. The Automatic Bond Evaluation System (ABES) has small platens (Figure 3.2 c) that hot press the veneers together and then measure the shear strength of the bond line by pulling the veneers apart. Platen temperature was set at 140°C for UF resin and 160°C for MF resin. The two veneers were placed on the ABES unit and pressed together at a pressure of 1 MPa. Hot pressing time for UF resin was 60s, and 240s for MF resin. 8 replicates for each resin treatment were tested.

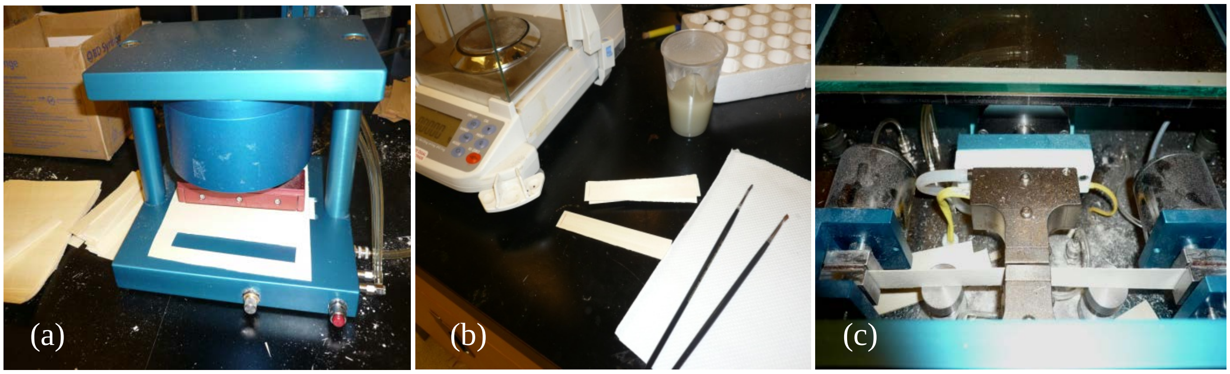

Figure 3.2: *(a)* air-operated clipper, *(b)* applying resin, *(c)* automatic bond evaluation system.

3.4 Manufacture of particle boards and evaluation of the effect of clay loading on board properties

The three clay-resin mixes: Cloisite30B mixed with coupling agent modified MF, Nanofil116 in MF, and Nanofil116 mixed with coupling agent modified MF had higher lap-shear strengths. These mixes were selected as the Clay Type factor for trials in fabricating particleboards to evaluate the effect of clay loading level on board properties. Three clay loading levels, 2%, 4% and 6%, were used.

Three-layer particle boards measuring 25 by 25 by 5/8 inches were made; the experimental parameters are listed in Table 3.3. The mass of each component was calculated using the oven dried furnish mass as the basis for the calculations. There are 3 clay types each with three different loading plus one control treatment containing no clay for a total of 10 treatments; 3 replicate particleboards were made for a total of 30 boards in this phase of the work.

Table 3.3: Experimental parameters and response variables for the large board production.

Variables:		
Clay Content	0, 2%, 4%, 6%wt of resin weight	
Clay type	Cloisite30B Cloisite30B with10% (clay wt.) coupling agent Nanofil116 Nanofil116 with 10% (clay wt.) coupling agent	
Replicates	3	
Constants:		
Resin Type	MF	
Resin Solids Content	57 wt%	
Board type	3 layers	
Board Length	25 inches	
Board Width	25 inches	
Board Thickness	5/8 inches	
Board Resin Content	10 wt% odw for both face and core layers	
Board Wax Content	1.5wt% odw	
Face Furnish Moisture Content	7% odw	
Core Furnish Moisture Content	7% odw	
Board Moisture Content	2% odw	
Shipping Density of Board	45pcf	
The Ratio of Face Furnish	46% of the total furnish mass	
Responses variables:	Number of samples per board	Number of samples per treatment
Internal bond (IB)	14	42
Screw Withdrawal Resistance (SWR)	8	24
Thickness Swell (TS)	2	6
Bending properties (MOR/MOE)	2	6

3.4.1 Three layer particle board manufacturing process

The required amounts of materials were weighted out and transferred into the Drais particleboard batch-blender (Figure 3.3 *left*). The surface furnish was blended first and due to the small size of the blender, furnish was blended with resin in two batches with the first batch used for the first two replicates and the second batch was blended for the third replicate. The same strategy was used for blending core layer furnish. The Pathex hot press (Figure 3.3 *Right*) was preheated from room temperature to 180˚C.

Figure 3.3: *(left)* Drais particleboard batch-blender and *(right)* Pathex press.

Resin and clay and coupling agent (if applicable) were mixed as described previously and the resin-clay mixture added to a paint pot. The paint-pot was then closed and 30 kPa of pressurized air applied to it. The spray nozzle was then bled until resin began to spray from the nozzle at which point the ball valve on the top of the paint-pot was closed. This step was necessary in order to ensure that all air in the line leading-up to the spray nozzle had been displaced. Emulsified wax was added into to the furnish using a spray bottle before blending with resin to enhance moisture resistance.

The paint pot was then placed on top of a balance accurate to ±1 gm and the balance tared. The Drais blender, shown in Figure 3.3, was turned on, the furnish allowed tumble for 1 minute to help distribute the wax and then the nozzle inserted through a hole in the lid of the blender and the resin sprayed onto the particles. As resin was being sprayed, the mass of the paint pot was monitored and the ball value closed once the correct resin-clay mass had been sprayed onto the furnish. This process took approximately 10 minutes. At this point the spray nozzle was removed, the time noted and the blender left to run for an additional 10 minutes. This was done to ensure that the wood particles were evenly coated with resin. After that the blender was turned off and the furnish was left in blender for a further 10 minutes to allow any fine aerosol droplets to settle out. Then these furnish were ready to form a mat.

A 25” by 25”forming box was place on top of an aluminum caul for forming the mat. The top and bottom layers were fine surface furnish, and the middle layer was composed of the coarse furnish. All three layers were distributed into the forming box consecutively and flattened using a small thick plywood sheet by hand before adding the next layer. The final step was to use the tamper to compress the mat to reduce air gaps and reduce its height before removing the forming box to reveal an even square mat and transfer it into the hot press with another caul on top. The hot pressing schedule for all mats is given in Table 3.4. Pressed boards were cooled to room temperature and then transferred to the conditioning room for 2 weeks to equilibrate the moisture content.

Table 3.4: Hot press cycles parameters

Proj. Ref.	LPBNANO	Date	12-13-2010	Time	15:18:18
Prod. Ref	Particleboard	Pane ID	0M-1	File Name	lananopb0m1
Press ID	Pathex	Mat Length	25in	Mat width	25in
Density	45pcf	Thickness	0.625in	Caul thick	0.48in
SEG	Control	Set point	SEG time	End Condition	
1	fastposn	-0.500 in./s	30 s	Position<=80.01mm	
2	position	50.00%	1 s		
3	position	38.1mm(1.5 in.)	5 s		
4	position	25.4mm(1.000 in.)	5 s		
5	position	19.05mm (0.75in.)	5 s		
6	position	19.05mm (0.75in.)	20 s		
7	position	15.88mm(0.625in.)	5s		
8	position	15.88mm(0.625in.)	400s		
9	pressure	2.41MPa(349.54psi)	10s	Position<=15.88mm	
10	pressure	1.72MPa(249.9psi)	10s	Position<=15.88mm	
11	pressure	1.03MPa(149.6 psi)	10s	Position<=15.88mm	
12	pressure	0.69MPa(100.2psi)	10s	Position<=15.88mm	
13	pressure	0.52MPa(74.8psi)	10s	Position<=15.88mm	
14	pressure	0.34MPa(50.1psi)	10s	Position<=15.88mm	
15	pressure	0.17MPa(25.1psi)	10s	Position<=15.88mm	
16	pressure	0Mpa	20s	Position<=15.88mm	
17	position	380mm(15in)	20s		

3.4.2 Test of mechanical properties of large boards

Each 25” by 25” board was first trimmed to 22” by 22” and then cut into test specimens for MOR/MOE, SWR, TS/WA and IB tests, the dimensions of which are given in Figure 3.4. The dimensions of the SWR specimens was 6" by 3", 6" by 6" for the TS specimens, 2” by 2” for the IB specimens, and 17” by 3” for the MOR/MOE specimens. All specimens were stored in the conditioning room for one week prior to testing. Specimen moisture content were around 7%-8%, density was around 0.66-0.69g/cm^3.

3.4.3 Board properties testing

Specimens for flexure test, screw withdrawal (SWR) resistance test, thickness swelling (TS) test, internal bonding (IB) test were prepared and tested according to ASTM standard D1037-06a. All mechanical tests were carried out on the Sintech 30/D machine using the TestWorks testing control system.

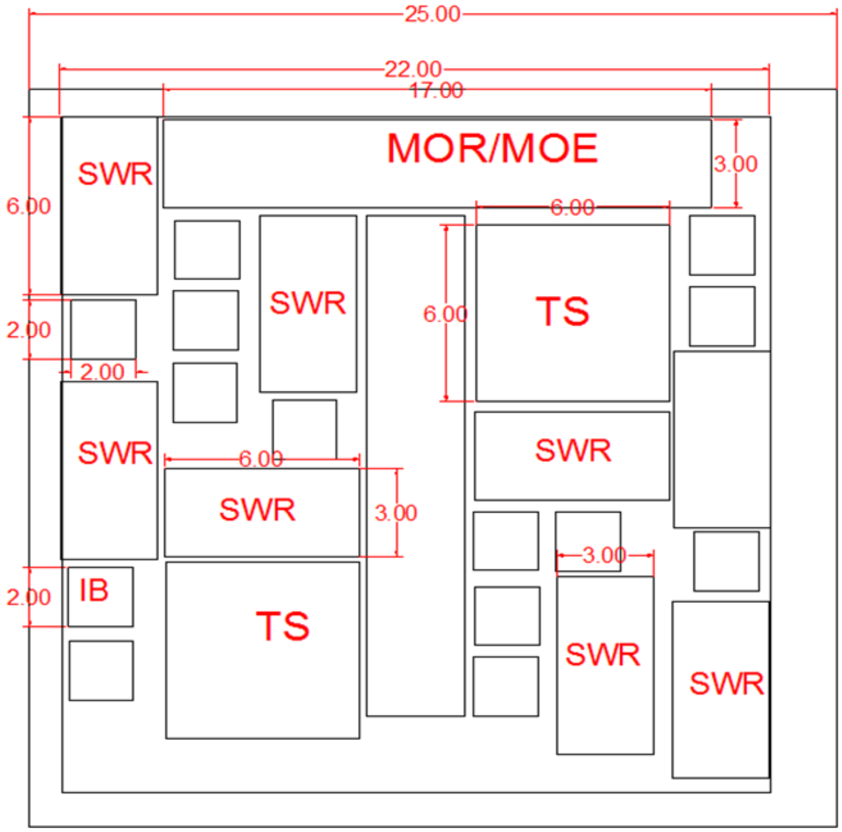

Figure 3.4: Cutting pattern of 25" by 25" particle board

For the static bending test, the width and thickness of the samples were measured for calculation of MOR and MOE. The static bending tests were carried out in the center-point loading mode (Figure 3.5) with a 15" span between the two supporting bars. The load was applied to the sample mid-point at a rate of 0.3 in/min (determined according to the standard). The MOR was calculated as follows: and the MOE was decided by the thickness, width of the samples as well as the slope of the deflection curve.

$$\mathbf{MOR} = \frac{3P_{max}L}{2bd^2} \qquad (3.1)$$

$$\mathbf{MOE} = \frac{\mathbf{L^3}}{\mathbf{4bd^3}} \frac{\mathbf{\Delta P}}{\mathbf{\Delta y}} \qquad (3.\ 2)$$

where:

a = area under load-deflection curve to maximum load, lbf·in. (N·m),

b = width of specimen measured in dry condition, in. (mm),

d = thickness (depth) of specimen measured in dry condition, in. (mm),

L= length of span, in. (mm),

MOR= modulus of rupture, psi (kPa)

MOE = apparent modulus of elasticity, psi (kPa),

$\frac{\Delta P}{\Delta y}$ = slope of the straight line portion of the load- deflection curve. lbf/in. (N/mm),

P_{max} = maximum load, lbf (N),

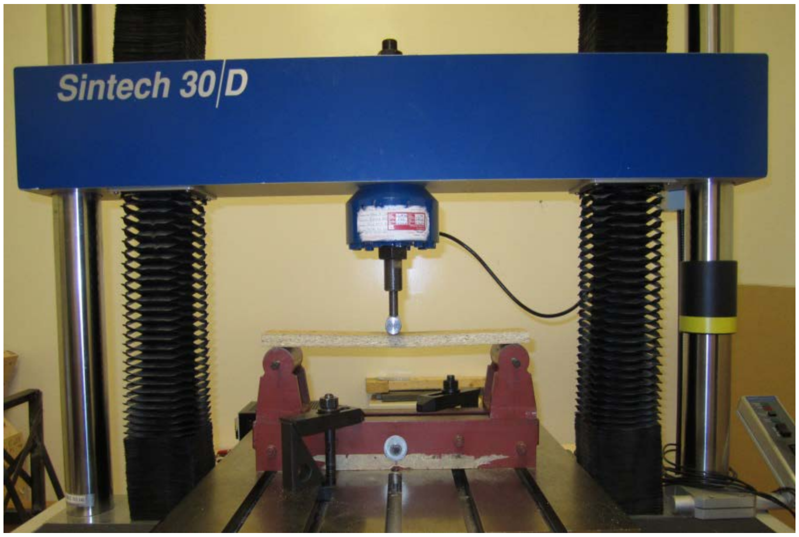

Figure 3.5: Apparatus of center-point loading flexural test.

For screw withdrawal testing, the screws were supplied by Pro-Fasten Inc., measuring 0.138±0.0003 in. in root diameter and 1 inch in length, with a thread pitch of 16 threads per inch. A 2/3 inch deep lead-hole was drilled into the center of the specimen's edge surface using an 1/8-inch drill bit. Samples were tested the same day that the screws were inserted. The testing machine (Sintech 30/D Test System) was assembled for SWR testing as shown in Figure 3.6. The specimen was fitted into the holder, and tensile force applied to the screw at a rate of 0.06 in./min and the maximum force in N was recorded by the system. 8 specimens were tested per board for a total of 24 per treatment.

Figure 3.6: The assembly for edge screw withdrawal test

For the IB tests, specimens were first glued to aluminum blocks on both surfaces using hot melt glue and the samples then placed in the test jig in the load-frame (Figure 3.7). A tension load was applied perpendicular to the specimen surface at a uniform rate of 0.05 in/min until failure occurred. The maximum load for every specimen was recorded and then divided by the sample's cross section area 2" by 2" (which is 50.8mm by 50.8mm). IB test values for treatments were the average of 14 specimens per board or 42 samples per treatment. If failure of the IB specimen occurred at the adhesive layer between the block and sample, the record was discarded

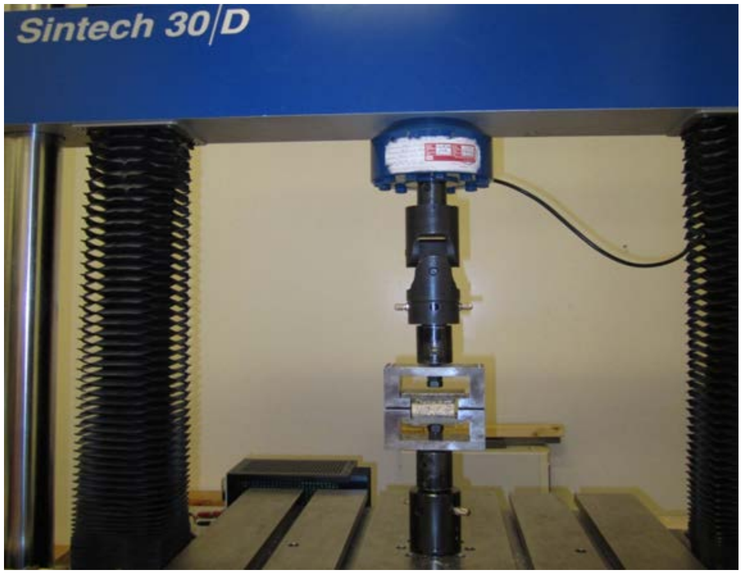

Figure 3.7: The assembly of internal bonding (IB) test

For Thickness Swell/Water Absorption (TS/WA) tests, the mass and four midway thicknesses of each specimen were measured prior immersion in water. Samples were submerged horizontally into the 20˚C water for 24h, and held at a distance of 1inch below the water level (Figure 3.8), leaving sufficient space for sample swelling. After 24h continual submersion, samples were removed from the water and drained for 5 min to remove the residual water on the surface, and the weight and thicknesses at the same four points were measured immediately. Two specimens were tested per board for a total of six per treatment.

Figure 3.8: Thickness swell samples in the tank.

Thickness swell (TS) and water absorption (WA) are calculated following the ASTM standards 1037-06a, as follows

$$\mathbf{WA}(\%) = \frac{(\mathbf{m_t} - \mathbf{m_0})}{\mathbf{m_o}} \times \mathbf{100} \qquad (3.\ 3)$$

where m_t is the mass of the sample after immersion (g) and m_0 is the mass of the sample before immersion.

$$\mathbf{TS}(\%) = \frac{(\boldsymbol{\delta}_\mathbf{t} - \boldsymbol{\delta}_\mathbf{0})}{\boldsymbol{\delta}_\mathbf{o}} \times \mathbf{100} \qquad (3.\ 4)$$

where δ_t and δ_0 are the sample thicknesses (mm) after and before the water immersion, respectively.

4 Results and discussion

4.1 XRD analysis

X-Ray diffraction is useful for evaluating the degree of clay dispersion in polymer matrices (Ray and Okamoto, 2003). The result of an XRD test is a pattern of X-ray intensity vs the diffraction angle. The distance between the clay layers (d-spacing) can be determined from Bragg's law if the diffraction angle which corresponds to the intensity peak is known. The mean d-spacings are listed in Table 4.1.

Typical XRD patterns of pure nanoclay and the nanoclay in the cured resin matrix are given in Figure 4.1 to Figure 4. 8. Due to the difficulty of computing a mean distribution, the replicate response closest to the mean is shown in the figure; to identify those figures where this was done, those figure captions begin with the word "typical". The intensity peaks of Cloisite30B disappeared after being dispersed into the UF resin by mechanical mixing. With the addition of a coupling agent, there is also no intensity peak for Cloisite30B. At higher loading (6%) of Cloisite30B, the intensity peak also disappeared, indicating its exfoliation into the UF resin (Figure 4.1). MF resin containing Cloisite30B had no intensity peak for any of the three clay loading levels.

The d-space of Nanofil116 in UF resin increased (Figure 4.3, Figure 4.4), which appears in the pattern as the intensity peak of Nanofil116 shifting to a lower 2θ, indicating that the unmodified Nanofil116 were all intercalated with UF resin. The intensity and location of the peak for the clay mix was not changed by clay loading.

The intensity peak for Nanofil116-MF mix also appeared at a lower 2θ (Figure 4.7). Adding coupling agent, the intensity peak appeared almost at the same 2θ (Figure 4.8). Higher clay concentration resulted in a higher intensity peak. MF resin was also able to enter the interlayer space of Naonofill116.

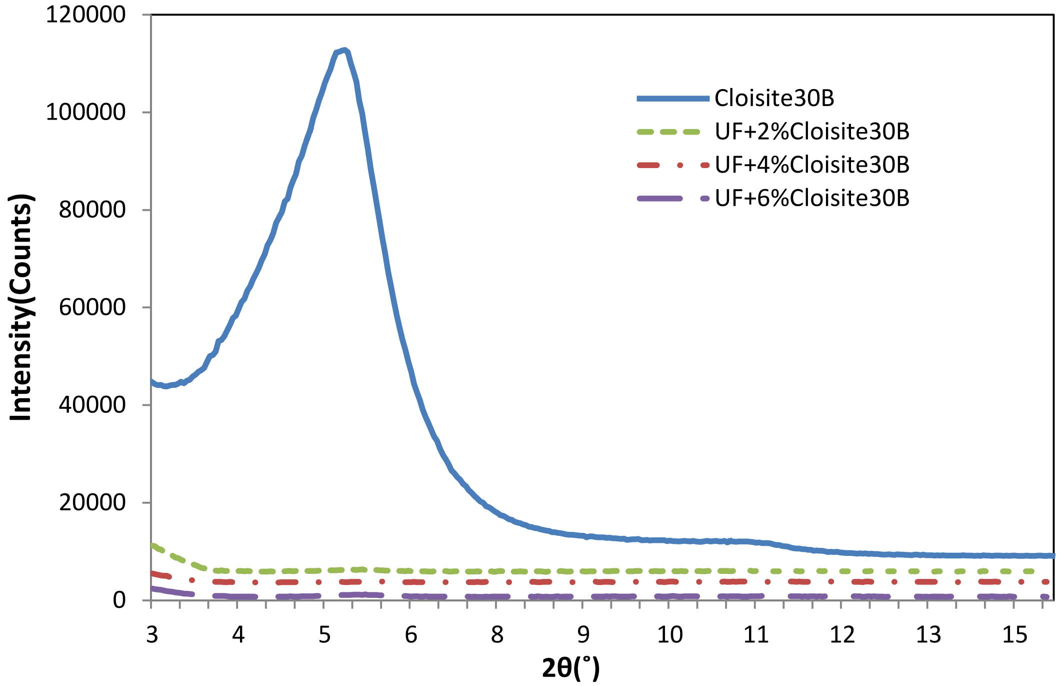

Figure 4.1: Typical XRD patterns of Cloisite30B, Cloisite30B + UF resin.

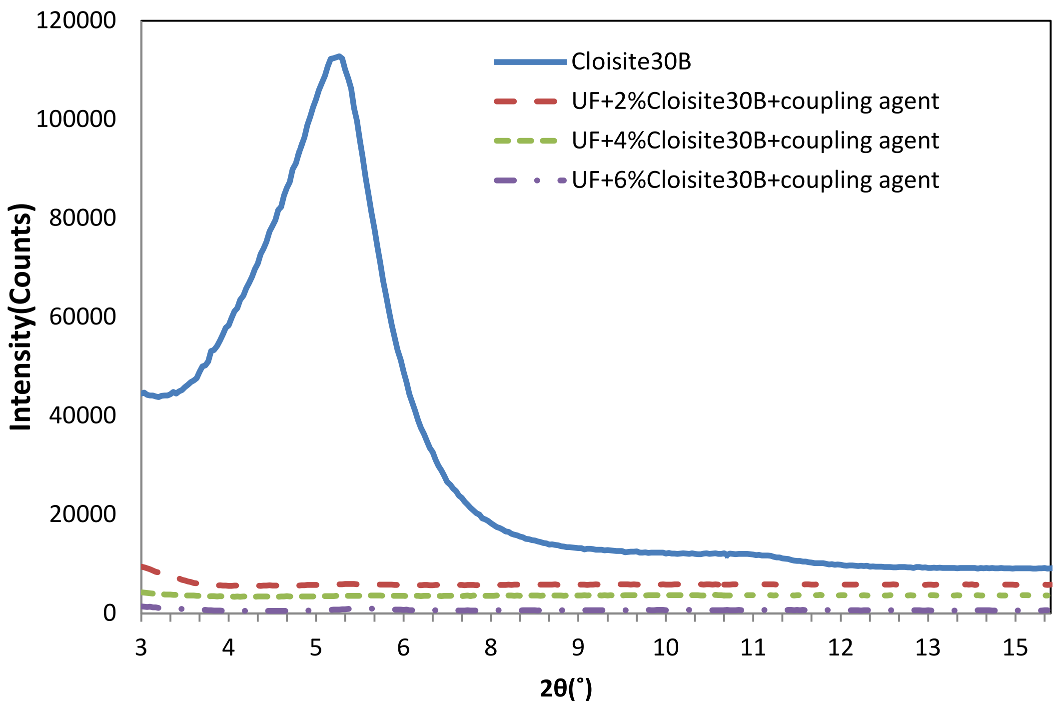

Figure 4.2: Typical XRD patterns of Cloisite30B, Cloisite30B and coupling agent + UF resin.

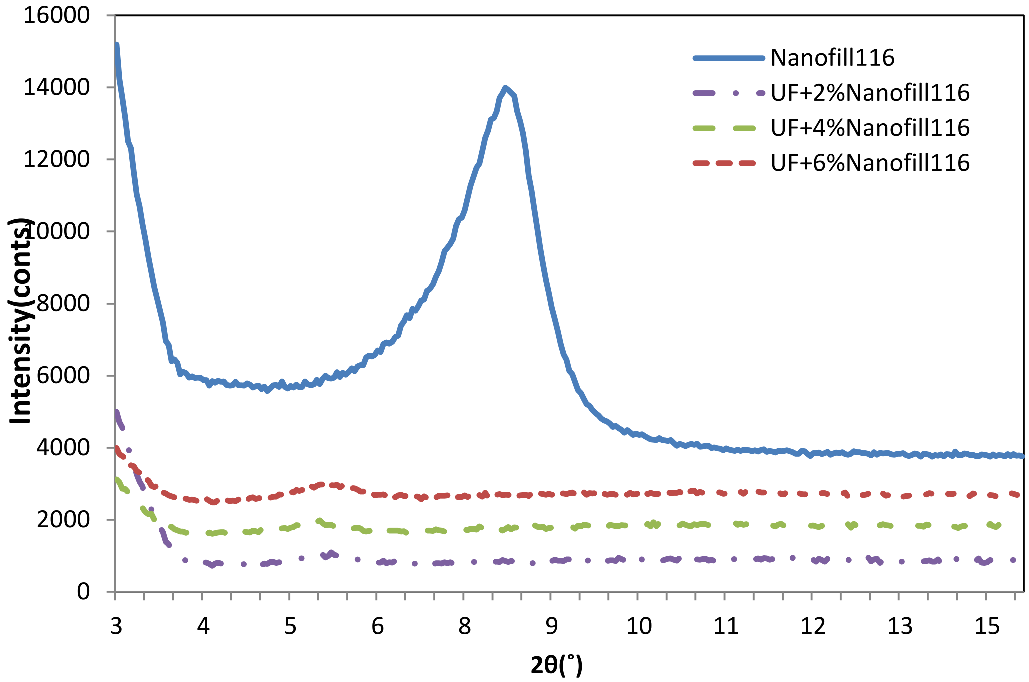

Figure 4.3: Typical XRD patterns of Nanofil116 and Nanofil116 + UF resin.

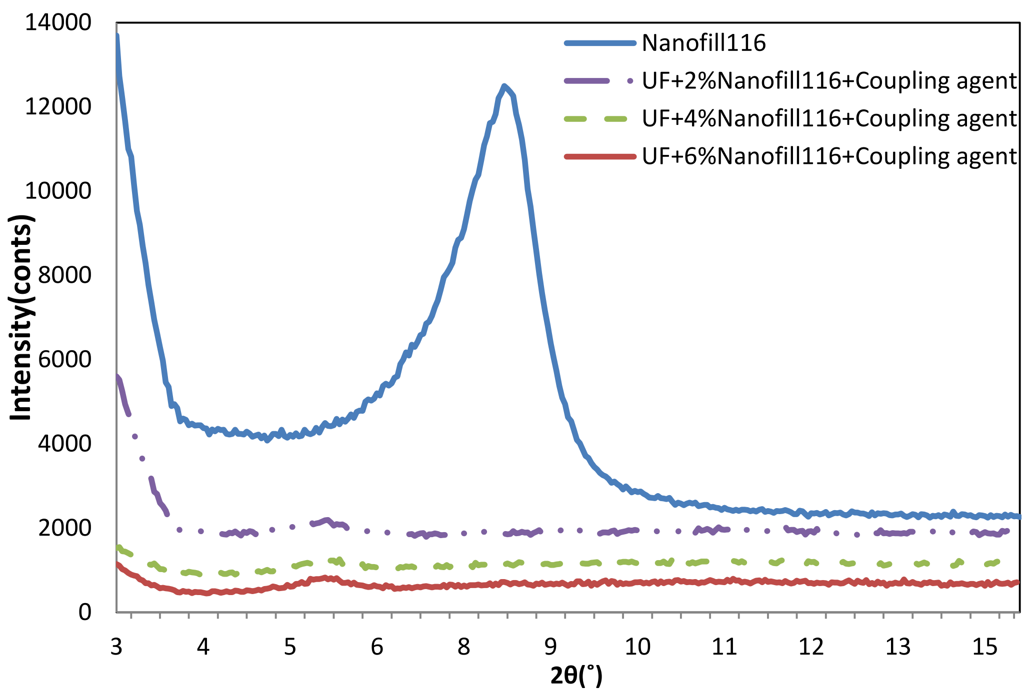

Figure 4.4: Typical XRD patterns of Nanofil116, Nanofil116 and coupling agent + UF resin.

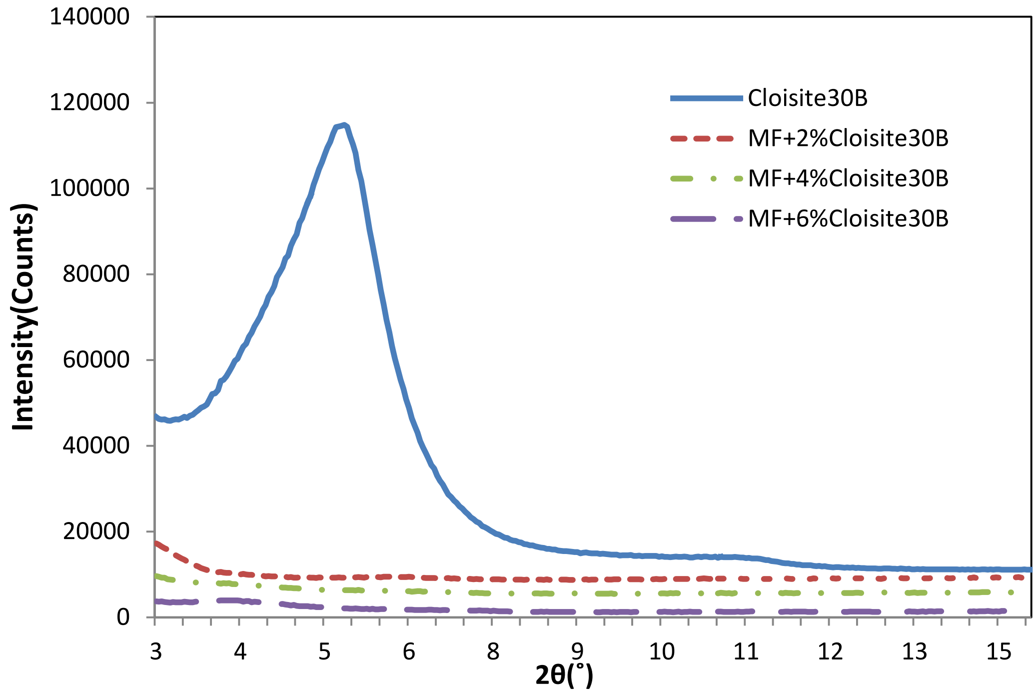

Figure 4.5: Typical XRD patterns of Cloisite30B, Cloisite30B + MF resin.

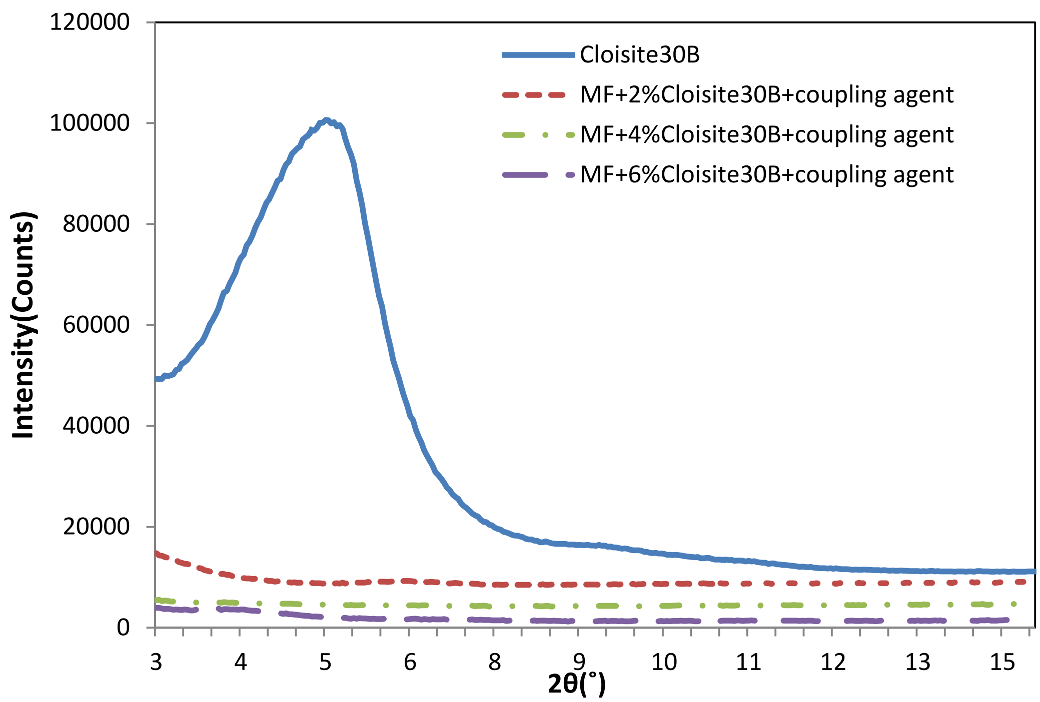

Figure 4.6: Typical XRD patterns of Cloisite30B, Cloisite30B and coupling agent +MF resin.

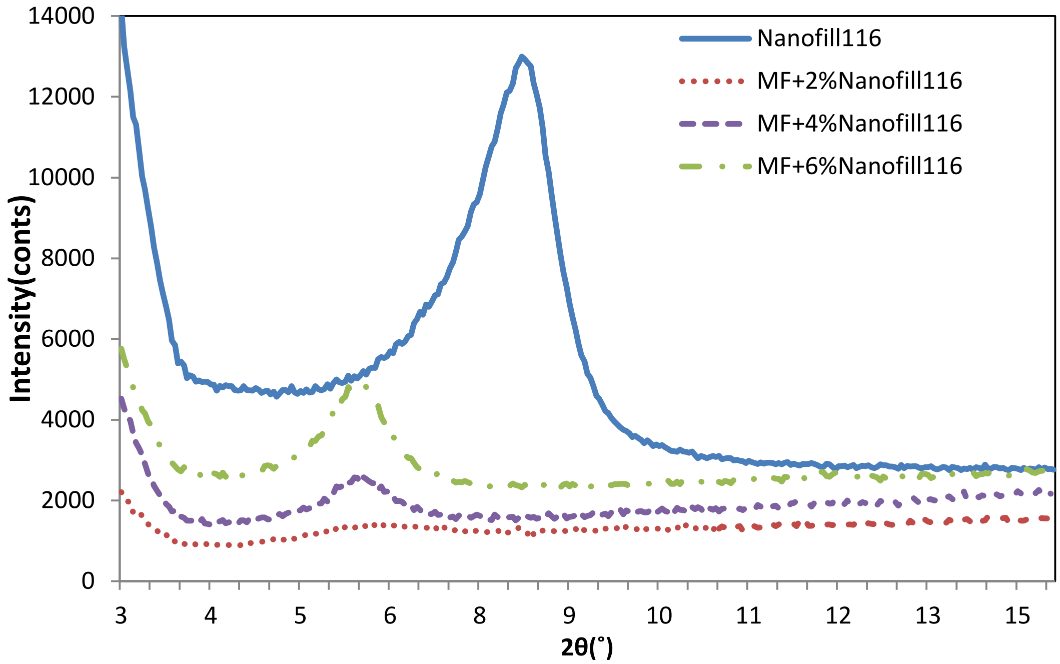

Figure 4.7: Typical XRD patterns of Nanofil116, Nanofil116 + MF resin.

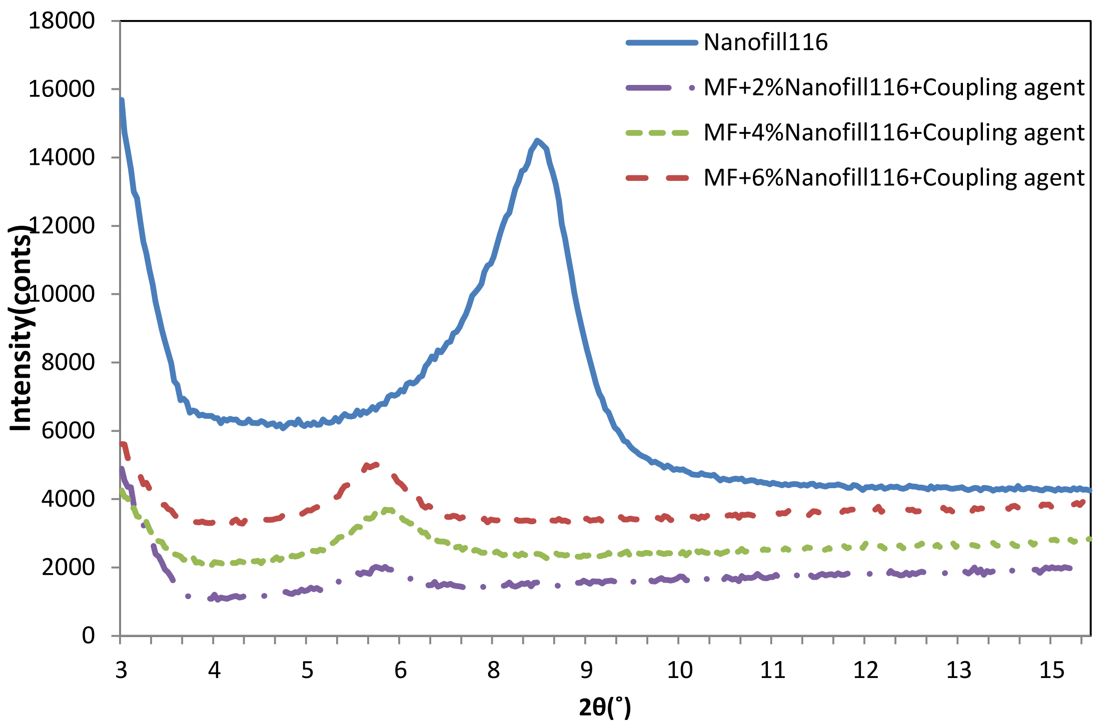

Figure 4.8: Typical XRD patterns of Nanofil116, Nanofil116 and coupling agent + MF resin.

The coupling agent has one end compatible with the polymer and the other end reacts/interacts or glues better to the filler; it is supposed to have similar effects as the organic modifier, helping extend distance between the clay platelets (Han *et al.*, 2008). The addition of the coupling agent did not show significant effects on the XRD patterns, i.e. the separation of clay platelets. The intensity peak positions were almost at the same 2θ for Nanofil116 + resin and the Nanofil116 + resin + coupling agent. The coupling agent did not aid the separation of unmodified clay either, ie the intensity peak did not shift to a lower 2θ with the addition of coupling agent.

The d-spacing of Nanofil116 was larger in UF resin than that in MF, and the intensity peak in of Nanofil116 + MF mixes was lower than that of the Nanofil116 + UF. This may be because the monomers of UF resin are smaller than those of MF resin and can therefore more easily enter the interstitial spaces between the clay platelets resulting in enhanced separation. The XRD results showed that the mechanical mixing method was able to exfoliate the organic-modified nanoclay Cloisite30B into both UF and MF resin, and enlarged the interlayer spacing of unmodified clay when it was dispersed into UF and MF resin.

Table 4.1: 2 θ and d-space values from XRD patterns (Some of the samples had no intensity peak and this is denoted by the 'np' entry in the table).

Clay or clay added resins	**2θ(˚)**	**d-space(A)**
Cloisite30B	6.226	16.663
UF+ 2%Cloisite30B	np	np
UF+ 4%Cloisite30B	np	np
UF+ 6%Cloisite30B	np	np
UF+ 4%Cloisite30B+Coupling agent	np	np
UF+ 6%Cloisite30B+Coupling agent	np	np
UF+ 6%Cloisite30B+Coupling agent	np	np
MF+ 2%Cloisite30B	np	np
MF+ 4%Cloisite30B	np	np
MF+ 6%Cloisite30B	np	np
MF+ 4%Cloisite30B+Coupling agent	np	np
MF+ 6%Cloisite30B+Coupling agent	np	np
MF+ 2%Cloisite30B+Coupling agent	np	np
Nanofil116	8.155	12.579
UF+ 2% Nanofil116	5.844	17.546
UF+ 4% Nanofil116	5.799	17.682
UF+ 6% Nanofil116	5.833	17.579
UF+ 2% Nanofil116+Coupling agent	5.869	17.489
UF+ 4% Nanofil116+Coupling agent	5.886	17.421
UF+ 6% Nanofil116+Coupling agent	5.702	17.983
MF+ 2% Nanofil116	6.076	16.877
MF+ 4% Nanofil116	6.101	16.809
MF+ 6% Nanofil116	6.276	16.342
MF+ 2% Nanofil116+Coupling agent	6.152	16.668
MF+ 4% Nanofil116+Coupling agent	6.243	16.425
MF+ 6% Nanofil116+Coupling agent	6.188	16.342

4.2 DSC analysis of the curing process

The curing of a thermosetting resin such as UF and MF is an irreversible exothermic reaction which shows an exothermic peak in the DSC curve. The enthalpy of transition (ΔH) based on peak area and the peak temperature (T_{peak}) is the point at which the reaction rate is the fastest (Ton-That, *et al.*, 2004). In this work, all of the liquid resins and resin-clay mixes were heated from B-stage monomers and cured in an amorphous state. Glass transition was observed in all of the curing processes for all resins and was not affected by nanoclay addition.

The mean test values were listed in Table 4.2. In order to get a representative comparison of each treatment, the response curves closest to the mean value were used. To signify this to readers, the word “Typical” has been placed at the beginning of each figure caption.

Adding Cloisite30B to UF resin had little effect on ΔH and onset temperature compared with pure UF. Adding nanoclay means that the peak temperature was slightly delayed, and with a higher curing temperature (Figure 4.9 to Figure 4.12). Similar results were obtained when coupling agent and Cloiste30B applied together.

The onset temperature and the peak temperature of UF resins increased also when Nanofil116 was added, which means the presence of clay delayed the curing reaction. As the clay loading increased, the area under the curing peak decreased (Table 4.2). ΔH decreased significantly as the clay content increased, and this effect was further exacerbated when coupling agent was also added. These suggest that Nanofil116 negatively affected curing and decreased the crosslinking density of UF resin network.

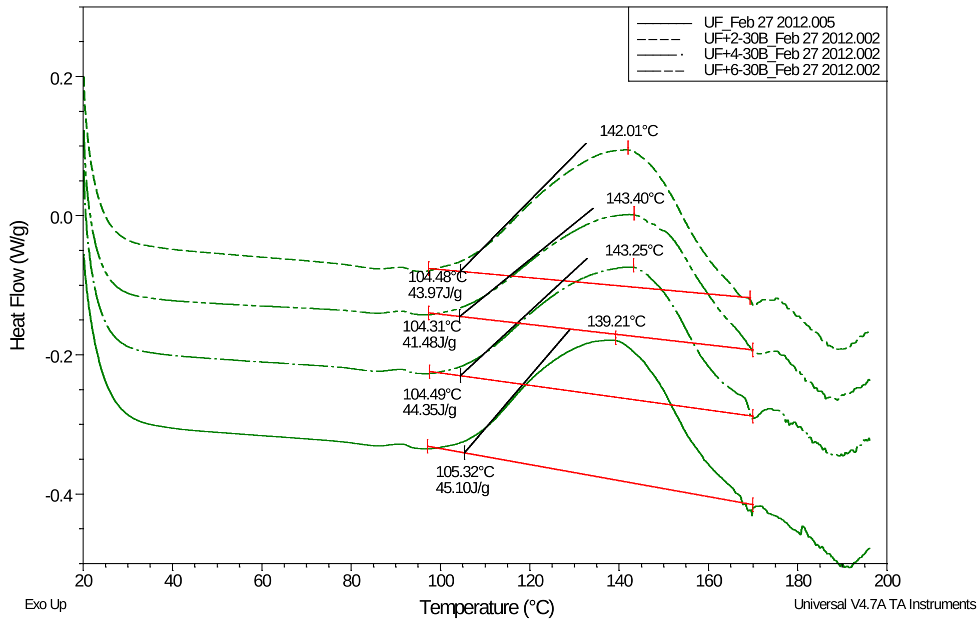

Figure 4.9: Typical heat flow curves of different UF resins with different loading of Closiste30B.

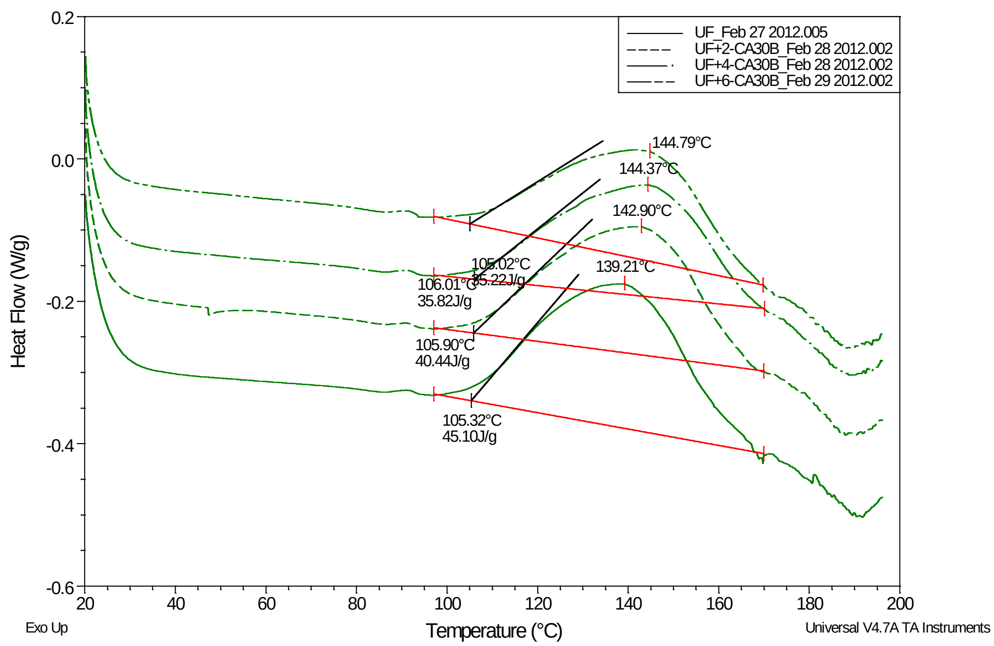

Figure 4.10: Typical heat flow curves of different UF resins with different loading of Closiste30B and coupling agent.

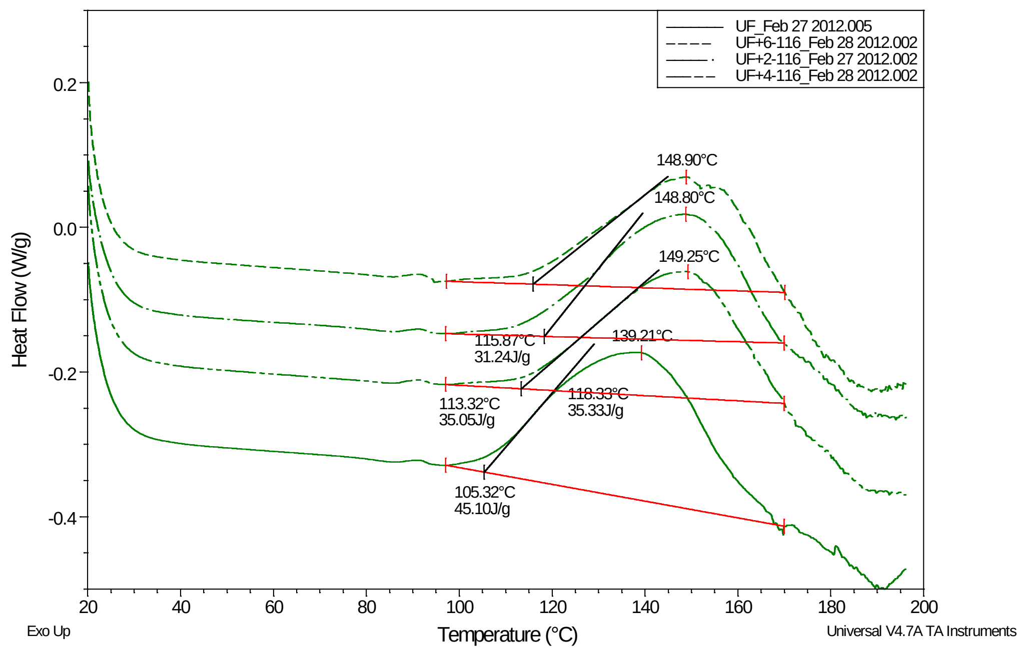

Figure 4.11: Typical heat flow curves of different UF resins with different loading of Nanofil116.

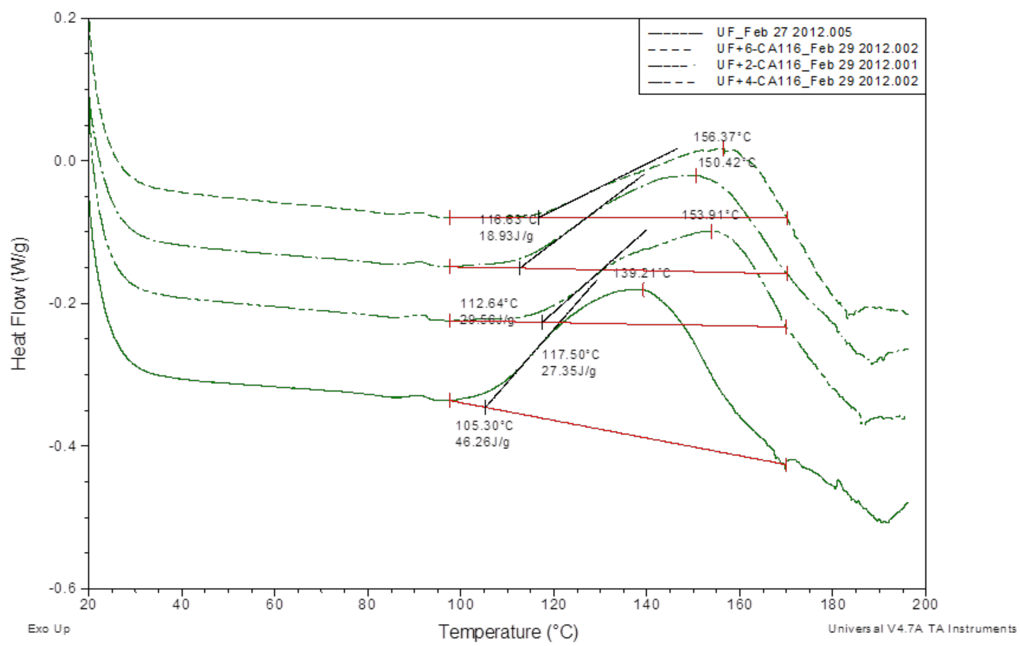

Figure 4.12: Typical heat flow curves of different UF resins with different loading of Nanofil116 and coupling agent.

For the MF resin (Figures 4. 13 to 4. 16) the onset temperature of pure MF resin is around 125 ˚C and curing peak temperature is around 147˚C. In contrast to the UF resin, adding Cloisite30B at different loadings did not change the ΔH, or the onset and peak temperatures. However using a coupling agent as well had a deleterious effect on the curing of the clay-resin mixes. The ΔH of the MF resin containing Cloisite30B and coupling agent was decreased compared to the pure MF, which means less reaction heat had been generated by this mix.

Nanofil116 decreased the ΔH of MF resin and delayed the curing temperature. Increasing clay concentration led to a lower ΔH and higher peak temperature, and the effect was further exacerbated by the addition of coupling agent.

The organic modifier of Cloisite30B is hydrophilic and likely to interact with the resin monomers (Giannelis, 1996). This interaction may not be as strong as the bonding of the resin so it slightly decreased the curing. While the unmodified clay Nanofil116 found it difficult to interact with the resin and probably blocked the connection of the resin network. The use of coupling agent may further extent the gaps between original resin chain connection therefore it further reduced the curing reaction heat (Table 4. 2) (The Tukey analysis of the treatments are listed in Appendix A pages 87-94).

In summary, low loading of Cloisite30B 2% 30B did not have a strong effect on the curing reactions of UF resin and MF resin. Higher concentrations of Cloisiste30B and the presence of coupling agent adversely affected the curing of both resin types. The Nanofil116 significantly reduced the reaction heat and delayed the curing reaction of both resin types, and the addition of coupling agent further compounded this effect.

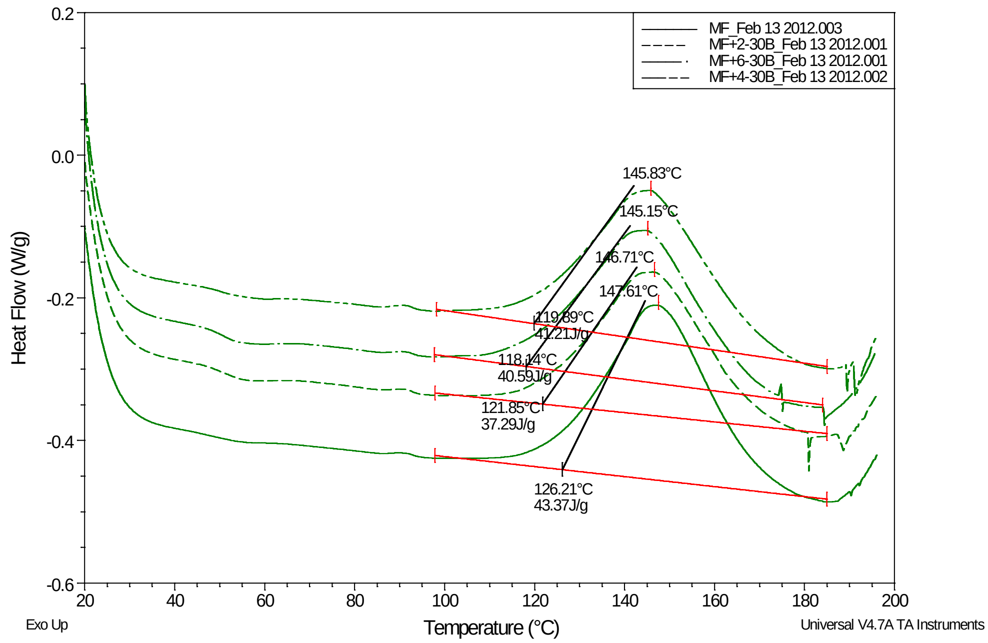

Figure 4.13: Typical heat flow curves of different MF resins with different loading of Closiste30B.

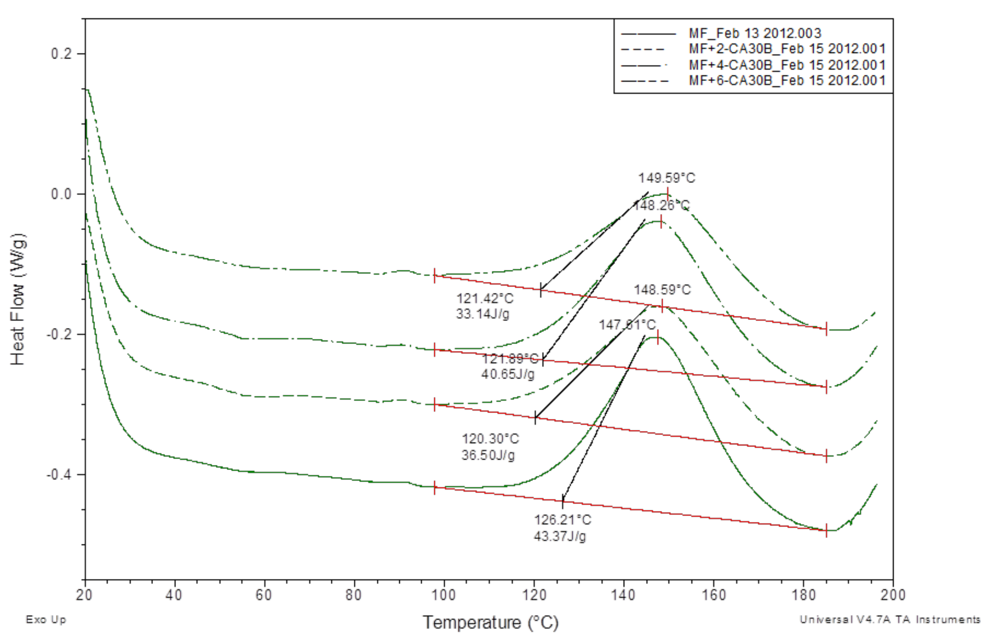

Figure 4.14: Typical heat flow curves of different MF resins with different loading of Closiste30B and coupling agent.

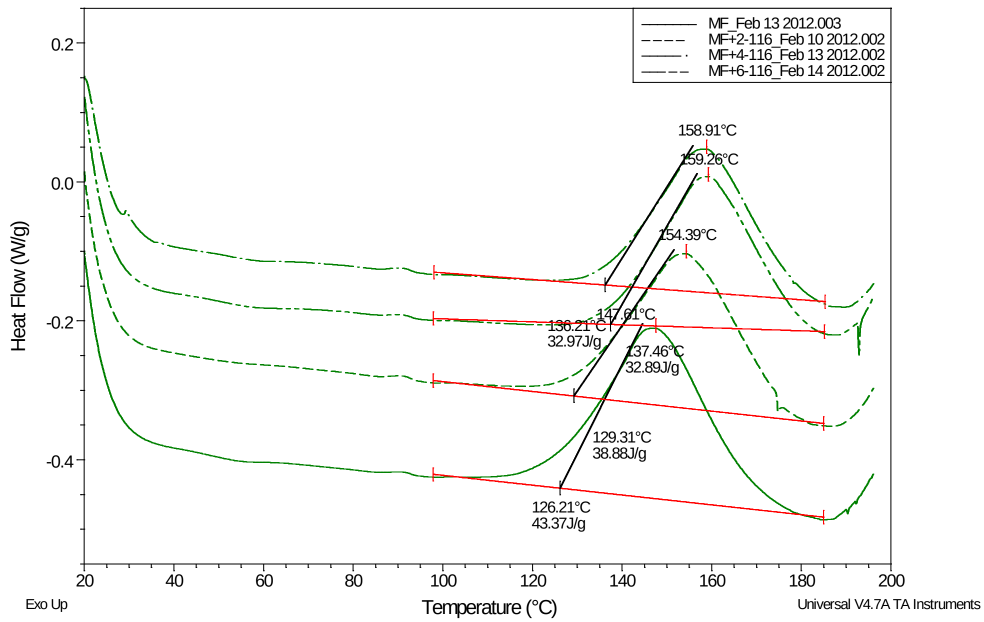

Figure 4.15: Typical heat flow curves of different MF resins with different loading of Nanofil116.

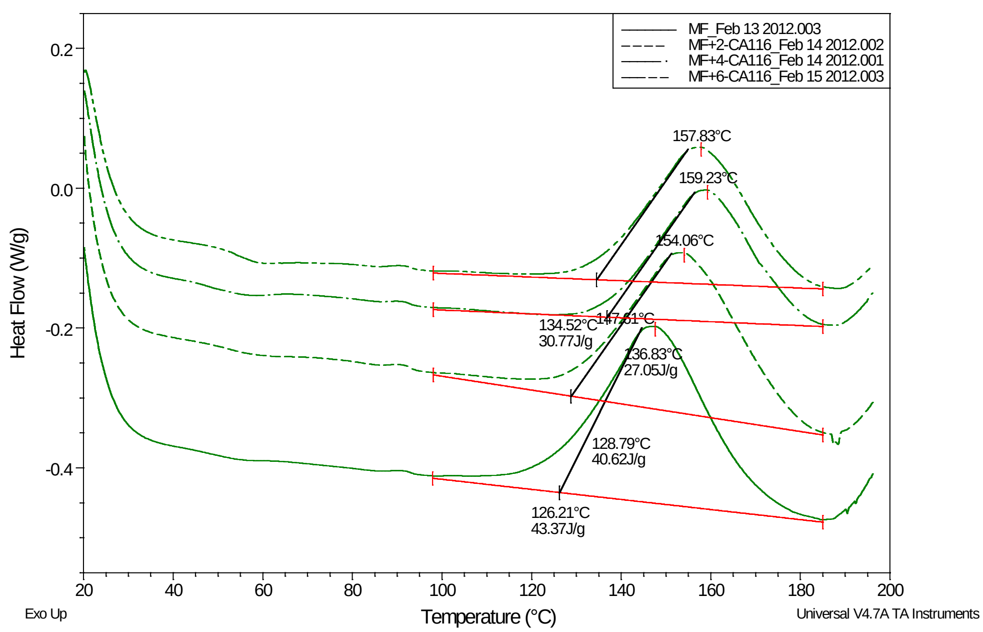

Figure 4.16: Typical heat flow curves of different MF resins with different loading of Nanofil116 and coupling agent.

Table 4.2: Mean values of 3 measurements for T_{onset}, ΔH, T_{peak}

Resins	Onset Temperature T_{onset} (˚C)	ΔH(J/g)	Peak Temperature T_{peak} (˚C)
UF	105.28	43.82	139.49
UF+2%30B	104.91	42.75	142.43
UF+4%30B	104.84	41.11	142.58
UF+6%30B	104.21	42.17	144.32
UF+2%30B Coupling agent	105.73	41.06	142.49
UF+4%30B Coupling agent	106.03	38.99	144.43
UF+6%30B Coupling agent	106.33	38.57	144.13
UF+2%116	114.06	36.29	150.40
UF+4%116	116.07	34.68	148.27
UF+6%116	115.13	33.83	147.70
UF+2%116 Coupling agent	112.68	28.72	150.73
UF+4%116 Coupling agent	115.18	28.12	154.99
UF+6%116 Coupling agent	119.44	19.28	154.43
MF	124.15	42.46	146.91
MF+2%30B	119.19	38.47	121.10
MF+4%30B	121.10	37.22	145.22
MF+6%30B	118.31	40.07	147.20
MF+2%30B Coupling agent	119.52	34.86	148.74
MF+4%30B Coupling agent	118.95	39.91	148.44
MF+6%30B Coupling agent	119.38	33.18	147.75
MF+2%116	130.53	36.57	154.35
MF+4%116	134.27	35.75	157.51
MF+6%116	137.92	32.39	159.61
MF+2%116 Coupling agent	130.05	37.55	153.62
MF+4%116 Coupling agent	137.17	30.90	159.23
MF+6%116 Coupling agent	134.82	26.43	158.07

4.3 DMA Test

Usually, DMA tests are used to detect the glass transition temperature of thermoplastics and their composites. However, the glass transition temperature (T_g) of thermosetting resins depends on the degree of curing of the resin (Louis *et al*., 2010, Hon 2003). Therefore, in this study, T_g is not used as the basis for quantifying and comparing the resins. Instead, the DMA test was used to study the curing process and compare the final rigidity of thermosetting resins and clay mixtures. Also, the results presented in the figures are typical curves from replicates for representative comparison.

The storage modulus increased as temperature increased, and the difference between the maximum and minimum E' (ΔE') represents the rigidity of the resin network (He and Riedl, 2003; Park and Kim, 2008). The minimum point is the gel point of the resin, which marks the onset of curing. For UF resin, E' decreased at first as the temperature increased, because of the softening of the pre cured UF resin. Once the storage modulus reaches the minimum point, it increases again before reaching its maximum value as the polymerization reaction continues, forming a cross-linked molecular network (Kim *et al*., 2006). The storage modulus increased during the curing process and reached the maximum value when the curing reaction was complete.

The UF resins containing Nanoclay and coupling agent had a higher ΔE' than the control resin alone and nanoclay + UF resin mixtures (Figure 4.17), indicating that their rigidity was higher than that of pure UF resins. The storage modulus of Nanofil116 + UF resin mix was higher than Cloisite30B + UF, and this might be because the Nanofil116 intercalated with UF and Closisite30B exfoliated in UF. The intercalated structure resulted in a stiffer UF resin than the exfoliated structure did. ΔE' of pure UF resin was lower than the other resin - clay mixes, which means it was less rigid.

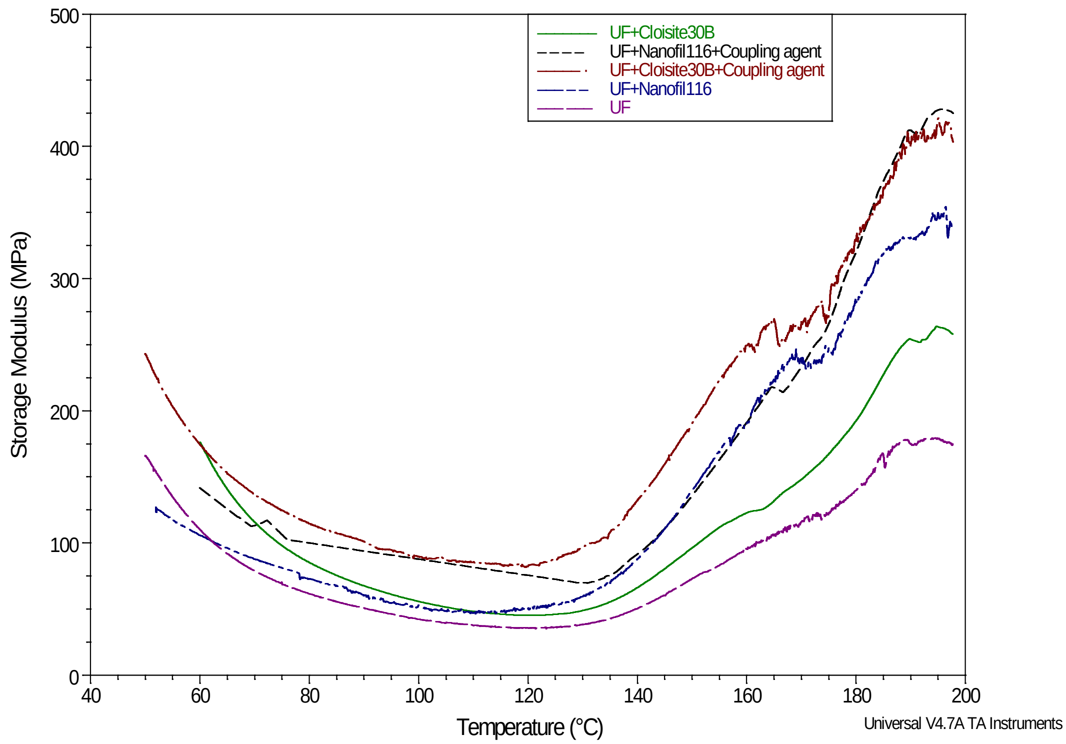

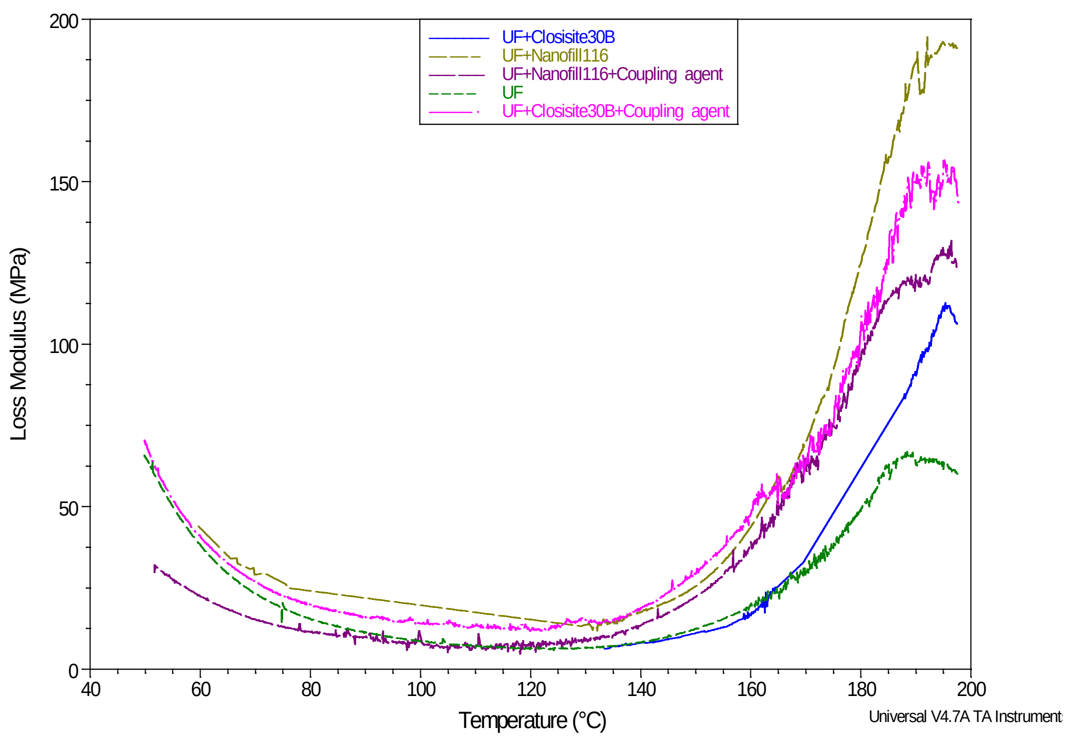

Figure 4.17: Typical storage modulus and loss modulus of UF resin and clay added UF resins.

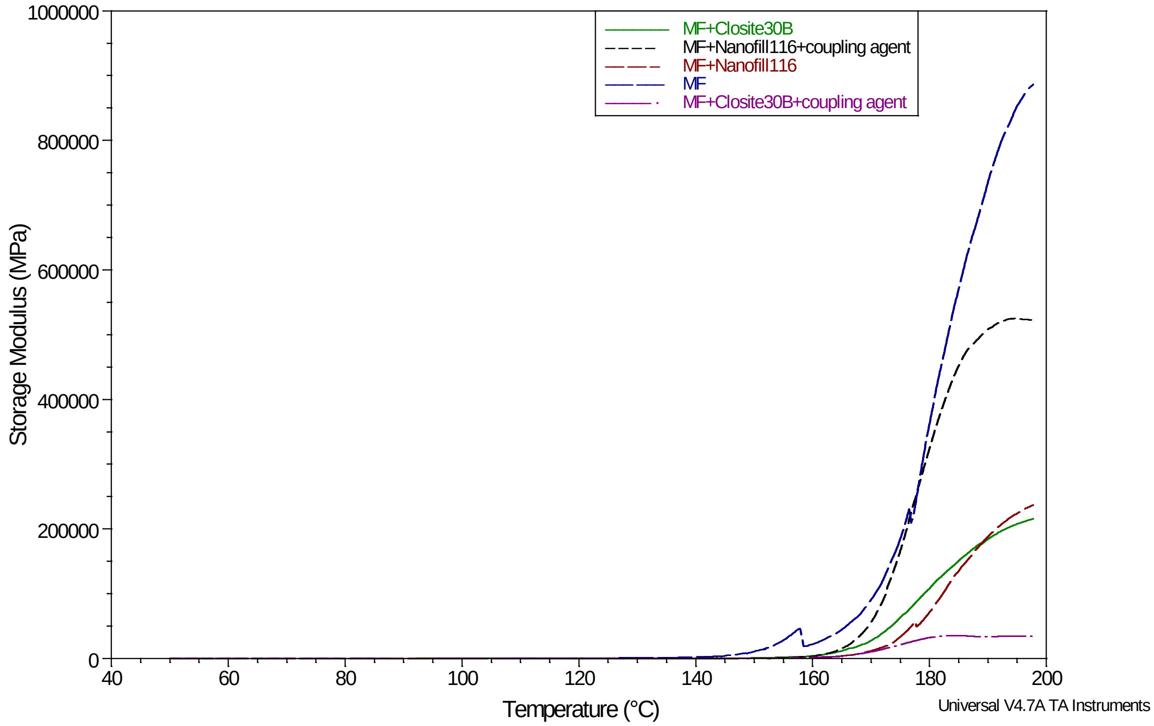

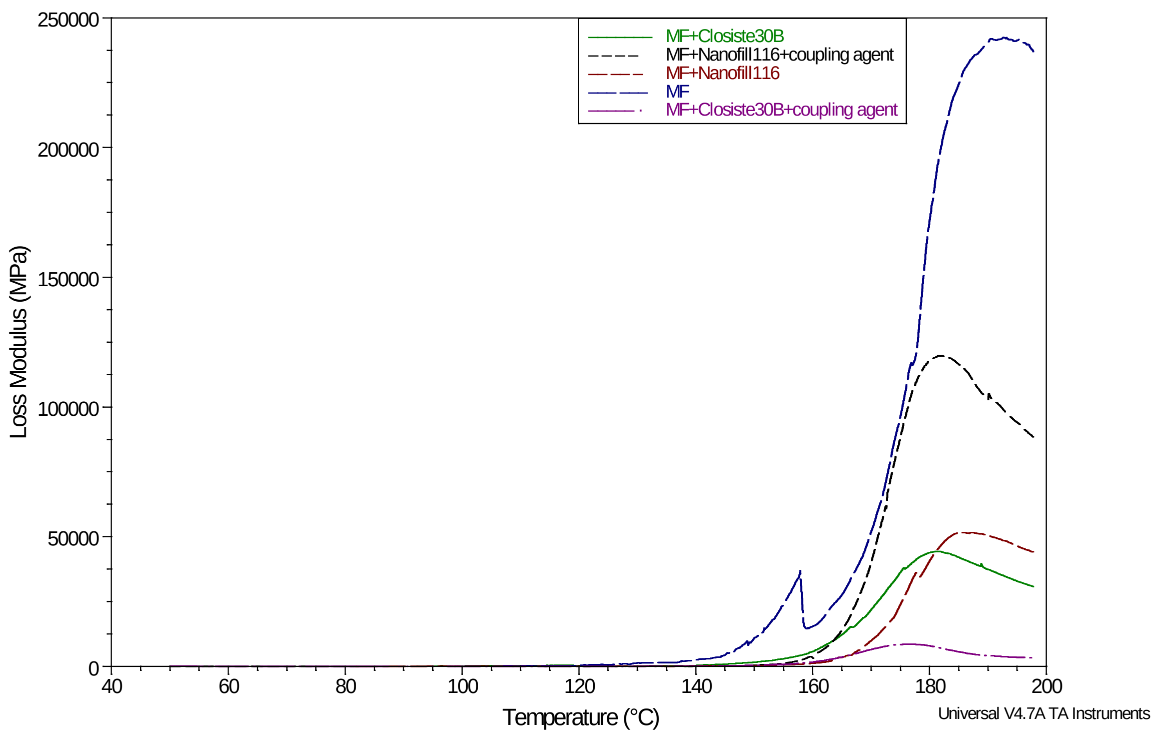

Figure 4.18: Typical storage modulus and loss modulus of MF resin and clay added MF resins.

For the MF resin, the storage modulus did not show a sharp increase until 160˚C, which also indicates curing of resin and increasing rigidity. Storage modulus of clay + MF resin mixes increased at a higher temperature of 170˚C which also indicates a delay of curing. In contrast to the UF resin, the storage modulus of pure MF resin was higher than all of the clay+ MF mixtures, which indicates rigidity and lower crosslinking density in resin containing clay. 30B+MF mixes had a lower ΔE' than the 116 + MF mixes, further indicating that the exfoliated organic clay results in more gaps and a more loose resin network connection than unmodified clay did. 30B+coupling agent had the lowest E' and it is likely that the coupling agent further exacerbated the extent of gaps between the resin network and further reduced cross-linking.

The storage modulus (E') of MF resin was much higher than that of UF resin due to the higher crosslink density and greater rigidity of the MF structure, as mentioned earlier. It might also be because the original resin network of urea is lower than the ring structure of melamine (Kim, Sumin 2006). The density and stiffness of pure MF resin is among the highest of the thermoset resins, and several attempts have been made to improve the chain flexibility to provide a more flexible structure and reduce material cost. (Dolye M, *et al.*, 2003). Our results show that the addition of clay and coupling agent can slightly increase the rigidity of UF resin, but have the potential to decrease the high crosslinking density of pure MF resin, improving its flexibility.

4.4 Lap-shear test - automatic bonding evaluation system (ABES) approach

The average lap-shear strengths for each resin and resin-clay mix are shown in Figure 4.19 and Figure 4.20. The average shear strength of glue lines bonded with nanoclay/resin mixtures were slightly lower than those of pure UF resin. Bond strength was further reduced with the addition of coupling agent. However, the treatments were not significantly different from the pure resin controls at p=0.05 (refer to Appendix B for Tukey analysis, page:103-105). For MF resin, most of the treatments had higher average shear strengths than pure MF resin except for the Cloisite30B treated MF resin. However these effects were not significant. The only significant difference at p=0.05 was between MF + Cloisite30B (low) and MF+116 with or without coupling agent. Adding coupling agent seems to have improved the bond strength of MF containing Cloisite30B.

UF resin has a loose resin network, adding nanoclays further reduced the connection of resin, therefore the shear strength decreased. The clay addition reduced the high crosslink MF resin network and likely acted as buffer for its brittle facture. That may be the reason for the slight improvement in shear strength. The lap-shear tests suggest that adding nanoclay to either UF or MF resin will not have a detrimental effect on its ability to bond wood elements. In the case of UF resin it may not even have a beneficial effect. The clay and MF resin treatments (MF+ 30B + coupling agent, MF+ 116, MF+ 30B + coupling agent) that yielded higher average shear strength values have the potential to improve particle board properties.

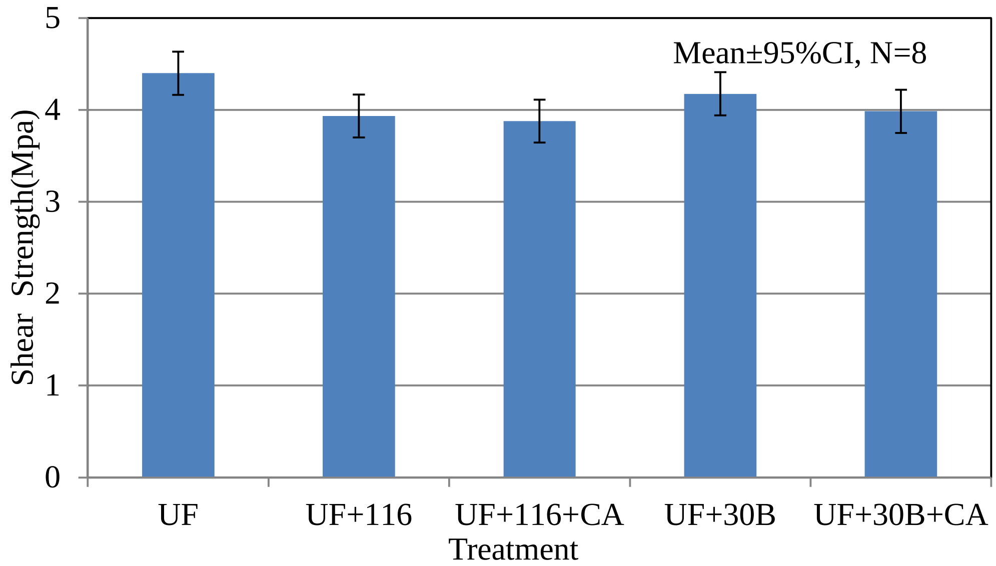

Figure 4.19: Shear strength of UF and clay added UF resins.

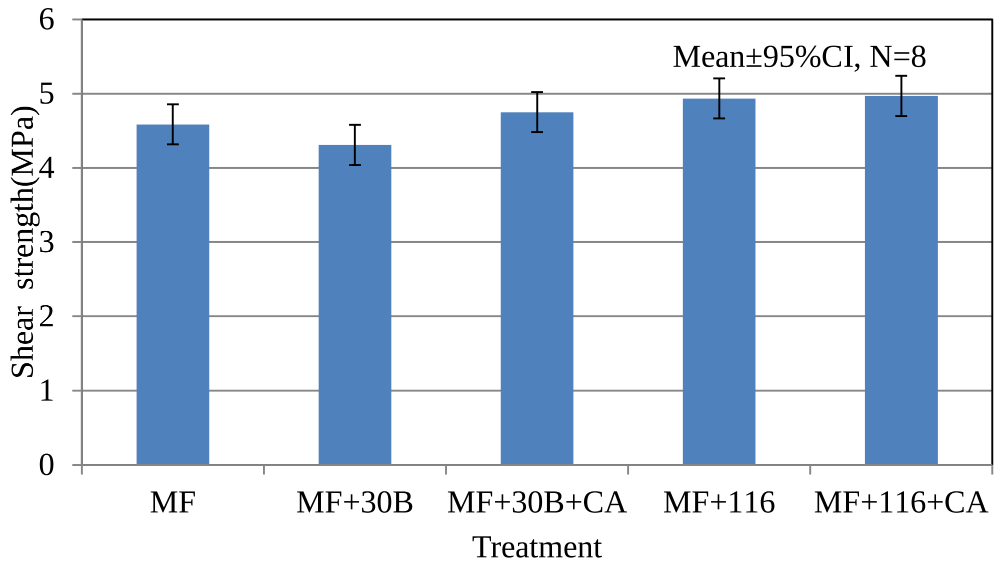

Figure 4.20: Shear strength of MF and clay added MF resins.

4.5 Particle board properties test results

Particleboard strength properties tests include MOR/MOE (Figure 4.21 and Figure 4.22), Edge SWR (Figure 4.23), Internal Bond (Figure 4.24), and Thickness Swell/Water Absorption (Figure 4.25). In the graphs, M0 denotes the control group, i.e. boards bonded with pure MF resin. 2bc, 4bc, 6bc, are the nanoclay treatments with 2%, 4%, 6% Colisite30B with coupling agent. “f” stands for Nanofil116, and “fc” denotes Nanofil116 with coupling agent. Mean values are shown for the specified number of test specimens (N) in the upper right corner of the graphs, and the error bars indicate the 95% confident interval (CI). All results were analyzed using the Tuke-Kramer pairwise means comparison test in SAS (See Appendix C pages:106-113), at a 5% significance level.

4.5.1 MOR/MOE test

As shown in Figure 4.21 and Figure 4.22, the variance within a group was large such that there were no significant different between treatments (Appendix C pages:106-107). The addition of Colisite30B with coupling agent or Nanofil116 only did not change the bending strength and elastic modulus greatly. In the treatments with Nanofil116 and coupling agent, higher clay loading decreased MOR and lower MOE. 6% Nanofil116 with coupling agent resulted in lower MOR than the control. When clay loading was higher than 4% clay, the average MOE was also lower than control. Therefore, the effect of nanclay on PB’s bending strength was minor or even negative.

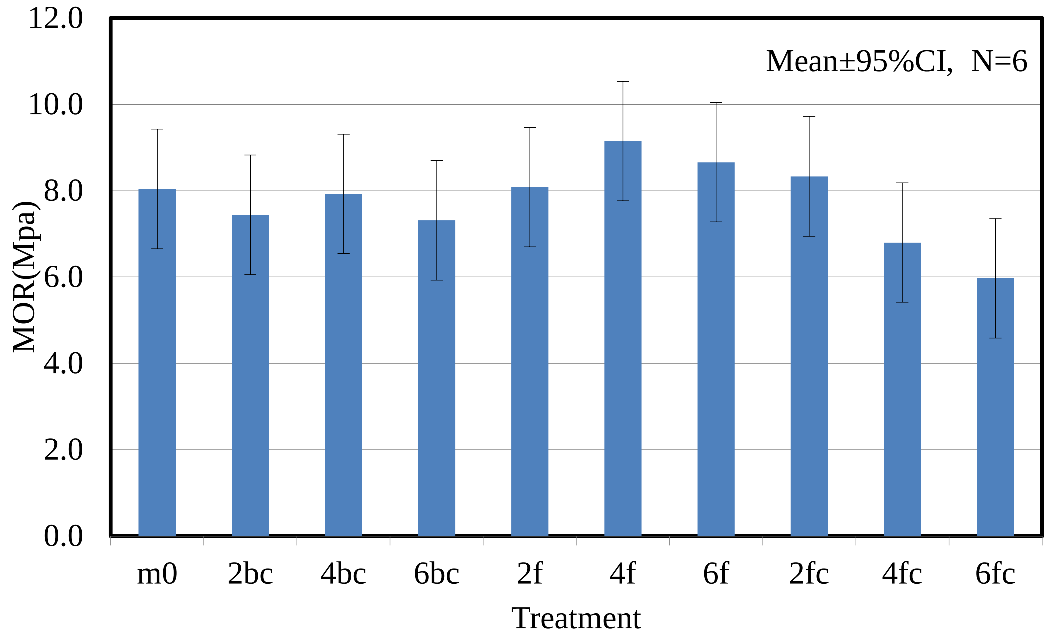

Figure 4.21: Average modulus of rupture for particleboards bonded with different MF resin + clay mixes.

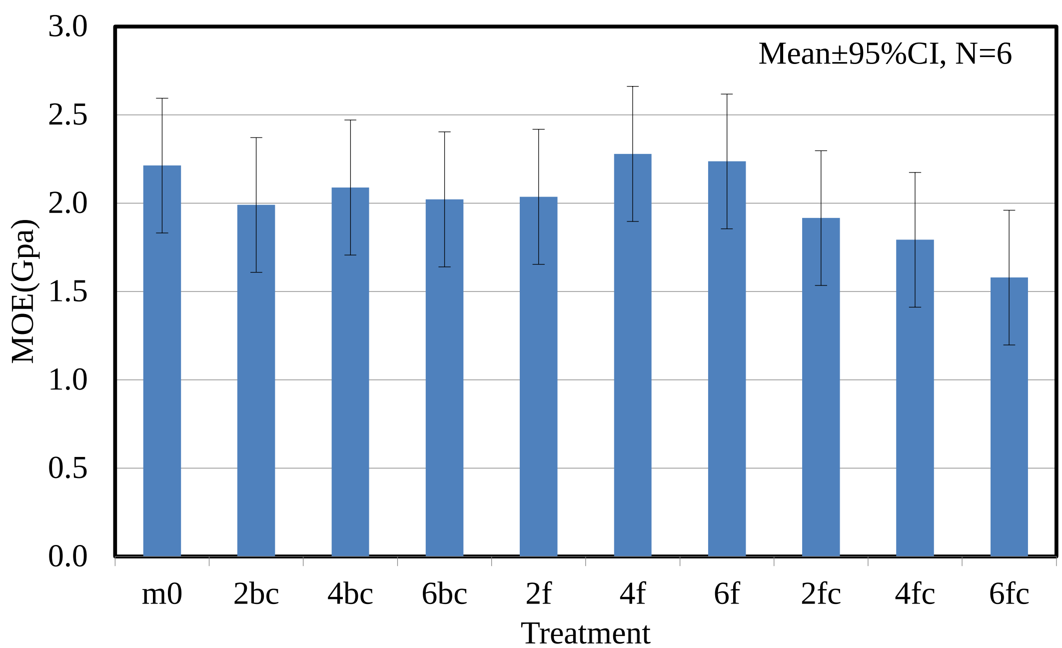

Figure 4.22: Average modulus of elasticity for particleboards bonded with different MF resin + clay mixes.

4.5.2 Edge screw withdrawal (SWR) test

SWR (Figure 4. 23), was largely unaffected by resin-clay mixes, except for the Nanofil116 with coupling agent (i.e. the fc). 2% Nanofil116 with coupling agent resulted in a higher average SWR than the control (Appendix C page:108), and subsequently reduced significantly at higher concentrations of clay. A trend was observed for all treatments with only Nanofil116 where higher clay loading decreased SWR values, but not significantly. The edge SWR were said related to bond strength(Semple and Smith, 2005), so it is likely that the result of these two tests were similar.

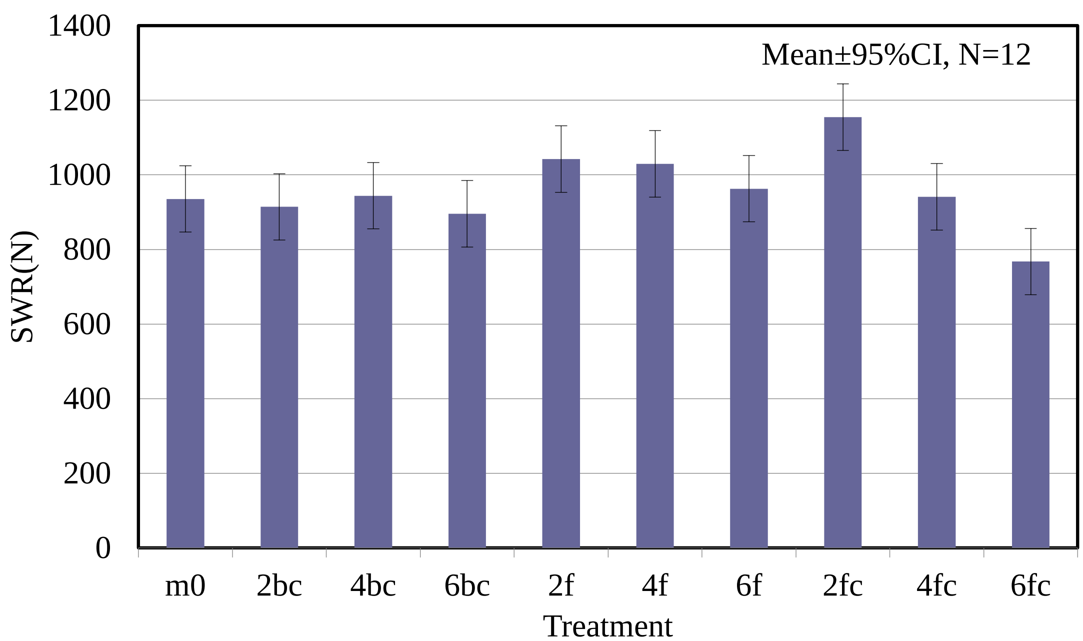

Figure 4.23: Test values of the screw withdrawal test

4.5.3 Internal bonding (IB) test

The results for IB strength were similar to those for SWR. Most resin clay mixes increased IB slightly, some to a significant extent, e.g. 2% Cloisite30B with coupling agent and 2% nanofil116 with coupling agent (Appendix C pages:109-111) This result is consistent with the lap shear strength that 2%Cloisite30B and Nanofil116+coupling agent increased the average bond strength. There was also a trend that the IB value declined as the clay loading increased, and the decrease was significant for 6% Nanofil116 with coupling agent. During testing failure in some of the samples occurred in the bond line between the test specimen and the metal block, the test values for these samples were not taken into consideration during data analysis.

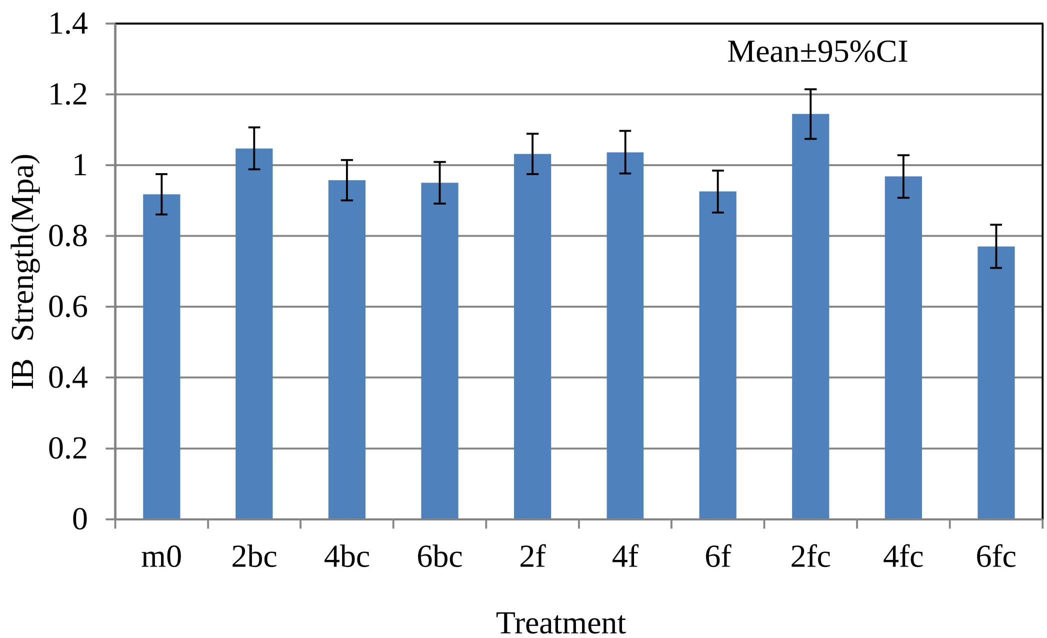

Figure 4.24: Internal bond strength values of different treatments

4.5.4 Thickness swelling test

Most of clay-resin mixes produced a slight improvement in the water resistance properties of particleboard, particularly TS (Figure4.25). However none of the treatments were significantly different (Appendix C pages:112-113). For the three treatments, the average thickness swelling rate tended to decrease as the clay loading increased but not significant different. This was similar with previous studies on adding nanoclay to MDF and solid wood(Ashori and Nourbakhsh, 2009; Cai *et al*., 2010) . The decrease in the thickness swelling rate might be because the clay filled some of the voids in thecomposite and the lumens preventing the penetration of water (Ashori and Nourbakhsh, 2009). In the end, neither the clay type nor the clay loading had a strong impact on thickness swell and water absorption rate, that is, the dimensional stability of the particleboard was not greatly improved by the addition of nanoclay.

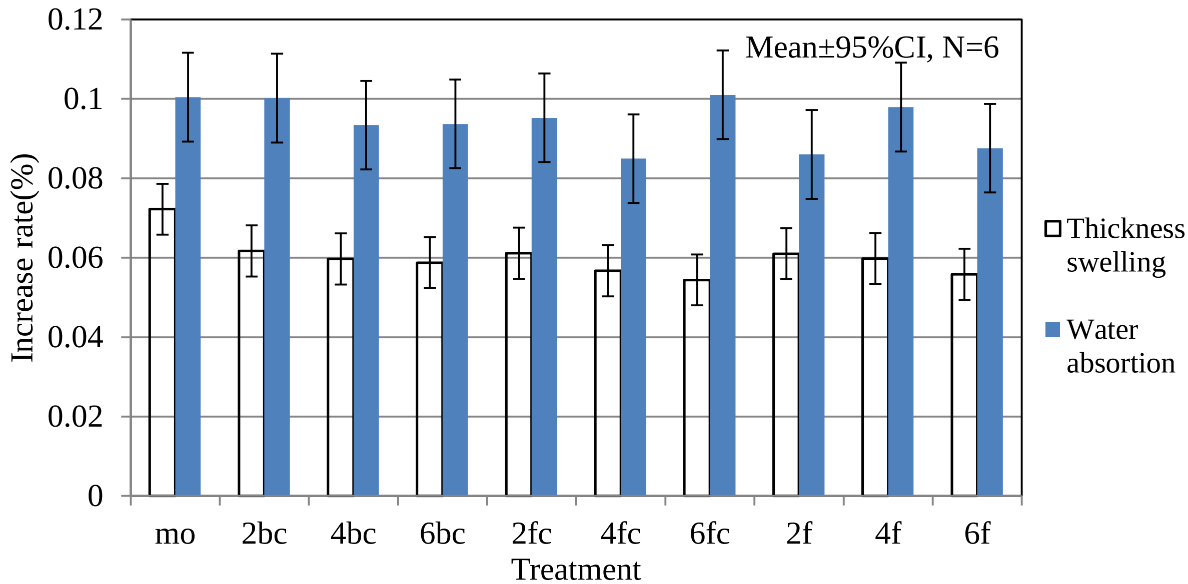

Figure 4.25: Water absorption and thickness swelling rate by different treatments

Over all, the addition of nanoclay and coupling agent to MF did not produce a dramatic improvement in particle board properties, in fact, strength properties (MOR, MOE, SWR and IB) decreased at higher clay loading. These results are consistent with those of the lap shear test conducted on the resin, when 2% clay loading was applied the mean strength was increased but not significantly so. When higher clay amounts were applied the mechanical properties decreased, this can also be predict by the DSC results where less ΔH was generated at higher clay loading, indicating that less effective bonding was generated between wood and the resin, resin and resin.

Colisite30B with coupling agent had no effect on the bending strength and the screw withdrawal properties, but was able to slightly improve the water resistance properties. Interestingly adding up to 6% of this clay did not significantly reduce board properties, suggesting that higher amount of this clay can be used to replace the resin in particle board production in terms of resin cost.

Nanofil116 also had no significant effect on board properties, except when used at higher concentrations, whereby strength properties (MOR, MOE, SWR and IB) were reduced. Nano116+MF with or without coupling agent also reduced thickness swelling to a small extent; however the change was not statistically significant.

MF resin containing 2% Nanofil116+coupling agent improved some of the mechanical properties, including SWR and IB strength however properties decreased as clay loading increased. When 6% clay was used, most mechanical properties were significantly lower than the controls bonded with pure MF resin. Nanofil116 with coupling agent, regardless of concentration, was able to decrease the average thickness swell rate of particleboard however which was still not significant in statistic.

In conclusion, the addition of nanoclays (with or without coupling agent) mostly had no statistically significant effects on the mechanical properties of the particleboard, with the exception of 2% Nanofil116 and coupling agent which resulted in a significant improvement in SWR and 2% Colisite30B-coupling agent treatment significantly improved internal bond strength. This suggests that adding very small amounts of nanoclays to resin can potentially improve mechanical strength. However, increasing clay addition (especially Nanofil116 with coupling agent) had a deleterious effect on board properties.

4.6 Conclusion and general discussion

This work demonstrated the possibility of using nanoclay as fillers and reinforcement for two common thermosetting resins used in the manufacture of particleboard. Mechanical mixing using a high speed stirrer was shown to be effective at dispersing nanoclays into liquid UF and MF resin. Based on evidence from XRD, organic-modified nanoclay is believed to have been exfoliated (i.e. complete separation and even distribution of platelets) in UF resin and MF resin. The unmodified nanoclay is believed to have been intercalated (i.e. opening up the gaps between platelets) within the resin matrix.

The addition of nanoclays to UF did not change the heat of reaction (peak curing temperature and ΔH) in curing to any large extent whereas the enthalpy of MF resin-clay mixes was reduced compared with controls, suggesting that less chemical bonds were generated when nanoclays were added.

The curing process of both UF resin and MF resin were slightly delayed by the presence of modified nanoclay (30B) and the heat of curing reaction was decreased. The addition of coupling agent into the clay-resin mix further compounded this effect. Adding unmodified nanoclay (116) significantly delayed the curing reaction of both resins and decreased the heat of reaction in curing, and again the addition of coupling agent further exacerbated this effect.

Adding nanoclays to UF resin had no, or a slightly reducing, effect on its capacity to bond wood elements. On the other hand the bonding strength of wood veneers cured with MF resin containing the organic nanoclay 30B and coupling agent, or 116 with or without coupling agent was improved but the effect was not statistically significant. Nevertheless MF resin was selected as the binder for testing the effect of nanoclay and coupling agent addition on the fabrication of particleboard.

Adding nanoclays and coupling agents mostly had no significant effects on the strength properties of particleboard, although adding small quantities (2%) appears to have some beneficial effect on board properties (SWR and IB). This is also consistent with the result of the shear strength. That may be because small amounts of clay filler in MF resin can share the facture stress and delay the cracking (Adam, 2001). Using higher concentrations of nanoclay, board properties were decreased, particularly in the case of Nanofil116 with coupling agent. This may be explained by the DSC results that higher clay content results in less effective curing reaction therefore the resin is weaker in bonding.

In summary, the nanoclay fillers did not significantly enhance the wood adhesive strength or the particle board properties. On the other hand, 2% nanoclay addition in wood adhesive did not significantly compromise the resin properties and particleboard properties, this method can still be applied in actual particleboard production to reduce cost. Greater amount of clay can be added into resin to lower the production cost as long as the board properties are maintain.

5 Comments and future work

In this work the effects of adding nanoclays and coupling agents to UF and MF wood adhesives was assessed. At low clay loading (2%) there appears to be some positive effects on MF resin bond strength, however since board properties deteriorate with higher clay loadings less clay filled MF resin can be used for making particle board to verify whether lower amount of this resin can maintain the board properties. Even though the amount of nanoclay that could be supplemented into the resin is restricted to a low content, nanoclay fillers are able to replace some of the resin in particle board and reduce production cost.

Fortunately, simple mechanical mixing can effectively disperse the nanoclay in the resin matrix. Other mixing methods can also be applied to disperse nanoclay into resins. If not limited by the cost and time, the ultrasonic dispersion method is also possible to get ideal clay distribution in resin matrix (Lin, *et al*., 2005). However, in the actual application of particleboard production in plants, the mixing instrument should sufficiently disperse the clay in greater amount of resin at a lower cost and minimum time.

Visual techniques for characterizing materials including TEM (Transmitting Electron Microscopy) and SEM (Scanning Electron Microscopy) can be used to investigate the clay dispersion and the cracking process of resins containing nanoclay. A useful further investigation would be to conduct blended furnish open time experiments to determine whether the presence of nanoclays can inhibit the penetration of resin into the wood element subsurface, which results in starvation of the glue line and reduced inter particle bond strength. Another useful investigation would be to test the air and water permeability of particle board bonded with resin-nanoclay mixtures to further investigate the effects on void space, connectivity and ease of water ingress. This would help explain why particleboard bonded with resin-clay mixes is more resistant to thickness swelling than the controls.

Due to confidentiality agreement with the resin supply company, there is no chemical analysis available for the commercial UF and MF resins used in this study. It would be desirable to undertake further tests on the chemical interaction between nanoclay and resin, using techniques such as Fourier transform spectroscopy (FTIR) and Nuclear magnetic resonance **(**NMR**)** to examine whether any extra or stronger chemical bonding takes place between the clay platelets and the cured resin polymer that may help further explain the reinforcement mechanism of nanoclays within the resin matrix.

References

ASTM. (2008). Standard Test Method for Plastics : Dynamic Mechanical Properties : Cure Behavior 1. *Annual Book of ASTM Standards*. doi:10.1520/D4473-08.2

Adam S. Zerda, A. J. L. (2001). Intercalated clay nanocomposites: Morphology, mechanics, and fracture behavior. *Journal of Polymer Science Part B: Polymer Physics, 39*(11), 1137-1146.

Alexandre, M., & Dubois, P. (2000). Polymer-layered silicate nanocomposites: preparation, properties and uses of a new class of materials. *Materials Science and Engineering: R: Reports*, *28*(1-2), 1-63. doi:10.1016/S0927-796X(00)00012-7

Ashori, A., & Nourbakhsh, A. (2009). Effects of Nanoclay as a Reinforcement Filler on the Physical and Mechanical Properties of Wood-based Composite. *Journal of Composite Materials*, *43*(18), 1869-1875. doi:10.1177/0021998309340936

Becker, O., Cheng, Y.-B., Varley, R. J., & Simon, G. P. (2003). Layered Silicate Nanocomposites Based on Various High-Functionality Epoxy Resins: The Influence of Cure Temperature on Morphology, Mechanical Properties, and Free Volume. *Macromolecules*, *36*(5), 1616-1625. doi:10.1021/ma0213448

Bragg, W. H., & Bragg, W. L. (1913). The Reflection of X-rays by Crystals. *Proceedings of the Royal Society A: Mathematical, Physical and Engineering Sciences*, *88*(605), 428-438. doi:10.1098/rspa.1913.0040

Cai, X., Riedl, B., Wan, H., Zhang, S. Y., & Wang, X.-M. (2010). A study on the curing and viscoelastic characteristics of melamine–urea–formaldehyde resin in the presence of aluminium silicate nanoclays. *Composites Part A: Applied Science and Manufacturing*, *41*(5), 604-611. doi:DOI: 10.1016/j.compositesa.2010.01.007

Cai, X., Riedl, B., Zhang, S. Y., & Wan, H. (2007). Effects of nanofillers on water resistance and dimensional stability of solid wood modified by melamine-urea-formaldehyde resin. *Wood and Fiber Science*, *39*(2), 307-318. CRB, Departement des Sciences du Bois et de la Foret, Universite Laval, Sainte-Foy, QC G1K 7P4, Canada: Allen Press Inc.

Cai, X., Riedl, B., Zhang, S. Y., & Wan, H. (2008). The impact of the nature of nanofillers on the performance of wood polymer nanocomposites. *Composites Part A: Applied Science and Manufacturing*, *39*(5), 727-737. doi:10.1016/j.compositesa.2008.02.004

Chen, L., Wong, S.-C., & Pisharath, S. (2003). Fracture properties of nanoclay-filled polypropylene. *Journal of Applied Polymer Science*, *88*(14), 3298-3305. Wiley Subscription Services, Inc., A Wiley Company. Retrieved from http://dx.doi.org/10.1002/app.12153

Chowdhury, F. H., Hosur, M. V., & Jeelani, S. (2006). Studies on the flexural and thermomechanical properties of woven carbon/nanoclay-epoxy laminates. *Internal stress* *and thermo-mechanical behavior in multi-component materials systems, TMS Annual Meeting, 2004*, *421*(1-2), 298-306. doi:DOI: 10.1016/j.msea.2006.01.074

Dean, K., Krstina, J., Tian, W., & Varley, R. J. (2007). Effect of Ultrasonic Dispersion Methods on Thermal and Mechanical Properties of Organoclay Epoxy Nanocomposites. *Macromolecular Materials and Engineering*, *292*(4), 415-427. doi:10.1002/mame.200600435

Deka, B. K., & Maji, T. K. (2010). Effect of coupling agent and nanoclay on properties of HDPE, LDPE, PP, PVC blend and Phargamites karka nanocomposite. *Composites Science and Technology*, *70*(12), 1755-1761. Elsevier Ltd. doi:10.1016/j.compscitech.2010.07.010

Douglas Clark. (2011). *Forestry Product annual market review 2010-2011*. *Review Literature And Arts Of The Americas* (pp. 1-153). Geneva.

Doyle, M., Hagstrand, P.-0., & Manson, J.-A. E. (2003). Influence of chemical composition on the rheological behavior of condensation reaction resins. *Polymer Engineering & Science*, *43*(2), 297-305. doi:10.1002/pen.10025

Edwards, K. (2004). Handbook of polymer blends and composites (4 Volumes). *Materials* (Vol. 25, pp. 263-264). iSmithers Rapra Publishing. doi:10.1016/j.matdes.2003.09.012

Faruk, O., & Matuana, L. (2008). Nanoclay reinforced HDPE as a matrix for wood-plastic composites. *Composites Science and Technology*, *68*(9), 2073-2077. doi:10.1016/j.compscitech.2008.03.004

Giannelis, E. P., Krishnamoorti, R., & Manias, E. (1999). Polymer-Silicate Nanocomposites : Model Systems for Confined Polymers and Polymer Brushes. *Advances in Polymer Science*, *138*, 106-147.

Groenewoud, W. M. (2001). Dynamic mechanical analysis. *Characterisation of Polymers by Thermal Analysis* (pp. 94-122). Amsterdam: Elsevier Science B.V. doi:DOI: 10.1016/B978-044450604-7/50005-4

Han, M. S., Kim, Y. H., Han, S. J., Choi, S. J., Kim, S. B., & Kim, W. N. (2008). Effects of a Silane Coupling Agent on the Exfoliation of Organoclay Layers in Polyurethane / Organoclay Nanocomposite Foams ? *Polymer*, *110*, 376-386. doi:10.1002/app

Hatakeyama, T., & Quinn, F. X. (1999). *Thermal Analysis Fundamentals and Applications to Polymer Science*. (T. Hatakeyama & F.X. Quinn, Eds.)*Recherche* (2nd ed., p. 131). Toko,Japan: John wiley& sons.

Hetzer, M., & Dekee, D. (2008). Wood/polymer/nanoclay composites, environmentally friendly sustainable technology: A review. *Chemical Engineering Research and Design*, *86*(10), 1083-1093. doi:10.1016/j.cherd.2008.05.003

Hon, D. . (2003). Analysis of Adhesives. In K. L. Pizzi, Antonio; Mittal (Ed.), *Hand book of wood Adheisve technology* (2nd ed.). M. Dekker.

Hussain, F., Chen, J., & Hojjati, M. (2007). Epoxy-silicate nanocomposites: Cure monitoring and characterization. *Materials Science and Engineering: A*, *445-446*, 467-476. doi:10.1016/j.msea.2006.09.071

Kim, J.-tae, Lee, D.-yeoul, Oh, T.-su, & Lee, D.-ho. (2003). Characteristics of Nitrile – Butadiene Rubber Layered Silicate Nanocomposites with Silane Coupling Agent. *Journal of Applied Polymer Science*, *89*, 2633–2640.

Kim, M. G., Nieh, W. L. S., & Meacham, R. M. (1991). Study on the curing of phenol-formaldehyde resol resins by dynamic mechanical analysis. *Industrial & Engineering Chemistry Research*, *30*(4), 798-803. doi:10.1021/ie00052a027

Kord, B., Hemmasi, A. H., & Ghasemi, I. (2010). Properties of PP/wood flour/organomodified montmorillonite nanocomposites. *Wood Science and Technology*, *45*(1), 111-119. doi:10.1007/s00226-010-0309-7

Kotsilkova, R., & Pissis, P. (2007). *Thermoset nanocomposites for engineering applications*. Shawbury: Smithers Rapra.

Kulshreshtha,A. K, & Vasile, C. (2002). *Handbook of polymer blends and composites,*. (C. V. A. K. Kulshreshtha, Ed.). Rapra Technonogy Limited.

Labidi, S., Azema, N., Perrin, D., & Lopez-Cuesta, J.-M. (2010). Organo-modified montmorillonite/poly(ε-caprolactone) nanocomposites prepared by melt intercalation in a twin-screw extruder. *Polymer Degradation and Stability*, *95*(3), 382-388. doi:10.1016/j.polymdegradstab.2009.11.013

Lan, T., & Pinnavaia, T. J. (1994). Clay-Reinforced Epoxy Nanocomposites. *Chemistry of Materials*, *6*(12), 2216-2219. American Chemical Society. Retrieved from http://dx.doi.org/10.1021/cm00048a006

Landry, V., Riedl, B., & Blanchet, P. (2008). Nanoclay dispersion effects on UV coatings curing. *Progress in Organic Coatings*, *62*(4), 400-408. doi:10.1016/j.porgcoat.2008.02.010

Lapique, F. (2002). Curing effects on viscosity and mechanical properties of a commercial epoxy resin adhesive. *International Journal of Adhesion and Adhesives*, *22*(4), 337-346. doi:10.1016/S0143-7496(02)00013-1

Lebaron, P. C., Wang, Z., & Pinnavaia, T. J. (1999). Polymer-layered silicate nanocomposites : an overview. *Applied Clay Science*, *15*, 11-29.

Lee, J., Jung, D., Hong, C., Rhee, K., & Advani, S. (2005). Properties of polyethylene-layered silicate nanocomposites prepared by melt intercalation with a PP-g-MA compatibilizer.

Composites Science and Technology, *65*(13), 1996-2002. doi:10.1016/j.compscitech.2005.03.015

Lee, Y. H. (2008). *Foaming of Wood Flour / Polyolefin / Layered Silicate Composites by. Microscopy*. University of Toronto.

Lei, H., Du, G., Pizzi, A., & Celzard, A. (2008). Influence of Nanoclay on Urea-Formaldehyde Resins for Wood Adhesives and Its Model. *Journal of Applied Polymer Science*, *109*, 2442-2451. doi:10.1002/app

Lei, Y., Wu, Q., Clemons, C. M., Yao, F., & Xu, Y. (2007). Influence of Nanoclay on Properties of HDPE / Wood Composites. *Journal of Applied Polymer Science*, *106*, 3958–3966. doi:10.1002/app

Lin, Qiaojia Liu, Jinghong Rao, Jiuping Yang, G. (2005). Study on the property of nano-SiO2/urea formaldehyde resin. *Scientia silvae sinicae (China); Linye Kexue (China),*, *41*(2), 129-135.

Lv, W., & Zhao, G. (2004). Design of wood/montmorillonite (MMT) intercalation nanocomposite. *Forestry Studies in China*, *6*(1), 54-62. Retrieved from http://dx.doi.org/10.1007/s11632-004-0010-8

Lü, W., & Zhao, G. (2004). Design of wood/montmorillonite (MMT) intercalation nanocomposite. *Forestry Studies in China*, *6*(1), 54-62. doi:10.1007/s11632-004-0010-8

Lü, W.-hua, Zhao, G.-jie, & Xue, Z.-hua. (2006). Preparation and characterization of wood/montmorillonite nanocomposites. *Forestry Studies in China*, *8*(1), 35-40. doi:10.1007/s11632-006-0007-6

Maiti, P., Nam, P. H., & Okamoto, M. (2002). Influence of Crystallization on Intercalation , Morphology , and Mechanical Properties of Polypropylene / Clay Nanocomposites. *Marcomolecules*, *36*(6), 2042-2049.

Menczel, J. D., & Prime, R. B. (2008). *Polymers Thermal Analysis of Fundamentals and Applications*. (J. D. MENCZEL & R. B. PRIME, Eds.). Hoboken, New Jersey: A JOHN WILEY & SONS, INC., PUBLICATION.

Mequanint, K., & Sanderson, R. (2003). Nano-structure phosphorus-containing polyurethane dispersions: synthesis and crosslinking with melamine formaldehyde resin. *Polymer*, *44*(9), 2631-2639. doi:10.1016/S0032-3861(03)00154-X

Miyagawa, H., Rich, M. J., & Drzal, L. T. (2004). Amine-cured epoxy/clay nanocomposites. II. The effect of the nanoclay aspect ratio. *Journal of Polymer Science Part B: Polymer Physics*, *42*(23), 4391-4400. doi:10.1002/polb.20289

Morgan, A. B., & Gilman, J. W. (2002). Characterization of Polymer-Layered Silicate (Clay) Nanocomposites by Transmission Electron Microscopy and X-Ray Diffraction : A Comparative Study. *Inorganic Materials*, *87*, 1329-1338.

Nishizawa, Y., Furukawa, T., Teruo, G., & Hirotsugu, O. (1982). Process for Producing Filler for Adhesive for Bonding Wood.

Nourbakhsh, Amir, & Ashori, A. (2009). Influence of Nanoclay and Coupling Agent on the Physical and Mechanical Properties of Polypropylene / Bagasse Nanocomposite. *Polymer*. doi:10.1002/app

Park, B.-dae, & Kim, J.-woo. (2008). Dynamic Mechanical Analysis of Urea – Formaldehyde Resin Adhesives with Different Formaldehyde-to-Urea Molar Ratios. *Polymer*. doi:10.1002/app

Pavlidou, S., & Papaspyrides, C. D. (2008). A reviewon polymer–layered silicate nanocomposites. *Progress in Polymer Science*, *33*(12), 1119-1198. doi:10.1016/j.progpolymsci.2008.07.008

Pegoretti, A. (2007). Tensile mechanical response of polyethylene – clay nanocomposites. *eXPRESS Polymer Letters*, *1*(3), 123-131. doi:10.3144/expresspolymlett.2007.21

Pepke, E. (2010). *FOREST PRODUCTS ANNUAL MARKET REVIEW 2009-2010*. *UNECE*.

Perrin-Sarazin, F., Ton-That, M.-T., Bureau, M. N., & Denault, J. (2005). Micro- and nano-structure in polypropylene/clay nanocomposites. *Polymer*, *46*(25), 11624-11634. doi:DOI: 10.1016/j.polymer.2005.09.076

Pilato David Nagy, Ellen, L. V. (2010). Phenolic Resins: A Century of Progress Analyses/Testing (pp. 93-135).

Pizzi, A, & Mittal, K. L. (1994). *Advanced wood adhesives technology* (1st ed., p. 289). New York, USA: Marcel Dekker, Inc.

RISI. (2011). *Particleboard and MDF Commentary*. *Production*. Retrieved from www.risi.com

Sarrazin, P., Blake, D., Feldman, S., Chipera, S., Vaniman, D., & Bish, D. (2005). Field deployment of a portable X-ray diffraction/X-ray flourescence instrument on Mars analog terrain. *Powder Diffraction*, *20*(2), 128. doi:10.1154/1.1913719

Semple, K. E., & Smith, G. D. (2005). PREDICTION OF INTERNAL BOND STRENGTH IN PARTICLEBOARD FROM SCREW WITHDRAWAL RESISTANCE MODELS. *Wood Science and Technology*, *38*(2), 256-267.

Sheshmani, S., Ashori, A., & Hamzeh, Y. (2010). Physical Properties of Polyethylene – Wood Fiber – Clay Nanocomposites. *Journal ofAppliedPolymer Science*, *118*, 3255–3259. doi:10.1002/app

Shi, Y., Qiu, J., & Zheng, Z. (2004). Mineralogy Characters of Yunnan Wollastonite and Application of M ineral Filler in Wood-based Panel Industry. *China Forestry product inductry*, *31*(4), 7-10. China Forest Product Industry.

Sichina, W. J., & Manager, I. M. (2000). Prediction of Epoxy Cure Properties Using Pyris DSC Scanning Kinetics Software. *Manager*. Norwalk.

Siddiqui, N. A., Woo, R. S. C., Kim, J.-K., Leung, C. C. K., & Munir, A. (2007). Mode I interlaminar fracture behavior and mechanical properties of CFRPs with nanoclay-filled epoxy matrix. *Composites Part A: Applied Science and Manufacturing*, *38*(2), 449-460. doi:DOI: 10.1016/j.compositesa.2006.03.001

Sinha Ray, S., & Okamoto, M. (2003). Polymer/layered silicate nanocomposites: a review from preparation to processing. *Progress in Polymer Science*, *28*(11), 1539-1641. doi:10.1016/j.progpolymsci.2003.08.002

Sui, G., Zhong, W.-H., Fuqua, M. a., & Ulven, C. a. (2007). Crystalline Structure and Properties of Carbon Nanofiber Composites Prepared by Melt Extrusion. *Macromolecular Chemistry and Physics*, *208*(17), 1928-1936. doi:10.1002/macp.200700170

Ton-That, M.-T., Ngo, T.-D., Ding, P., Fang, G., Cole, K. C., & Hoa, S. V. (2004). Epoxy nanocomposites: Analysis and kinetics of cure. *Polymer Engineering and Science*, *44*(6), 1132-1141. doi:10.1002/pen.20106

Vaia, R. a., & Liu, W. (2002). X-ray powder diffraction of polymer/layered silicate nanocomposites: Model and practice. *Journal of Polymer Science Part B: Polymer Physics*, *40*(15), 1590-1600. doi:10.1002/polb.10214

Vermogen, A., Masenelli-Varlot, K., Séguéla, R., Duchet-Rumeau, J., Boucard, S., & Prele, P. (2005). Evaluation of the Structure and Dispersion in Polymer-Layered Silicate Nanocomposites. *Macromolecules*, *38*(23), 9661-9669. doi:10.1021/ma051249+

Wang, Ke, Chen, L., Wu, J., Toh, M. L., He, C., & Yee, A. F. (2005). Epoxy Nanocomposites with Highly Exfoliated Clay : Mechanical Properties and Fracture Mechanisms. *Macromolecules*, *38*(3), 788-800.

Wang, S., Qiu, H., Zhou, J., & Wellwood, R. (2008). Phyllosilicate Modifided Resins for Lignocellulousic Fiber Based Composite Panels.

Wang, Z.-yu, Han, E.-hou, & Ke, W. (2007). Fire-resistant effect of nanoclay on intumescent nanocomposite coatings. *Journal of Applied Polymer Science*, *103*(3), 1681-1689. Wiley

Subscription Services, Inc., A Wiley Company. Retrieved from http://dx.doi.org/10.1002/app.25096

Wong, D. C. (2008). Particleboard performance requirements of secondary wood products manufacturers in Canada. *Forestry Productd Journal*, *58*(3), 34-41.

Yeh, S.-K. (2007). *POLYPROPYLENE-BASED WOOD-PLASTIC COMPOSITES REINFORCED WITH NANOCLAY*. West Virginia University.

Young No, B., & Kim, M. G. (2005). Curing of low level melamine-modified urea-formaldehyde particleboard binder resins studied with dynamic mechanical analysis (DMA). *Journal of Applied Polymer Science*, *97*(1), 377-389. doi:10.1002/app.21759

Zerda, A. S., & Lesser, A. J. (2001). Intercalated Clay Nanocomposites : Morphology , Mechanics , and Fracture Behavior. *Journal of Polymer Science Part B: Polymer Physics*, *39*, 1137-1146.

Zhang, J., Hereid, J., Hagen, M., Bakirtzis, D., Delichatsios, M. A., Fina, A., Castrovinci, A., et al. (2009). Effects of nanoclay and fire retardants on fire retardancy of a polymer blend of EVA and LDPE. *Fire Safety Journal*, *44*(4), 504-513. doi:10.1016/j.firesaf.2008.10.005

Zhao, Y., Wang, K., Zhu, F., Xue, P., & Jia, M. (2006). Properties of poly(vinyl chloride)/wood flour/montmorillonite composites: Effects of coupling agents and layered silicate. *Polymer Degradation and Stability*, *91*(12), 2874-2883. doi:10.1016/j.polymdegradstab.2006.09.001

Appendix A: Statistical analysis result of DSC test

This appendix is the test result of the Tukey's test, grouping the means of board properties tests. The means of which are significantly different will be grouped by different letters or mark.

UF resin DSC test

Oneway Analysis of ΔH By TREATMENT

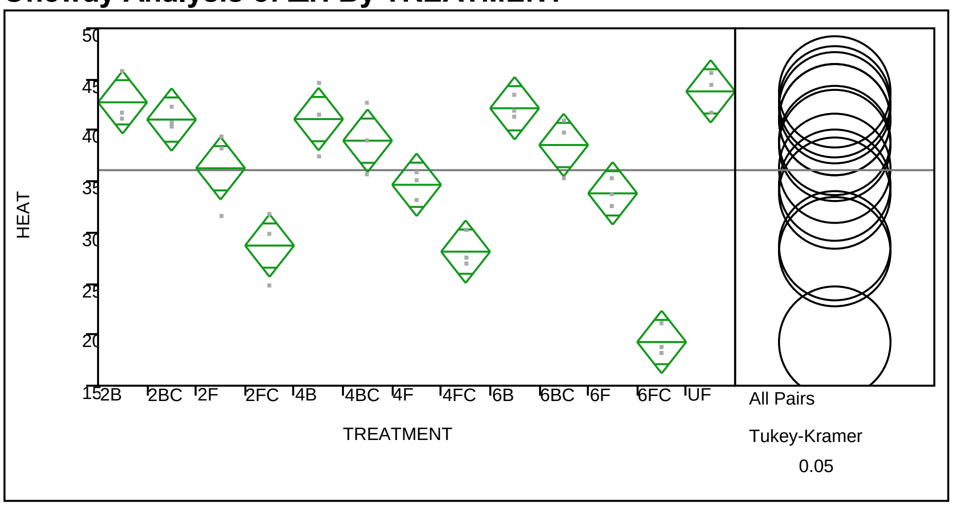

Excluded Rows
3

Means Comparisons

Comparisons for all pairs using Tukey-Kramer HSD

q*	Alpha
3.63404	0.05

Abs(Dif)-HSD	UF	2B	6B	4B	2BC	4BC	6BC
UF	-7.663	-6.593	-6.010	-4.950	-4.900	-2.833	-2.410
2B	-6.593	-7.663	-7.080	-6.020	-5.970	-3.903	-3.480
6B	-6.010	-7.080	-7.663	-6.603	-6.553	-4.486	-4.063
4B	-4.950	-6.020	-6.603	-7.663	-7.613	-5.546	-5.123
2BC	-4.900	-5.970	-6.553	-7.613	-7.663	-5.596	-5.173
4BC	-2.833	-3.903	-4.486	-5.546	-5.596	-7.663	-7.240
6BC	-2.410	-3.480	-4.063	-5.123	-5.173	-7.240	-7.663
2F	-0.133	-1.203	-1.786	-2.846	-2.896	-4.963	-5.386
4F	1.484	0.414	-0.170	-1.230	-1.280	-3.346	-3.770
6F	2.324	1.254	0.670	-0.390	-0.440	-2.506	-2.930
2FC	7.437	6.367	5.784	4.724	4.674	2.607	2.184
4FC	8.034	6.964	6.380	5.320	5.270	3.204	2.780
6FC	16.884	15.814	15.230	14.170	14.120	12.054	11.630

Abs(Dif)-HSD	2F	4F	6F	2FC	4FC	6FC
UF	-0.133	1.484	2.324	7.437	8.034	16.884
2B	-1.203	0.414	1.254	6.367	6.964	15.814
6B	-1.786	-0.170	0.670	5.784	6.380	15.230
4B	-2.846	-1.230	-0.390	4.724	5.320	14.170
2BC	-2.896	-1.280	-0.440	4.674	5.270	14.120
4BC	-4.963	-3.346	-2.506	2.607	3.204	12.054
6BC	-5.386	-3.770	-2.930	2.184	2.780	11.630
2F	-7.663	-6.046	-5.206	-0.093	0.504	9.354
4F	-6.046	-7.663	-6.823	-1.710	-1.113	7.737
6F	-5.206	-6.823	-7.663	-2.550	-1.953	6.897
2FC	-0.093	-1.710	-2.550	-7.663	-7.066	1.784
4FC	0.504	-1.113	-1.953	-7.066	-7.663	1.187
6FC	9.354	7.737	6.897	1.784	1.187	-7.663

Positive values show pairs of means that are significantly different.

Level	Mean

Level							Mean
UF	A						43.823333
2B	A						42.753333
6B	A	B					42.170000
4B	A	B	C				41.110000
2BC	A	B	C				41.060000
4BC	A	B	C				38.993333
6BC	A	B	C				38.570000
2F	A	B	C	D			36.293333
4F		B	C	D	E		34.676667
6F			C	D	E		33.836667
2FC				D	E		28.723333
4FC					E		28.126667
6FC						F	19.276667

Levels not connected by same letter are significantly different.

Level	- Level	Difference	Std Err Dif	Lower CL	Upper CL	p-Value	Difference
UF	6FC	24.54667	2.108642	16.8838	32.20956	<.0001*	
2B	6FC	23.47667	2.108642	15.8138	31.13956	<.0001*	
6B	6FC	22.89333	2.108642	15.2304	30.55622	<.0001*	
4B	6FC	21.83333	2.108642	14.1704	29.49622	<.0001*	
2BC	6FC	21.78333	2.108642	14.1204	29.44622	<.0001*	
4BC	6FC	19.71667	2.108642	12.0538	27.37956	<.0001*	
6BC	6FC	19.29333	2.108642	11.6304	26.95622	<.0001*	
2F	6FC	17.01667	2.108642	9.3538	24.67956	<.0001*	
UF	4FC	15.69667	2.108642	8.0338	23.35956	<.0001*	
4F	6FC	15.40000	2.108642	7.7371	23.06289	<.0001*	
UF	2FC	15.10000	2.108642	7.4371	22.76289	<.0001*	
2B	4FC	14.62667	2.108642	6.9638	22.28956	<.0001*	
6F	6FC	14.56000	2.108642	6.8971	22.22289	<.0001*	
6B	4FC	14.04333	2.108642	6.3804	21.70622	<.0001*	
2B	2FC	14.03000	2.108642	6.3671	21.69289	<.0001*	
6B	2FC	13.44667	2.108642	5.7838	21.10956	<.0001*	
4B	4FC	12.98333	2.108642	5.3204	20.64622	0.0001*	
2BC	4FC	12.93333	2.108642	5.2704	20.59622	0.0001*	
4B	2FC	12.38667	2.108642	4.7238	20.04956	0.0002*	
2BC	2FC	12.33667	2.108642	4.6738	19.99956	0.0002*	
4BC	4FC	10.86667	2.108642	3.2038	18.52956	0.0013*	
6BC	4FC	10.44333	2.108642	2.7804	18.10622	0.0021*	
4BC	2FC	10.27000	2.108642	2.6071	17.93289	0.0026*	
UF	6F	9.98667	2.108642	2.3238	17.64956	0.0036*	
6BC	2FC	9.84667	2.108642	2.1838	17.50956	0.0043*	
2FC	6FC	9.44667	2.108642	1.7838	17.10956	0.0069*	
UF	4F	9.14667	2.108642	1.4838	16.80956	0.0097*	
2B	6F	8.91667	2.108642	1.2538	16.57956	0.0126*	
4FC	6FC	8.85000	2.108642	1.1871	16.51289	0.0136*	
6B	6F	8.33333	2.108642	0.6704	15.99622	0.0243*	
2F	4FC	8.16667	2.108642	0.5038	15.82956	0.0292*	
2B	4F	8.07667	2.108642	0.4138	15.73956	0.0322*	
2F	2FC	7.57000	2.108642	-0.0929	15.23289	0.0551	
UF	2F	7.53000	2.108642	-0.1329	15.19289	0.0574	
6B	4F	7.49333	2.108642	-0.1696	15.15622	0.0596	
4B	6F	7.27333	2.108642	-0.3896	14.93622	0.0746	
2BC	6F	7.22333	2.108642	-0.4396	14.88622	0.0785	
4F	4FC	6.55000	2.108642	-1.1129	14.21289	0.1496	
2B	2F	6.46000	2.108642	-1.2029	14.12289	0.1622	
4B	4F	6.43333	2.108642	-1.2296	14.09622	0.1662	
2BC	4F	6.38333	2.108642	-1.2796	14.04622	0.1737	
4F	2FC	5.95333	2.108642	-1.7096	13.61622	0.2501	
6B	2F	5.87667	2.108642	-1.7862	13.53956	0.2659	

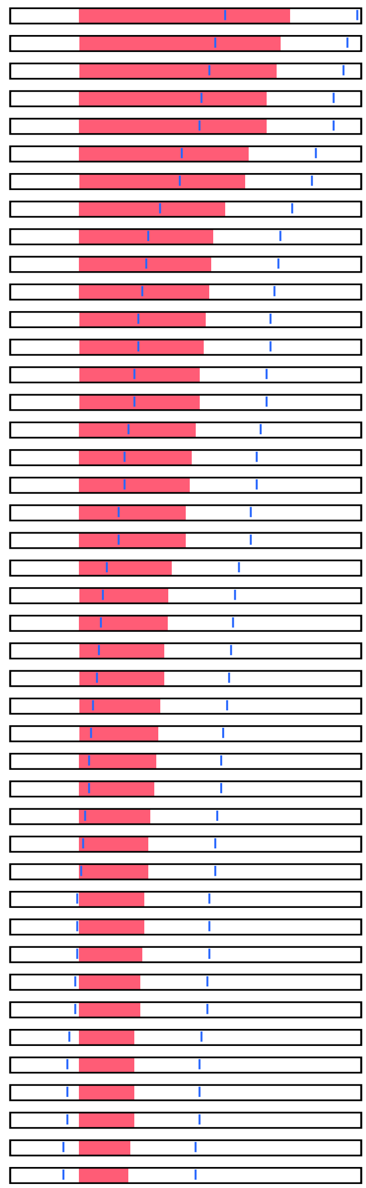

Level	- Level	Difference	Std Err Dif	Lower CL	Upper CL	p-Value	Difference
6F	4FC	5.71000	2.108642	-1.9529	13.37289	0.3027	
UF	6BC	5.25333	2.108642	-2.4096	12.91622	0.4189	
4BC	6F	5.15667	2.108642	-2.5062	12.81956	0.4459	
6F	2FC	5.11333	2.108642	-2.5496	12.77622	0.4583	
UF	4BC	4.83000	2.108642	-2.8329	12.49289	0.5418	
4B	2F	4.81667	2.108642	-2.8462	12.47956	0.5458	
2BC	2F	4.76667	2.108642	-2.8962	12.42956	0.5609	
6BC	6F	4.73333	2.108642	-2.9296	12.39622	0.5710	
4BC	4F	4.31667	2.108642	-3.3462	11.97956	0.6956	
2B	6BC	4.18333	2.108642	-3.4796	11.84622	0.7335	
6BC	4F	3.89333	2.108642	-3.7696	11.55622	0.8097	
2B	4BC	3.76000	2.108642	-3.9029	11.42289	0.8409	
6B	6BC	3.60000	2.108642	-4.0629	11.26289	0.8745	
6B	4BC	3.17667	2.108642	-4.4862	10.83956	0.9417	
UF	2BC	2.76333	2.108642	-4.8996	10.42622	0.9784	
UF	4B	2.71333	2.108642	-4.9496	10.37622	0.9812	
4BC	2F	2.70000	2.108642	-4.9629	10.36289	0.9819	
4B	6BC	2.54000	2.108642	-5.1229	10.20289	0.9889	
2BC	6BC	2.49000	2.108642	-5.1729	10.15289	0.9906	
2F	6F	2.45667	2.108642	-5.2062	10.11956	0.9916	
6BC	2F	2.27667	2.108642	-5.3862	9.93956	0.9956	
4B	4BC	2.11667	2.108642	-5.5462	9.77956	0.9977	
2BC	4BC	2.06667	2.108642	-5.5962	9.72956	0.9982	
2B	2BC	1.69333	2.108642	-5.9696	9.35622	0.9997	
UF	6B	1.65333	2.108642	-6.0096	9.31622	0.9998	
2B	4B	1.64333	2.108642	-6.0196	9.30622	0.9998	
2F	4F	1.61667	2.108642	-6.0462	9.27956	0.9998	
6B	2BC	1.11000	2.108642	-6.5529	8.77289	1.0000	
UF	2B	1.07000	2.108642	-6.5929	8.73289	1.0000	
6B	4B	1.06000	2.108642	-6.6029	8.72289	1.0000	
4F	6F	0.84000	2.108642	-6.8229	8.50289	1.0000	
2FC	4FC	0.59667	2.108642	-7.0662	8.25956	1.0000	
2B	6B	0.58333	2.108642	-7.0796	8.24622	1.0000	
4BC	6BC	0.42333	2.108642	-7.2396	8.08622	.	
4B	2BC	0.05000	2.108642	-7.6129	7.71289	.	

Oneway Analysis of PEAKTEMP By TREATMENT

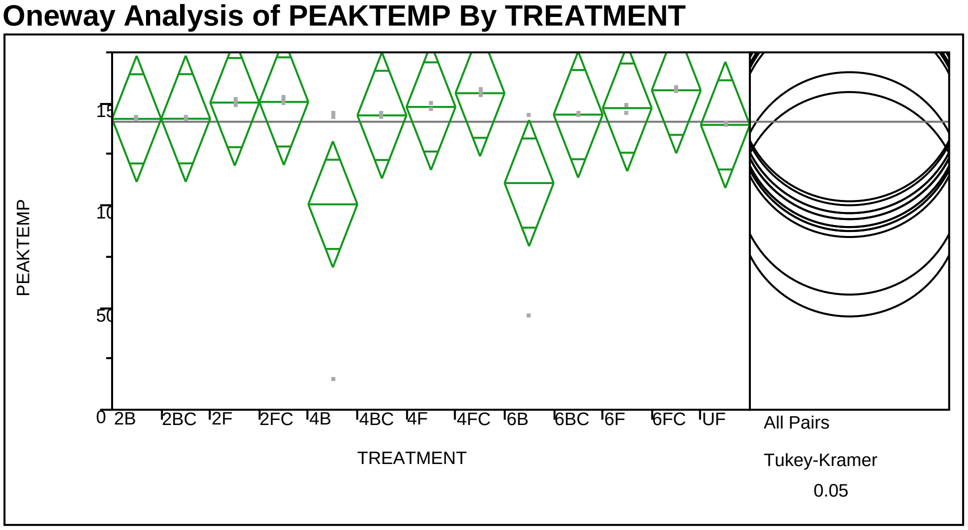

Excluded Rows
3

Means Comparisons
Comparisons for all pairs using Tukey-Kramer HSD

q*	Alpha
3.63404	0.05

Abs(Dif)-HSD	6FC	4FC	2FC	2F	4F	6F	6BC	4BC	2BC	2B	UF	6B	4B
6FC	-77.205	-75.768	-71.502	-71.172	-69.045	-68.465	-65.282	-64.902	-63.258	-63.198	-60.265	-31.762	-21.355
4FC	-75.768	-77.205	-72.938	-72.608	-70.482	-69.902	-66.718	-66.338	-64.695	-64.635	-61.702	-33.198	-22.792
2FC	-71.502	-72.938	-77.205	-76.875	-74.748	-74.168	-70.985	-70.605	-68.962	-68.902	-65.968	-37.465	-27.058
2F	-71.172	-72.608	-76.875	-77.205	-75.078	-74.498	-71.315	-70.935	-69.292	-69.232	-66.298	-37.795	-27.388
4F	-69.045	-70.482	-74.748	-75.078	-77.205	-76.625	-73.442	-73.062	-71.418	-71.358	-68.425	-39.922	-29.515
6F	-68.465	-69.902	-74.168	-74.498	-76.625	-77.205	-74.022	-73.642	-71.998	-71.938	-69.005	-40.502	-30.095
6BC	-65.282	-66.718	-70.985	-71.315	-73.442	-74.022	-77.205	-76.825	-75.182	-75.122	-72.188	-43.685	-33.278
4BC	-64.902	-66.338	-70.605	-70.935	-73.062	-73.642	-76.825	-77.205	-75.562	-75.502	-72.568	-44.065	-33.658
2BC	-63.258	-64.695	-68.962	-69.292	-71.418	-71.998	-75.182	-75.562	-77.205	-77.145	-74.212	-45.708	-35.302
2B	-63.198	-64.635	-68.902	-69.232	-71.358	-71.938	-75.122	-75.502	-77.145	-77.205	-74.272	-45.768	-35.362
UF	-60.265	-61.702	-65.968	-66.298	-68.425	-69.005	-72.188	-72.568	-74.212	-74.272	-77.205	-48.702	-38.295
6B	-31.762	-33.198	-37.465	-37.795	-39.922	-40.502	-43.685	-44.065	-45.708	-45.768	-48.702	-77.205	-66.798
4B	-21.355	-22.792	-27.058	-27.388	-29.515	-30.095	-33.278	-33.658	-35.302	-35.362	-38.295	-66.798	-77.205

Positive values show pairs of means that are significantly different.

Level		Mean
6FC	A	156.43333
4FC	A	154.99667
2FC	A	150.73000
2F	A	150.40000
4F	A	148.27333
6F	A	147.69333
6BC	A	144.51000
4BC	A	144.13000
2BC	A	142.48667
2B	A	142.42667
UF	A	139.49333
6B	A	110.99000
4B	A	100.58333

Levels not connected by same letter are significantly different.

Level	- Level	Difference	Std Err Dif	Lower CL	Upper CL	p-Value	Difference
6FC	4B	55.85000	21.24498	-21.3551	133.0551	0.3426	
4FC	4B	54.41333	21.24498	-22.7918	131.6184	0.3791	
2FC	4B	50.14667	21.24498	-27.0584	127.3518	0.4979	

Level	- Level	Difference	Std Err Dif	Lower CL	Upper CL	p-Value	Difference
2F	4B	49.81667	21.24498	-27.3884	127.0218	0.5076	
4F	4B	47.69000	21.24498	-29.5151	124.8951	0.5710	
6F	4B	47.11000	21.24498	-30.0951	124.3151	0.5884	
6FC	6B	45.44333	21.24498	-31.7618	122.6484	0.6383	
4FC	6B	44.00667	21.24498	-33.1984	121.2118	0.6806	
6BC	4B	43.92667	21.24498	-33.2784	121.1318	0.6830	
4BC	4B	43.54667	21.24498	-33.6584	120.7518	0.6940	
2BC	4B	41.90333	21.24498	-35.3018	119.1084	0.7403	
2B	4B	41.84333	21.24498	-35.3618	119.0484	0.7419	
2FC	6B	39.74000	21.24498	-37.4651	116.9451	0.7971	
2F	6B	39.41000	21.24498	-37.7951	116.6151	0.8052	
UF	4B	38.91000	21.24498	-38.2951	116.1151	0.8173	
4F	6B	37.28333	21.24498	-39.9218	114.4884	0.8539	
6F	6B	36.70333	21.24498	-40.5018	113.9084	0.8659	
6BC	6B	33.52000	21.24498	-43.6851	110.7251	0.9215	
4BC	6B	33.14000	21.24498	-44.0651	110.3451	0.9270	
2BC	6B	31.49667	21.24498	-45.7084	108.7018	0.9476	
2B	6B	31.43667	21.24498	-45.7684	108.6418	0.9483	
UF	6B	28.50333	21.24498	-48.7018	105.7084	0.9742	
6FC	UF	16.94000	21.24498	-60.2651	94.1451	0.9998	
4FC	UF	15.50333	21.24498	-61.7018	92.7084	0.9999	
6FC	2B	14.00667	21.24498	-63.1984	91.2118	1.0000	
6FC	2BC	13.94667	21.24498	-63.2584	91.1518	1.0000	
4FC	2B	12.57000	21.24498	-64.6351	89.7751	1.0000	
4FC	2BC	12.51000	21.24498	-64.6951	89.7151	1.0000	
6FC	4BC	12.30333	21.24498	-64.9018	89.5084	1.0000	
6FC	6BC	11.92333	21.24498	-65.2818	89.1284	1.0000	
2FC	UF	11.23667	21.24498	-65.9684	88.4418	1.0000	
2F	UF	10.90667	21.24498	-66.2984	88.1118	1.0000	
4FC	4BC	10.86667	21.24498	-66.3384	88.0718	1.0000	
4FC	6BC	10.48667	21.24498	-66.7184	87.6918	1.0000	
6B	4B	10.40667	21.24498	-66.7984	87.6118	1.0000	
4F	UF	8.78000	21.24498	-68.4251	85.9851	1.0000	
6FC	6F	8.74000	21.24498	-68.4651	85.9451	1.0000	
2FC	2B	8.30333	21.24498	-68.9018	85.5084	1.0000	
2FC	2BC	8.24333	21.24498	-68.9618	85.4484	1.0000	
6F	UF	8.20000	21.24498	-69.0051	85.4051	1.0000	
6FC	4F	8.16000	21.24498	-69.0451	85.3651	1.0000	
2F	2B	7.97333	21.24498	-69.2318	85.1784	1.0000	
2F	2BC	7.91333	21.24498	-69.2918	85.1184	1.0000	
4FC	6F	7.30333	21.24498	-69.9018	84.5084	1.0000	
4FC	4F	6.72333	21.24498	-70.4818	83.9284	1.0000	
2FC	4BC	6.60000	21.24498	-70.6051	83.8051	1.0000	
2F	4BC	6.27000	21.24498	-70.9351	83.4751	1.0000	
2FC	6BC	6.22000	21.24498	-70.9851	83.4251	1.0000	
6FC	2F	6.03333	21.24498	-71.1718	83.2384	1.0000	
2F	6BC	5.89000	21.24498	-71.3151	83.0951	1.0000	
4F	2B	5.84667	21.24498	-71.3584	83.0518	1.0000	
4F	2BC	5.78667	21.24498	-71.4184	82.9918	1.0000	
6FC	2FC	5.70333	21.24498	-71.5018	82.9084	1.0000	
6F	2B	5.26667	21.24498	-71.9384	82.4718	1.0000	
6F	2BC	5.20667	21.24498	-71.9984	82.4118	1.0000	
6BC	UF	5.01667	21.24498	-72.1884	82.2218	1.0000	
4BC	UF	4.63667	21.24498	-72.5684	81.8418	1.0000	
4FC	2F	4.59667	21.24498	-72.6084	81.8018	1.0000	
4FC	2FC	4.26667	21.24498	-72.9384	81.4718	.	
4F	4BC	4.14333	21.24498	-73.0618	81.3484	.	
4F	6BC	3.76333	21.24498	-73.4418	80.9684	.	
6F	4BC	3.56333	21.24498	-73.6418	80.7684	.	
6F	6BC	3.18333	21.24498	-74.0218	80.3884	.	

Level	- Level	Difference	Std Err Dif	Lower CL	Upper CL	p-Value	Difference
2FC	6F	3.03667	21.24498	-74.1684	80.2418	.	
2BC	UF	2.99333	21.24498	-74.2118	80.1984	.	
2B	UF	2.93333	21.24498	-74.2718	80.1384	.	
2F	6F	2.70667	21.24498	-74.4984	79.9118	.	
2FC	4F	2.45667	21.24498	-74.7484	79.6618	.	
2F	4F	2.12667	21.24498	-75.0784	79.3318	.	
6BC	2B	2.08333	21.24498	-75.1218	79.2884	.	
6BC	2BC	2.02333	21.24498	-75.1818	79.2284	.	
4BC	2B	1.70333	21.24498	-75.5018	78.9084	.	
4BC	2BC	1.64333	21.24498	-75.5618	78.8484	.	
6FC	4FC	1.43667	21.24498	-75.7684	78.6418	.	
4F	6F	0.58000	21.24498	-76.6251	77.7851	.	
6BC	4BC	0.38000	21.24498	-76.8251	77.5851	.	
2FC	2F	0.33000	21.24498	-76.8751	77.5351	.	
2BC	2B	0.06000	21.24498	-77.1451	77.2651	.	

Oneway Analysis of T ON SET By TREATMENT

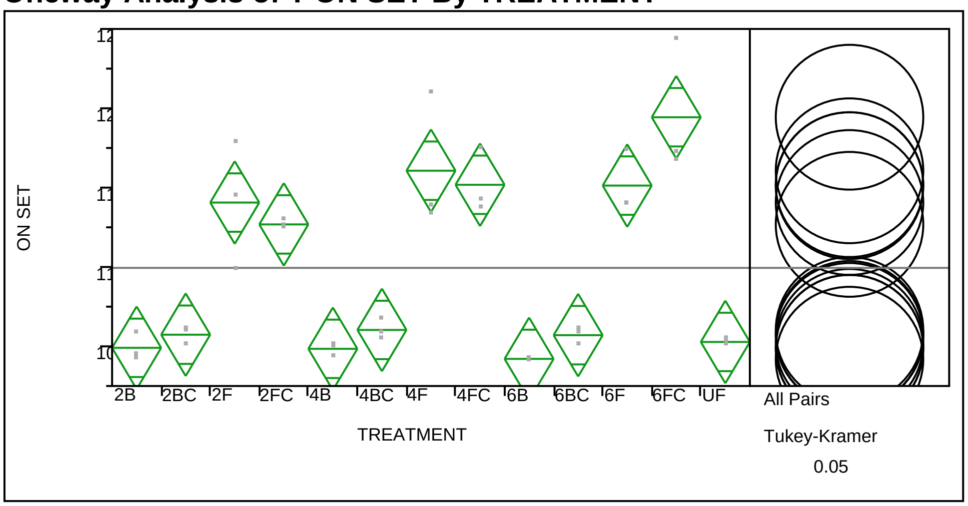

Excluded Rows
3

Oneway Anova

Analysis of Variance

Source	DF	Sum of Squares	Mean Square	F Ratio	Prob > F
TREATMENT	12	1090.2421	90.8535	18.8906	<.0001*
Error	26	125.0456	4.8094		
C. Total	38	1215.2877			

Means for Oneway Anova

Level	Number	Mean	Std Error	Lower 95%	Upper 95%
2B	3	104.907	1.2662	102.30	107.51
2BC	3	105.733	1.2662	103.13	108.34
2F	3	114.060	1.2662	111.46	116.66
2FC	3	112.683	1.2662	110.08	115.29
4B	3	104.843	1.2662	102.24	107.45
4BC	3	106.033	1.2662	103.43	108.64
4F	3	116.067	1.2662	113.46	118.67
4FC	3	115.180	1.2662	112.58	117.78
6B	3	104.210	1.2662	101.61	106.81
6BC	3	105.703	1.2662	103.10	108.31
6F	3	115.130	1.2662	112.53	117.73

Level	Number	Mean	Std Error	Lower 95%	Upper 95%
6FC	3	119.437	1.2662	116.83	122.04
UF	3	105.277	1.2662	102.67	107.88

Std Error uses a pooled estimate of error variance

Means Comparisons

Comparisons for all pairs using Tukey-Kramer HSD

q*	Alpha
3.63404	0.05

Abs(Dif)-HSD	6FC	4F	4FC	6F	2F	2FC	4BC	2BC	6BC	UF	2B	4B	6B
6FC	-6.5072	-3.1372	-2.2505	-2.2005	-1.1305	0.2462	6.8962	7.1962	7.2262	7.6528	8.0228	8.0862	8.7195
4F	-3.1372	-6.5072	-5.6205	-5.5705	-4.5005	-3.1238	3.5262	3.8262	3.8562	4.2828	4.6528	4.7162	5.3495
4FC	-2.2505	-5.6205	-6.5072	-6.4572	-5.3872	-4.0105	2.6395	2.9395	2.9695	3.3962	3.7662	3.8295	4.4628
6F	-2.2005	-5.5705	-6.4572	-6.5072	-5.4372	-4.0605	2.5895	2.8895	2.9195	3.3462	3.7162	3.7795	4.4128
2F	-1.1305	-4.5005	-5.3872	-5.4372	-6.5072	-5.1305	1.5195	1.8195	1.8495	2.2762	2.6462	2.7095	3.3428
2FC	0.2462	-3.1238	-4.0105	-4.0605	-5.1305	-6.5072	0.1428	0.4428	0.4728	0.8995	1.2695	1.3328	1.9662
4BC	6.8962	3.5262	2.6395	2.5895	1.5195	0.1428	-6.5072	-6.2072	-6.1772	-5.7505	-5.3805	-5.3172	-4.6838
2BC	7.1962	3.8262	2.9395	2.8895	1.8195	0.4428	-6.2072	-6.5072	-6.4772	-6.0505	-5.6805	-5.6172	-4.9838
6BC	7.2262	3.8562	2.9695	2.9195	1.8495	0.4728	-6.1772	-6.4772	-6.5072	-6.0805	-5.7105	-5.6472	-5.0138
UF	7.6528	4.2828	3.3962	3.3462	2.2762	0.8995	-5.7505	-6.0505	-6.0805	-6.5072	-6.1372	-6.0738	-5.4405
2B	8.0228	4.6528	3.7662	3.7162	2.6462	1.2695	-5.3805	-5.6805	-5.7105	-6.1372	-6.5072	-6.4438	-5.8105
4B	8.0862	4.7162	3.8295	3.7795	2.7095	1.3328	-5.3172	-5.6172	-5.6472	-6.0738	-6.4438	-6.5072	-5.8738
6B	8.7195	5.3495	4.4628	4.4128	3.3428	1.9662	-4.6838	-4.9838	-5.0138	-5.4405	-5.8105	-5.8738	-6.5072

Positive values show pairs of means that are significantly different.

Level				Mean
6FC	A			119.43667
4F	A	B		116.06667
4FC	A	B		115.18000
6F	A	B		115.13000
2F	A	B		114.06000
2FC		B		112.68333
4BC			C	106.03333
2BC			C	105.73333
6BC			C	105.70333
UF			C	105.27667
2B			C	104.90667
4B			C	104.84333
6B			C	104.21000

Levels not connected by same letter are significantly different.

Level	- Level	Difference	Std Err Dif	Lower CL	Upper CL	p-Value	Difference

Level	- Level	Difference	Std Err Dif	Lower CL	Upper CL	p-Value	Difference
6FC	6B	15.22667	1.790614	8.71950	21.73383	<.0001*	
6FC	4B	14.59333	1.790614	8.08617	21.10050	<.0001*	
6FC	2B	14.53000	1.790614	8.02284	21.03716	<.0001*	
6FC	UF	14.16000	1.790614	7.65284	20.66716	<.0001*	
6FC	6BC	13.73333	1.790614	7.22617	20.24050	<.0001*	
6FC	2BC	13.70333	1.790614	7.19617	20.21050	<.0001*	
6FC	4BC	13.40333	1.790614	6.89617	19.91050	<.0001*	
4F	6B	11.85667	1.790614	5.34950	18.36383	<.0001*	
4F	4B	11.22333	1.790614	4.71617	17.73050	<.0001*	
4F	2B	11.16000	1.790614	4.65284	17.66716	<.0001*	
4FC	6B	10.97000	1.790614	4.46284	17.47716	0.0001*	
6F	6B	10.92000	1.790614	4.41284	17.42716	0.0001*	
4F	UF	10.79000	1.790614	4.28284	17.29716	0.0001*	
4F	6BC	10.36333	1.790614	3.85617	16.87050	0.0003*	
4FC	4B	10.33667	1.790614	3.82950	16.84383	0.0003*	
4F	2BC	10.33333	1.790614	3.82617	16.84050	0.0003*	
6F	4B	10.28667	1.790614	3.77950	16.79383	0.0003*	
4FC	2B	10.27333	1.790614	3.76617	16.78050	0.0003*	
6F	2B	10.22333	1.790614	3.71617	16.73050	0.0003*	
4F	4BC	10.03333	1.790614	3.52617	16.54050	0.0004*	
4FC	UF	9.90333	1.790614	3.39617	16.41050	0.0005*	
6F	UF	9.85333	1.790614	3.34617	16.36050	0.0005*	
2F	6B	9.85000	1.790614	3.34284	16.35716	0.0005*	
4FC	6BC	9.47667	1.790614	2.96950	15.98383	0.0009*	
4FC	2BC	9.44667	1.790614	2.93950	15.95383	0.0009*	
6F	6BC	9.42667	1.790614	2.91950	15.93383	0.0010*	
6F	2BC	9.39667	1.790614	2.88950	15.90383	0.0010*	
2F	4B	9.21667	1.790614	2.70950	15.72383	0.0013*	
2F	2B	9.15333	1.790614	2.64617	15.66050	0.0014*	
4FC	4BC	9.14667	1.790614	2.63950	15.65383	0.0014*	
6F	4BC	9.09667	1.790614	2.58950	15.60383	0.0015*	
2F	UF	8.78333	1.790614	2.27617	15.29050	0.0024*	
2FC	6B	8.47333	1.790614	1.96617	14.98050	0.0037*	
2F	6BC	8.35667	1.790614	1.84950	14.86383	0.0043*	
2F	2BC	8.32667	1.790614	1.81950	14.83383	0.0045*	
2F	4BC	8.02667	1.790614	1.51950	14.53383	0.0068*	
2FC	4B	7.84000	1.790614	1.33284	14.34716	0.0088*	
2FC	2B	7.77667	1.790614	1.26950	14.28383	0.0096*	
2FC	UF	7.40667	1.790614	0.89950	13.91383	0.0157*	
2FC	6BC	6.98000	1.790614	0.47284	13.48716	0.0275*	
2FC	2BC	6.95000	1.790614	0.44284	13.45716	0.0286*	
6FC	2FC	6.75333	1.790614	0.24617	13.26050	0.0368*	
2FC	4BC	6.65000	1.790614	0.14284	13.15716	0.0419*	
6FC	2F	5.37667	1.790614	-1.13050	11.88383	0.1818	
6FC	6F	4.30667	1.790614	-2.20050	10.81383	0.4703	
6FC	4FC	4.25667	1.790614	-2.25050	10.76383	0.4875	
4F	2FC	3.38333	1.790614	-3.12383	9.89050	0.7869	
6FC	4F	3.37000	1.790614	-3.13716	9.87716	0.7909	
4FC	2FC	2.49667	1.790614	-4.01050	9.00383	0.9659	
6F	2FC	2.44667	1.790614	-4.06050	8.95383	0.9705	
4F	2F	2.00667	1.790614	-4.50050	8.51383	0.9939	
4BC	6B	1.82333	1.790614	-4.68383	8.33050	0.9974	
2BC	6B	1.52333	1.790614	-4.98383	8.03050	0.9995	
6BC	6B	1.49333	1.790614	-5.01383	8.00050	0.9996	
2F	2FC	1.37667	1.790614	-5.13050	7.88383	0.9998	
4BC	4B	1.19000	1.790614	-5.31716	7.69716	1.0000	
4BC	2B	1.12667	1.790614	-5.38050	7.63383	1.0000	
4FC	2F	1.12000	1.790614	-5.38716	7.62716	1.0000	
6F	2F	1.07000	1.790614	-5.43716	7.57716	1.0000	
UF	6B	1.06667	1.790614	-5.44050	7.57383	1.0000	

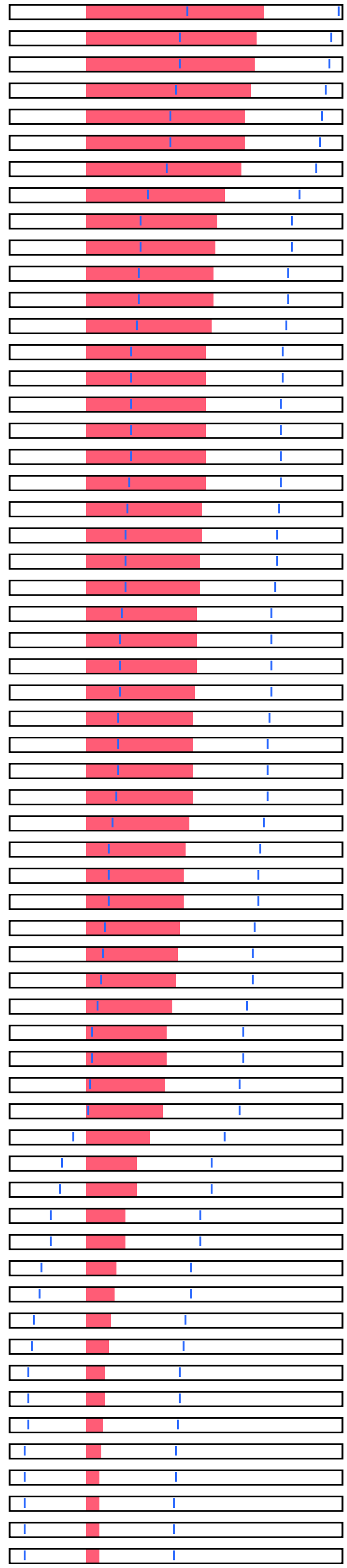

Level	- Level	Difference	Std Err Dif	Lower CL	Upper CL	p-Value	Difference
4F	6F	0.93667	1.790614	-5.57050	7.44383	1.0000	
2BC	4B	0.89000	1.790614	-5.61716	7.39716	1.0000	
4F	4FC	0.88667	1.790614	-5.62050	7.39383	1.0000	
6BC	4B	0.86000	1.790614	-5.64716	7.36716	1.0000	
2BC	2B	0.82667	1.790614	-5.68050	7.33383	1.0000	
6BC	2B	0.79667	1.790614	-5.71050	7.30383	1.0000	
4BC	UF	0.75667	1.790614	-5.75050	7.26383	1.0000	
2B	6B	0.69667	1.790614	-5.81050	7.20383	1.0000	
4B	6B	0.63333	1.790614	-5.87383	7.14050	1.0000	
2BC	UF	0.45667	1.790614	-6.05050	6.96383	1.0000	
UF	4B	0.43333	1.790614	-6.07383	6.94050	1.0000	
6BC	UF	0.42667	1.790614	-6.08050	6.93383	1.0000	
UF	2B	0.37000	1.790614	-6.13716	6.87716	.	
4BC	6BC	0.33000	1.790614	-6.17716	6.83716	.	
4BC	2BC	0.30000	1.790614	-6.20716	6.80716	.	
2B	4B	0.06333	1.790614	-6.44383	6.57050	.	
4FC	6F	0.05000	1.790614	-6.45716	6.55716	.	
2BC	6BC	0.03000	1.790614	-6.47716	6.53716	.	

MF resin DSC test

Oneway Analysis of Peak Temperature By TREATMENT

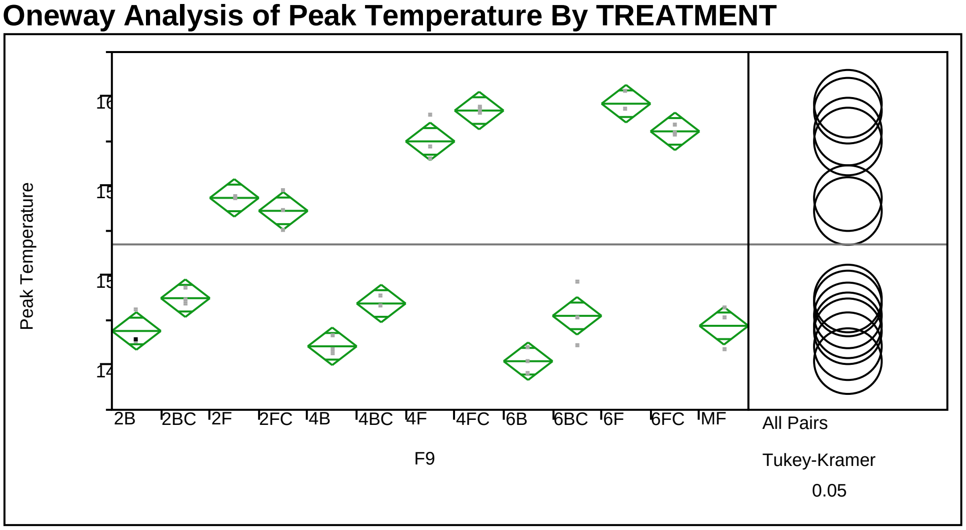

Missing Rows
3

Means Comparisons
Comparisons for all pairs using Tukey-Kramer HSD

q*	Alpha
3.63404	0.05

Abs(Dif)-HSD	6F	4FC	6FC	4F	2F	2FC	2BC	4BC	6BC	MF	2B	4B	6B
6F	-2.628	-2.245	-1.081	-0.521	2.639	3.362	8.245	8.542	9.232	9.789	10.079	10.935	11.769
4FC	-2.245	-2.628	-1.465	-0.905	2.255	2.979	7.862	8.159	8.849	9.405	9.695	10.552	11.385
6FC	-1.081	-1.465	-2.628	-2.068	1.092	1.815	6.699	6.995	7.685	8.242	8.532	9.389	10.222
4F	-0.521	-0.905	-2.068	-2.628	0.532	1.255	6.139	6.435	7.125	7.682	7.972	8.829	9.662
2F	2.639	2.255	1.092	0.532	-2.628	-1.905	2.979	3.275	3.965	4.522	4.812	5.669	6.502

Abs(Dif)-HSD	6F	4FC	6FC	4F	2F	2FC	2BC	4BC	6BC	MF	2B	4B	6B
2FC	3.362	2.979	1.815	1.255	-1.905	-2.628	2.255	2.552	3.242	3.799	4.089	4.945	5.779
2BC	8.245	7.862	6.699	6.139	2.979	2.255	-2.628	-2.331	-1.641	-1.085	-0.795	0.062	0.895
4BC	8.542	8.159	6.995	6.435	3.275	2.552	-2.331	-2.628	-1.938	-1.381	-1.091	-0.235	0.599
6BC	9.232	8.849	7.685	7.125	3.965	3.242	-1.641	-1.938	-2.628	-2.071	-1.781	-0.925	-0.091
MF	9.789	9.405	8.242	7.682	4.522	3.799	-1.085	-1.381	-2.071	-2.628	-2.338	-1.481	-0.648
2B	10.079	9.695	8.532	7.972	4.812	4.089	-0.795	-1.091	-1.781	-2.338	-2.628	-1.771	-0.938
4B	10.935	10.552	9.389	8.829	5.669	4.945	0.062	-0.235	-0.925	-1.481	-1.771	-2.628	-1.795
6B	11.769	11.385	10.222	9.662	6.502	5.779	0.895	0.599	-0.091	-0.648	-0.938	-1.795	-2.628

Positive values show pairs of means that are significantly different.

Level					Mean
6F	A				159.61333
4FC	A				159.23000
6FC	A				158.06667
4F	A				157.50667
2F		B			154.34667
2FC		B			153.62333
2BC			C		148.74000
4BC			C	D	148.44333
6BC			C	D E	147.75333
MF			C	D E	147.19667
2B			C	D E	146.90667
4B				D E	146.05000
6B				E	145.21667

Levels not connected by same letter are significantly different.

Level	- Level	Difference	Std Err Dif	Lower CL	Upper CL	p-Value
6F	6B	14.39667	0.7231354	11.7688	17.02457	<.0001*
4FC	6B	14.01333	0.7231354	11.3854	16.64124	<.0001*
6F	4B	13.56333	0.7231354	10.9354	16.19124	<.0001*
4FC	4B	13.18000	0.7231354	10.5521	15.80790	<.0001*
6FC	6B	12.85000	0.7231354	10.2221	15.47790	<.0001*
6F	2B	12.70667	0.7231354	10.0788	15.33457	<.0001*
6F	MF	12.41667	0.7231354	9.7888	15.04457	<.0001*
4FC	2B	12.32333	0.7231354	9.6954	14.95124	<.0001*
4F	6B	12.29000	0.7231354	9.6621	14.91790	<.0001*
4FC	MF	12.03333	0.7231354	9.4054	14.66124	<.0001*
6FC	4B	12.01667	0.7231354	9.3888	14.64457	<.0001*
6F	6BC	11.86000	0.7231354	9.2321	14.48790	<.0001*
4FC	6BC	11.47667	0.7231354	8.8488	14.10457	<.0001*
4F	4B	11.45667	0.7231354	8.8288	14.08457	<.0001*
6F	4BC	11.17000	0.7231354	8.5421	13.79790	<.0001*
6FC	2B	11.16000	0.7231354	8.5321	13.78790	<.0001*
6F	2BC	10.87333	0.7231354	8.2454	13.50124	<.0001*
6FC	MF	10.87000	0.7231354	8.2421	13.49790	<.0001*
4FC	4BC	10.78667	0.7231354	8.1588	13.41457	<.0001*
4F	2B	10.60000	0.7231354	7.9721	13.22790	<.0001*
4FC	2BC	10.49000	0.7231354	7.8621	13.11790	<.0001*
6FC	6BC	10.31333	0.7231354	7.6854	12.94124	<.0001*
4F	MF	10.31000	0.7231354	7.6821	12.93790	<.0001*
4F	6BC	9.75333	0.7231354	7.1254	12.38124	<.0001*
6FC	4BC	9.62333	0.7231354	6.9954	12.25124	<.0001*
6FC	2BC	9.32667	0.7231354	6.6988	11.95457	<.0001*
2F	6B	9.13000	0.7231354	6.5021	11.75790	<.0001*
4F	4BC	9.06333	0.7231354	6.4354	11.69124	<.0001*
4F	2BC	8.76667	0.7231354	6.1388	11.39457	<.0001*

Difference

Level	- Level	Difference	Std Err Dif	Lower CL	Upper CL	p-Value	Difference
2FC	6B	8.40667	0.7231354	5.7788	11.03457	<.0001*	
2F	4B	8.29667	0.7231354	5.6688	10.92457	<.0001*	
2FC	4B	7.57333	0.7231354	4.9454	10.20124	<.0001*	
2F	2B	7.44000	0.7231354	4.8121	10.06790	<.0001*	
2F	MF	7.15000	0.7231354	4.5221	9.77790	<.0001*	
2FC	2B	6.71667	0.7231354	4.0888	9.34457	<.0001*	
2F	6BC	6.59333	0.7231354	3.9654	9.22124	<.0001*	
2FC	MF	6.42667	0.7231354	3.7988	9.05457	<.0001*	
6F	2FC	5.99000	0.7231354	3.3621	8.61790	<.0001*	
2F	4BC	5.90333	0.7231354	3.2754	8.53124	<.0001*	
2FC	6BC	5.87000	0.7231354	3.2421	8.49790	<.0001*	
4FC	2FC	5.60667	0.7231354	2.9788	8.23457	<.0001*	
2F	2BC	5.60667	0.7231354	2.9788	8.23457	<.0001*	
6F	2F	5.26667	0.7231354	2.6388	7.89457	<.0001*	
2FC	4BC	5.18000	0.7231354	2.5521	7.80790	<.0001*	
4FC	2F	4.88333	0.7231354	2.2554	7.51124	<.0001*	
2FC	2BC	4.88333	0.7231354	2.2554	7.51124	<.0001*	
6FC	2FC	4.44333	0.7231354	1.8154	7.07124	0.0001*	
4F	2FC	3.88333	0.7231354	1.2554	6.51124	0.0007*	
6FC	2F	3.72000	0.7231354	1.0921	6.34790	0.0013*	
2BC	6B	3.52333	0.7231354	0.8954	6.15124	0.0026*	
4BC	6B	3.22667	0.7231354	0.5988	5.85457	0.0072*	
4F	2F	3.16000	0.7231354	0.5321	5.78790	0.0090*	
2BC	4B	2.69000	0.7231354	0.0621	5.31790	0.0413*	
6BC	6B	2.53667	0.7231354	-0.0912	5.16457	0.0658	
4BC	4B	2.39333	0.7231354	-0.2346	5.02124	0.0999	
6F	4F	2.10667	0.7231354	-0.5212	4.73457	0.2138	
MF	6B	1.98000	0.7231354	-0.6479	4.60790	0.2883	
2BC	2B	1.83333	0.7231354	-0.7946	4.46124	0.3936	
4FC	4F	1.72333	0.7231354	-0.9046	4.35124	0.4838	
6BC	4B	1.70333	0.7231354	-0.9246	4.33124	0.5010	
2B	6B	1.69000	0.7231354	-0.9379	4.31790	0.5125	
6F	6FC	1.54667	0.7231354	-1.0812	4.17457	0.6384	
2BC	MF	1.54333	0.7231354	-1.0846	4.17124	0.6413	
4BC	2B	1.53667	0.7231354	-1.0912	4.16457	0.6471	
4BC	MF	1.24667	0.7231354	-1.3812	3.87457	0.8674	
4FC	6FC	1.16333	0.7231354	-1.4646	3.79124	0.9115	
MF	4B	1.14667	0.7231354	-1.4812	3.77457	0.9190	
2BC	6BC	0.98667	0.7231354	-1.6412	3.61457	0.9708	
2B	4B	0.85667	0.7231354	-1.7712	3.48457	0.9903	
6BC	2B	0.84667	0.7231354	-1.7812	3.47457	0.9912	
4B	6B	0.83333	0.7231354	-1.7946	3.46124	0.9923	
2F	2FC	0.72333	0.7231354	-1.9046	3.35124	0.9978	
4BC	6BC	0.69000	0.7231354	-1.9379	3.31790	0.9986	
6FC	4F	0.56000	0.7231354	-2.0679	3.18790	0.9998	
6BC	MF	0.55667	0.7231354	-2.0712	3.18457	0.9998	
6F	4FC	0.38333	0.7231354	-2.2446	3.01124	1.0000	
2BC	4BC	0.29667	0.7231354	-2.3312	2.92457	1.0000	
MF	2B	0.29000	0.7231354	-2.3379	2.91790	1.0000	

Oneway Analysis of ΔH By F9

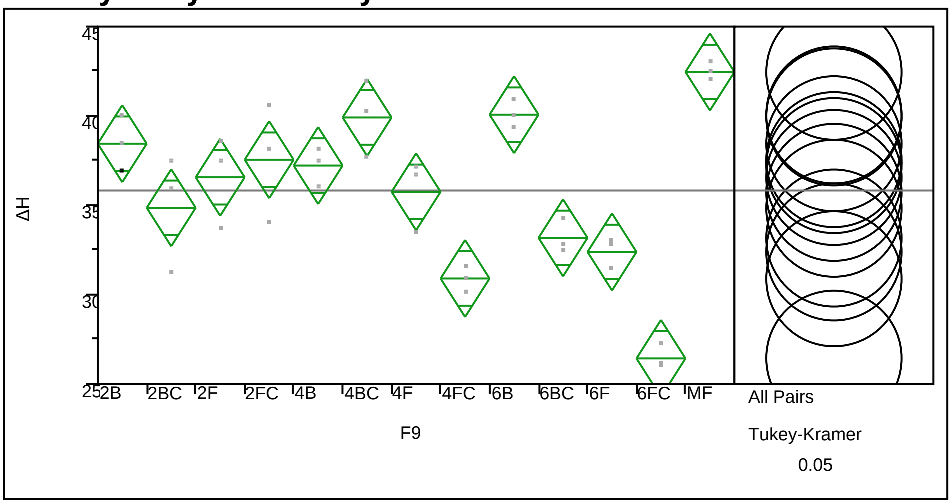

Missing Rows
3

Means Comparisons
Comparisons for all pairs using Tukey-Kramer HSD

q*	Alpha
3.63404	0.05

Abs(Dif)-HSD	MF	6B	4BC	2B	2FC	4B	2F	4F	2BC	6BC	6F	4FC	6FC
MF	-5.387	-2.997	-2.840	-1.373	-0.477	-0.150	0.507	1.320	2.213	3.897	4.683	6.170	10.643
6B	-2.997	-5.387	-5.230	-3.763	-2.867	-2.540	-1.883	-1.070	-0.177	1.507	2.293	3.780	8.253
4BC	-2.840	-5.230	-5.387	-3.920	-3.023	-2.697	-2.040	-1.227	-0.333	1.350	2.137	3.623	8.097
2B	-1.373	-3.763	-3.920	-5.387	-4.490	-4.163	-3.507	-2.693	-1.800	-0.117	0.670	2.157	6.630
2FC	-0.477	-2.867	-3.023	-4.490	-5.387	-5.060	-4.403	-3.590	-2.697	-1.013	-0.227	1.260	5.733
4B	-0.150	-2.540	-2.697	-4.163	-5.060	-5.387	-4.730	-3.917	-3.023	-1.340	-0.553	0.933	5.407
2F	0.507	-1.883	-2.040	-3.507	-4.403	-4.730	-5.387	-4.573	-3.680	-1.997	-1.210	0.277	4.750
4F	1.320	-1.070	-1.227	-2.693	-3.590	-3.917	-4.573	-5.387	-4.493	-2.810	-2.023	-0.537	3.937
2BC	2.213	-0.177	-0.333	-1.800	-2.697	-3.023	-3.680	-4.493	-5.387	-3.703	-2.917	-1.430	3.043
6BC	3.897	1.507	1.350	-0.117	-1.013	-1.340	-1.997	-2.810	-3.703	-5.387	-4.600	-3.113	1.360
6F	4.683	2.293	2.137	0.670	-0.227	-0.553	-1.210	-2.023	-2.917	-4.600	-5.387	-3.900	0.573
4FC	6.170	3.780	3.623	2.157	1.260	0.933	0.277	-0.537	-1.430	-3.113	-3.900	-5.387	-0.913
6FC	10.643	8.253	8.097	6.630	5.733	5.407	4.750	3.937	3.043	1.360	0.573	-0.913	-5.387

Positive values show pairs of means that are significantly different.

Level							Mean
MF	A						42.460000
6B	A	B					40.070000
4BC	A	B					39.913333
2B	A	B	C				38.446667
2FC	A	B	C	D			37.550000
4B	A	B	C	D			37.223333
2F		B	C	D			36.566667
4F		B	C	D	E		35.753333
2BC		B	C	D	E		34.860000
6BC			C	D	E		33.176667
6F				D	E		32.390000
4FC					E	F	30.903333

Level		Mean
6FC	F	26.430000

Levels not connected by same letter are significantly different.

Level	- Level	Difference	Std Err Dif	Lower CL	Upper CL	p-Value	Difference
MF	6FC	16.03000	1.482270	10.6434	21.41663	<.0001*	
6B	6FC	13.64000	1.482270	8.2534	19.02663	<.0001*	
4BC	6FC	13.48333	1.482270	8.0967	18.86996	<.0001*	
2B	6FC	12.01667	1.482270	6.6300	17.40330	<.0001*	
MF	4FC	11.55667	1.482270	6.1700	16.94330	<.0001*	
2FC	6FC	11.12000	1.482270	5.7334	16.50663	<.0001*	
4B	6FC	10.79333	1.482270	5.4067	16.17996	<.0001*	
2F	6FC	10.13667	1.482270	4.7500	15.52330	<.0001*	
MF	6F	10.07000	1.482270	4.6834	15.45663	<.0001*	
4F	6FC	9.32333	1.482270	3.9367	14.70996	<.0001*	
MF	6BC	9.28333	1.482270	3.8967	14.66996	<.0001*	
6B	4FC	9.16667	1.482270	3.7800	14.55330	<.0001*	
4BC	4FC	9.01000	1.482270	3.6234	14.39663	0.0001*	
2BC	6FC	8.43000	1.482270	3.0434	13.81663	0.0003*	
6B	6F	7.68000	1.482270	2.2934	13.06663	0.0012*	
MF	2BC	7.60000	1.482270	2.2134	12.98663	0.0014*	
2B	4FC	7.54333	1.482270	2.1567	12.92996	0.0015*	
4BC	6F	7.52333	1.482270	2.1367	12.90996	0.0016*	
6B	6BC	6.89333	1.482270	1.5067	12.27996	0.0045*	
6BC	6FC	6.74667	1.482270	1.3600	12.13330	0.0058*	
4BC	6BC	6.73667	1.482270	1.3500	12.12330	0.0059*	
MF	4F	6.70667	1.482270	1.3200	12.09330	0.0062*	
2FC	4FC	6.64667	1.482270	1.2600	12.03330	0.0068*	
4B	4FC	6.32000	1.482270	0.9334	11.70663	0.0116*	
2B	6F	6.05667	1.482270	0.6700	11.44330	0.0177*	
6F	6FC	5.96000	1.482270	0.5734	11.34663	0.0207*	
MF	2F	5.89333	1.482270	0.5067	11.27996	0.0230*	
2F	4FC	5.66333	1.482270	0.2767	11.04996	0.0329*	
2B	6BC	5.27000	1.482270	-0.1166	10.65663	0.0594	
MF	4B	5.23667	1.482270	-0.1500	10.62330	0.0624	
6B	2BC	5.21000	1.482270	-0.1766	10.59663	0.0649	
2FC	6F	5.16000	1.482270	-0.2266	10.54663	0.0697	
4BC	2BC	5.05333	1.482270	-0.3333	10.43996	0.0812	
MF	2FC	4.91000	1.482270	-0.4766	10.29663	0.0993	
4F	4FC	4.85000	1.482270	-0.5366	10.23663	0.1078	
4B	6F	4.83333	1.482270	-0.5533	10.21996	0.1103	
4FC	6FC	4.47333	1.482270	-0.9133	9.85996	0.1767	
2FC	6BC	4.37333	1.482270	-1.0133	9.75996	0.2000	
6B	4F	4.31667	1.482270	-1.0700	9.70330	0.2142	
2F	6F	4.17667	1.482270	-1.2100	9.56330	0.2525	
4BC	4F	4.16000	1.482270	-1.2266	9.54663	0.2573	
4B	6BC	4.04667	1.482270	-1.3400	9.43330	0.2921	
MF	2B	4.01333	1.482270	-1.3733	9.39996	0.3029	
2BC	4FC	3.95667	1.482270	-1.4300	9.34330	0.3218	
2B	2BC	3.58667	1.482270	-1.8000	8.97330	0.4615	
6B	2F	3.50333	1.482270	-1.8833	8.88996	0.4960	
2F	6BC	3.39000	1.482270	-1.9966	8.77663	0.5441	
4F	6F	3.36333	1.482270	-2.0233	8.74996	0.5555	
4BC	2F	3.34667	1.482270	-2.0400	8.73330	0.5627	
6B	4B	2.84667	1.482270	-2.5400	8.23330	0.7699	
2B	4F	2.69333	1.482270	-2.6933	8.07996	0.8245	
4BC	4B	2.69000	1.482270	-2.6966	8.07663	0.8256	
2FC	2BC	2.69000	1.482270	-2.6966	8.07663	0.8256	
4F	6BC	2.57667	1.482270	-2.8100	7.96330	0.8612	
MF	4BC	2.54667	1.482270	-2.8400	7.93330	0.8699	

Level	- Level	Difference	Std Err Dif	Lower CL	Upper CL	p-Value	Difference
6B	2FC	2.52000	1.482270	-2.8666	7.90663	0.8774	
2BC	6F	2.47000	1.482270	-2.9166	7.85663	0.8908	
MF	6B	2.39000	1.482270	-2.9966	7.77663	0.9102	
4BC	2FC	2.36333	1.482270	-3.0233	7.74996	0.9162	
4B	2BC	2.36333	1.482270	-3.0233	7.74996	0.9162	
6BC	4FC	2.27333	1.482270	-3.1133	7.65996	0.9345	
2B	2F	1.88000	1.482270	-3.5066	7.26663	0.9832	
2FC	4F	1.79667	1.482270	-3.5900	7.18330	0.9883	
2F	2BC	1.70667	1.482270	-3.6800	7.09330	0.9924	
2BC	6BC	1.68333	1.482270	-3.7033	7.06996	0.9932	
6B	2B	1.62333	1.482270	-3.7633	7.00996	0.9950	
6F	4FC	1.48667	1.482270	-3.9000	6.87330	0.9977	
4B	4F	1.47000	1.482270	-3.9166	6.85663	0.9980	
4BC	2B	1.46667	1.482270	-3.9200	6.85330	0.9980	
2B	4B	1.22333	1.482270	-4.1633	6.60996	0.9996	
2FC	2F	0.98333	1.482270	-4.4033	6.36996	1.0000	
2B	2FC	0.89667	1.482270	-4.4900	6.28330	1.0000	
4F	2BC	0.89333	1.482270	-4.4933	6.27996	1.0000	
2F	4F	0.81333	1.482270	-4.5733	6.19996	1.0000	
6BC	6F	0.78667	1.482270	-4.6000	6.17330	1.0000	
4B	2F	0.65667	1.482270	-4.7300	6.04330	1.0000	
2FC	4B	0.32667	1.482270	-5.0600	5.71330	1.0000	
6B	4BC	0.15667	1.482270	-5.2300	5.54330	.	

Oneway Analysis of Onset temperature By F9

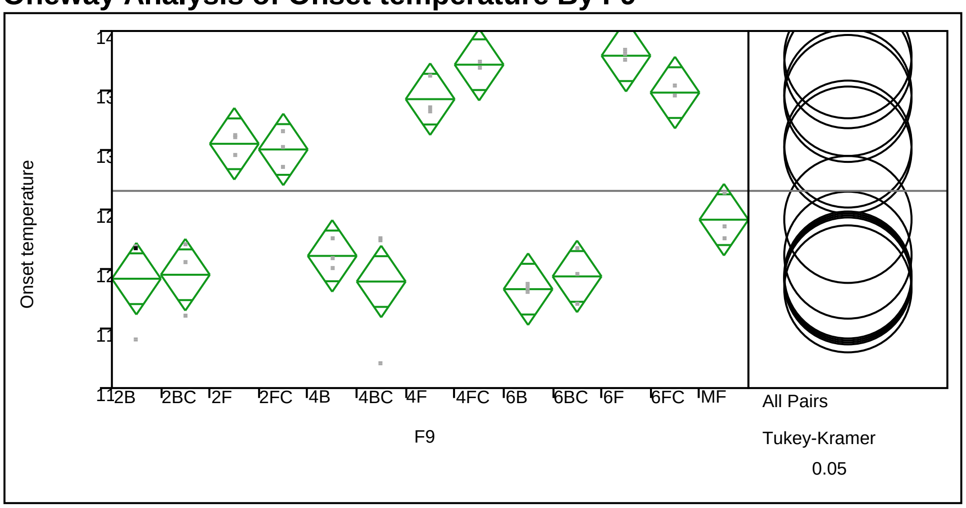

Missing Rows
3

Means Comparisons

Comparisons for all pairs using Tukey-Kramer HSD

q*	Alpha
3.63404	0.05

Abs(Dif)-HSD	6F	4FC	6FC	4F	2F	2FC	MF	4B	2BC	6BC	2B	4BC	6B
6F	-7.531	-6.777	-4.431	-3.881	-0.131	0.347	6.246	9.289	10.873	11.013	11.206	11.443	12.083
4FC	-6.777	-7.531	-5.184	-4.634	-0.884	-0.407	5.493	8.536	10.119	10.259	10.453	10.689	11.329
6FC	-4.431	-5.184	-7.531	-6.981	-3.231	-2.753	3.146	6.189	7.773	7.913	8.106	8.343	8.983
4F	-3.881	-4.634	-6.981	-7.531	-3.781	-3.303	2.596	5.639	7.223	7.363	7.556	7.793	8.433
2F	-0.131	-0.884	-3.231	-3.781	-7.531	-7.053	-1.154	1.889	3.473	3.613	3.806	4.043	4.683
2FC	0.347	-0.407	-2.753	-3.303	-7.053	-7.531	-1.631	1.412	2.995	3.135	3.329	3.565	4.205

Abs(Dif)-HSD	6F	4FC	6FC	4F	2F	2FC	MF	4B	2BC	6BC	2B	4BC	6B
MF	6.246	5.493	3.146	2.596	-1.154	-1.631	-7.531	-4.487	-2.904	-2.764	-2.571	-2.334	-1.694
4B	9.289	8.536	6.189	5.639	1.889	1.412	-4.487	-7.531	-5.947	-5.807	-5.614	-5.377	-4.737
2BC	10.873	10.119	7.773	7.223	3.473	2.995	-2.904	-5.947	-7.531	-7.391	-7.197	-6.961	-6.321
6BC	11.013	10.259	7.913	7.363	3.613	3.135	-2.764	-5.807	-7.391	-7.531	-7.337	-7.101	-6.461
2B	11.206	10.453	8.106	7.556	3.806	3.329	-2.571	-5.614	-7.197	-7.337	-7.531	-7.294	-6.654
4BC	11.443	10.689	8.343	7.793	4.043	3.565	-2.334	-5.377	-6.961	-7.101	-7.294	-7.531	-6.891
6B	12.083	11.329	8.983	8.433	4.683	4.205	-1.694	-4.737	-6.321	-6.461	-6.654	-6.891	-7.531

Positive values show pairs of means that are significantly different.

Level					Mean
6F	A				137.92333
4FC	A	B			137.17000
6FC	A	B			134.82333
4F	A	B			134.27333
2F	A	B	C		130.52333
2FC		B	C		130.04600
MF			C	D	124.14667
4B				D	121.10333
2BC				D	119.52000
6BC				D	119.38000
2B				D	119.18667
4BC				D	118.95000
6B				D	118.31000

Levels not connected by same letter are significantly different.

Level	- Level	Difference	Std Err Dif	Lower CL	Upper CL	p-Value	Difference
6F	6B	19.61333	2.072272	12.0826	27.14405	<.0001*	
6F	4BC	18.97333	2.072272	11.4426	26.50405	<.0001*	
4FC	6B	18.86000	2.072272	11.3293	26.39072	<.0001*	
6F	2B	18.73667	2.072272	11.2059	26.26739	<.0001*	
6F	6BC	18.54333	2.072272	11.0126	26.07405	<.0001*	
6F	2BC	18.40333	2.072272	10.8726	25.93405	<.0001*	
4FC	4BC	18.22000	2.072272	10.6893	25.75072	<.0001*	
4FC	2B	17.98333	2.072272	10.4526	25.51405	<.0001*	
4FC	6BC	17.79000	2.072272	10.2593	25.32072	<.0001*	
4FC	2BC	17.65000	2.072272	10.1193	25.18072	<.0001*	
6F	4B	16.82000	2.072272	9.2893	24.35072	<.0001*	
6FC	6B	16.51333	2.072272	8.9826	24.04405	<.0001*	
4FC	4B	16.06667	2.072272	8.5359	23.59739	<.0001*	
4F	6B	15.96333	2.072272	8.4326	23.49405	<.0001*	
6FC	4BC	15.87333	2.072272	8.3426	23.40405	<.0001*	
6FC	2B	15.63667	2.072272	8.1059	23.16739	<.0001*	
6FC	6BC	15.44333	2.072272	7.9126	22.97405	<.0001*	
4F	4BC	15.32333	2.072272	7.7926	22.85405	<.0001*	
6FC	2BC	15.30333	2.072272	7.7726	22.83405	<.0001*	
4F	2B	15.08667	2.072272	7.5559	22.61739	<.0001*	
4F	6BC	14.89333	2.072272	7.3626	22.42405	<.0001*	
4F	2BC	14.75333	2.072272	7.2226	22.28405	<.0001*	
6F	MF	13.77667	2.072272	6.2459	21.30739	<.0001*	
6FC	4B	13.72000	2.072272	6.1893	21.25072	<.0001*	
4F	4B	13.17000	2.072272	5.6393	20.70072	<.0001*	
4FC	MF	13.02333	2.072272	5.4926	20.55405	<.0001*	
2F	6B	12.21333	2.072272	4.6826	19.74405	0.0002*	
2FC	6B	11.73600	2.072272	4.2053	19.26672	0.0004*	
2F	4BC	11.57333	2.072272	4.0426	19.10405	0.0004*	
2F	2B	11.33667	2.072272	3.8059	18.86739	0.0006*	

Level	- Level	Difference	Std Err Dif	Lower CL	Upper CL	p-Value	Difference
2F	6BC	11.14333	2.072272	3.6126	18.67405	0.0007*	
2FC	4BC	11.09600	2.072272	3.5653	18.62672	0.0008*	
2F	2BC	11.00333	2.072272	3.4726	18.53405	0.0009*	
2FC	2B	10.85933	2.072272	3.3286	18.39005	0.0010*	
6FC	MF	10.67667	2.072272	3.1459	18.20739	0.0013*	
2FC	6BC	10.66600	2.072272	3.1353	18.19672	0.0013*	
2FC	2BC	10.52600	2.072272	2.9953	18.05672	0.0015*	
4F	MF	10.12667	2.072272	2.5959	17.65739	0.0025*	
2F	4B	9.42000	2.072272	1.8893	16.95072	0.0058*	
2FC	4B	8.94267	2.072272	1.4119	16.47339	0.0102*	
6F	2FC	7.87733	2.072272	0.3466	15.40805	0.0344*	
6F	2F	7.40000	2.072272	-0.1307	14.93072	0.0574	
4FC	2FC	7.12400	2.072272	-0.4067	14.65472	0.0765	
4FC	2F	6.64667	2.072272	-0.8841	14.17739	0.1227	
2F	MF	6.37667	2.072272	-1.1541	13.90739	0.1581	
2FC	MF	5.89933	2.072272	-1.6314	13.43005	0.2402	
MF	6B	5.83667	2.072272	-1.6941	13.36739	0.2530	
MF	4BC	5.19667	2.072272	-2.3341	12.72739	0.4094	
MF	2B	4.96000	2.072272	-2.5707	12.49072	0.4775	
6FC	2FC	4.77733	2.072272	-2.7534	12.30805	0.5325	
MF	6BC	4.76667	2.072272	-2.7641	12.29739	0.5357	
MF	2BC	4.62667	2.072272	-2.9041	12.15739	0.5787	
6FC	2F	4.30000	2.072272	-3.2307	11.83072	0.6784	
4F	2FC	4.22733	2.072272	-3.3034	11.75805	0.7000	
4F	2F	3.75000	2.072272	-3.7807	11.28072	0.8281	
6F	4F	3.65000	2.072272	-3.8807	11.18072	0.8509	
6F	6FC	3.10000	2.072272	-4.4307	10.63072	0.9444	
MF	4B	3.04333	2.072272	-4.4874	10.57405	0.9509	
4FC	4F	2.89667	2.072272	-4.6341	10.42739	0.9652	
4B	6B	2.79333	2.072272	-4.7374	10.32405	0.9733	
4FC	6FC	2.34667	2.072272	-5.1841	9.87739	0.9934	
4B	4BC	2.15333	2.072272	-5.3774	9.68405	0.9969	
4B	2B	1.91667	2.072272	-5.6141	9.44739	0.9989	
4B	6BC	1.72333	2.072272	-5.8074	9.25405	0.9996	
4B	2BC	1.58333	2.072272	-5.9474	9.11405	0.9998	
2BC	6B	1.21000	2.072272	-6.3207	8.74072	1.0000	
6BC	6B	1.07000	2.072272	-6.4607	8.60072	1.0000	
2B	6B	0.87667	2.072272	-6.6541	8.40739	1.0000	
6F	4FC	0.75333	2.072272	-6.7774	8.28405	1.0000	
4BC	6B	0.64000	2.072272	-6.8907	8.17072	1.0000	
2BC	4BC	0.57000	2.072272	-6.9607	8.10072	1.0000	
6FC	4F	0.55000	2.072272	-6.9807	8.08072	1.0000	
2F	2FC	0.47733	2.072272	-7.0534	8.00805	1.0000	
6BC	4BC	0.43000	2.072272	-7.1007	7.96072	.	
2BC	2B	0.33333	2.072272	-7.1974	7.86405	.	
2B	4BC	0.23667	2.072272	-7.2941	7.76739	.	
6BC	2B	0.19333	2.072272	-7.3374	7.72405	.	
2BC	6BC	0.14000	2.072272	-7.3907	7.67072	.	

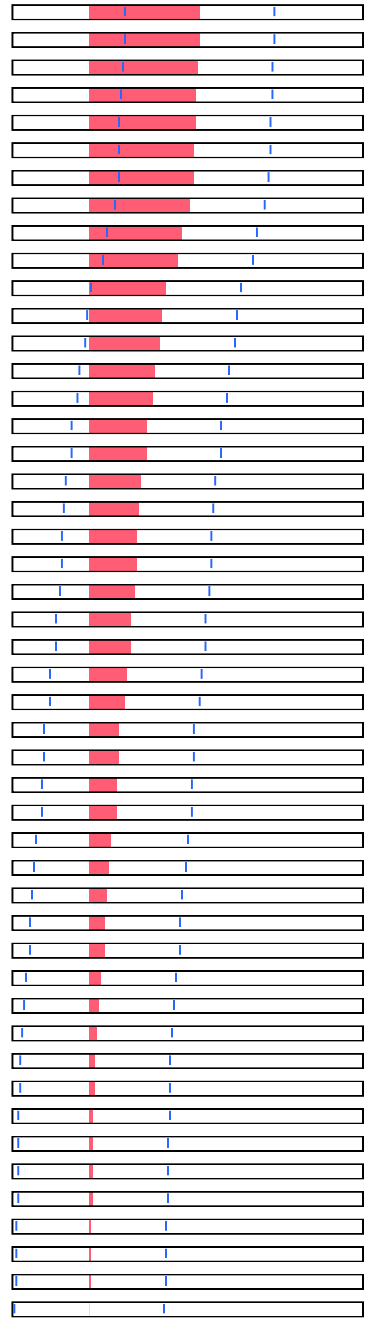

Appendix B: Statistical analysis result of Lap-shear test

UF resin Lap shear test

Oneway Analysis of UF_resin By Sample name

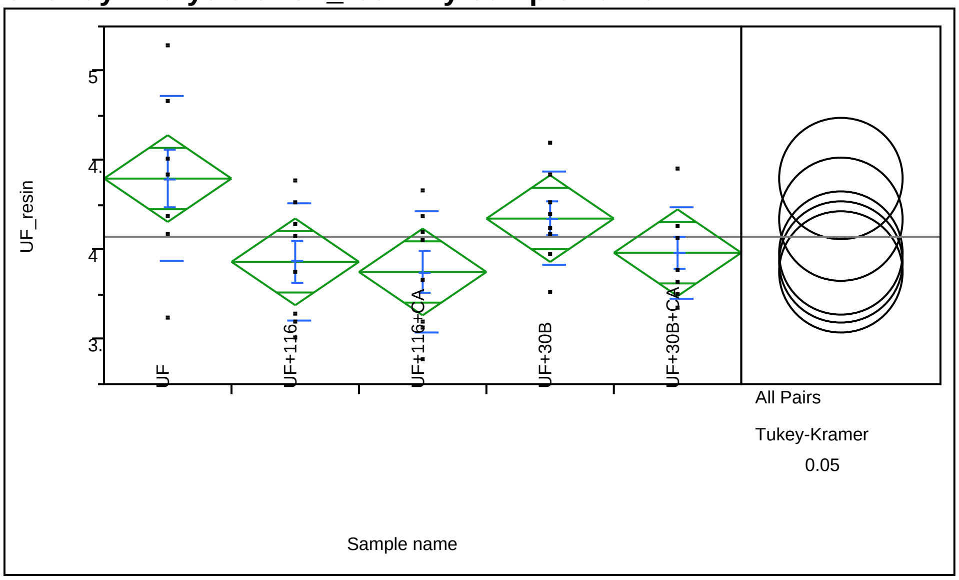

Means Comparisons

Comparisons for all pairs using Tukey-Kramer HSD

q*	Alpha
2.87506	0.05

Abs(Dif)-HSD	UF	UF+30B	UF+30B+CA	UF+116	UF+116+CA
UF	-0.48535	-0.26160	-0.07048	-0.01973	0.03690
UF+30B	-0.26160	-0.48535	-0.29423	-0.24348	-0.18685
UF+30B+CA	-0.07048	-0.29423	-0.48535	-0.43460	-0.37798
UF+116	-0.01973	-0.24348	-0.43460	-0.48535	-0.42873
UF+116+CA	0.03690	-0.18685	-0.37798	-0.42873	-0.48535

Positive values show pairs of means that are significantly different.

Level			Mean
UF	A		4.3995000
UF+30B	A	B	4.1757500
UF+30B+CA	A	B	3.9846250
UF+116	A	B	3.9338750
UF+116+CA		B	3.8772500

Levels not connected by same letter are significantly different.

Level	- Level	Difference	Std Err Dif	Lower CL	Upper CL	p-Value	Difference
UF	UF+116+CA	0.5222500	0.1688141	0.036899	1.007601	0.0297*	
UF	UF+116	0.4656250	0.1688141	-0.019726	0.950976	0.0653	
UF	UF+30B+CA	0.4148750	0.1688141	-0.070476	0.900226	0.1240	
UF+30B	UF+116+CA	0.2985000	0.1688141	-0.186851	0.783851	0.4076	
UF+30B	UF+116	0.2418750	0.1688141	-0.243476	0.727226	0.6113	

Level	- Level	Difference	Std Err Dif	Lower CL	Upper CL	p-Value	Difference
UF	UF+30B	0.2237500	0.1688141	-0.261601	0.709101	0.6776	
UF+30B	UF+30B+CA	0.1911250	0.1688141	-0.294226	0.676476	0.7885	
UF+30B+CA	UF+116+CA	0.1073750	0.1688141	-0.377976	0.592726	0.9681	
UF+116	UF+116+CA	0.0566250	0.1688141	-0.428726	0.541976	0.9971	
UF+30B+CA	UF+116	0.0507500	0.1688141	-0.434601	0.536101	0.9981	

MF Resin test

Oneway Analysis of MF_resin By Sample name

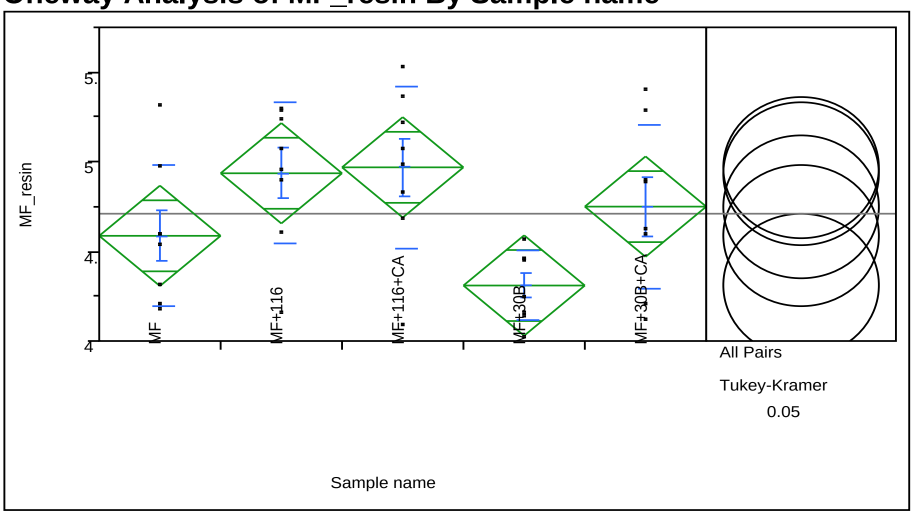

Means and Std Deviations

Level	Number	Mean	Std Dev	Std Err Mean	Lower 95%	Upper 95%
MF	8	4.58688	0.391489	0.13841	4.2596	4.9142
MF+116	8	4.93588	0.394249	0.13939	4.6063	5.2655
MF+116+CA	8	4.96900	0.450525	0.15928	4.5924	5.3456
MF+30B	8	4.30963	0.195046	0.06896	4.1466	4.4727
MF+30B+CA	8	4.74988	0.460388	0.16277	4.3650	5.1348

Means Comparisons

Comparisons for all pairs using Tukey-Kramer HSD

q*	Alpha
2.87506	0.05

Abs(Dif)-HSD	MF+116+CA	MF+116	MF+30B+CA	MF	MF+30B
MF+116+CA	-0.56107	-0.52794	-0.34194	-0.17894	0.09831
MF+116	-0.52794	-0.56107	-0.37507	-0.21207	0.06518
MF+30B+CA	-0.34194	-0.37507	-0.56107	-0.39807	-0.12082
MF	-0.17894	-0.21207	-0.39807	-0.56107	-0.28382
MF+30B	0.09831	0.06518	-0.12082	-0.28382	-0.56107

Positive values show pairs of means that are significantly different.

Level			Mean
MF+116+CA	A		4.9690000
MF+116	A		4.9358750
MF+30B+CA	A	B	4.7498750
MF	A	B	4.5868750
MF+30B		B	4.3096250

Levels not connected by same letter are significantly different.

Level	- Level	Difference	Std Err Dif	Lower CL	Upper CL	p-Value	Difference
MF+116+CA	MF+30B	0.6593750	0.1951497	0.098307	1.220443	0.0145*	
MF+116	MF+30B	0.6262500	0.1951497	0.065182	1.187318	0.0223*	
MF+30B+CA	MF+30B	0.4402500	0.1951497	-0.120818	1.001318	0.1836	
MF+116+CA	MF	0.3821250	0.1951497	-0.178943	0.943193	0.3071	
MF+116	MF	0.3490000	0.1951497	-0.212068	0.910068	0.3962	
MF	MF+30B	0.2772500	0.1951497	-0.283818	0.838318	0.6189	
MF+116+CA	MF+30B+CA	0.2191250	0.1951497	-0.341943	0.780193	0.7934	
MF+116	MF+30B+CA	0.1860000	0.1951497	-0.375068	0.747068	0.8739	
MF+30B+CA	MF	0.1630000	0.1951497	-0.398068	0.724068	0.9178	
MF+116+CA	MF+116	0.0331250	0.1951497	-0.527943	0.594193	0.9998	

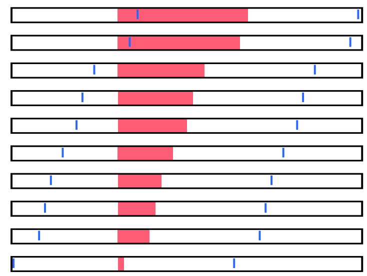

Appendix C: Statistical analysis result of PB properties test

MOR test

```
                          The SAS System                                 7
                                         16:38 Tuesday, March 22, 2011

                        The GLM Procedure

              Tukey's Studentized Range (HSD) Test for mor

NOTE: This test controls the Type I experimentwise error rate, but it
        generally has a higher Type II error rate than REGWQ.


             Alpha                                     0.05
             Error Degrees of Freedom                    50
             Error Mean Square                     2.988619
             Critical Value of Studentized Range  4.68143
             Minimum Significant Difference          3.304

     Means with the same letter are not significantly different.

    Tukey Grouping          Mean      N    treatment

                 A        9.1475      6    4f
                 A
                 A        8.6597      6    6f
                 A
                 A        8.3298      6    2fc
                 A
                 A        8.0822      6    2f
                 A
                 A        8.0417      6    none
                 A
                 A        7.9257      6    4bc
                 A
                 A        7.4419      6    2bc
                 A
                 A        7.3151      6    6bc
                 A
                 A        6.7991      6    4fc
                 A
                 A        5.9708      6    6fc
```

MOE test

The GLM Procedure

Tukey's Studentized Range (HSD) Test for mor

NOTE: This test controls the Type I experimentwise error rate, but it generally has a higher Type II error rate than REGWQ.

Alpha	0.05
Error Degrees of Freedom	50
Error Mean Square	2.988619
Critical Value of Studentized Range	4.68143
Minimum Significant Difference	3.304

Means with the same letter are not significantly different.

Tukey Grouping	Mean	N	treatment
A	2.2786	6	4f
A			
A	2.2360	6	6f
A			
A	2.1952	6	none
A			
A	2.0882	6	4bc
A			
A	2.0358	6	2f
A			
A	2.0214	6	6bc
A			
A	1.9902	6	2bc
A			
A	1.9158	6	4bc
A			
A	1.7922	6	4fc
A			
A	1.5786	6	6fc

SWR test

```
                 The SAS System                          14
                                     11:49 Tuesday, March 22, 2011

                    The GLM Procedure

            Tukey's Studentized Range (HSD) Test for SWR

NOTE: This test controls the Type I experimentwise error rate, but it
        generally has a higher Type II error rate than REGWQ.


             Alpha                                     0.05
             Error Degrees of Freedom                   110
             Error Mean Square                     24739.44
             Critical Value of Studentized Range    4.56737
             Minimum Significant Difference          207.38


     Means with the same letter are not significantly different.


       Tukey Grouping          Mean       N    treatment

               A            1154.83      12    2fc
               A
          B    A            1042.50      12    2f
          B    A
          B    A            1029.58      12    4f
          B    A
          B    A    C        962.92      12    6f
          B         C
          B         C        944.00      12    4bc
          B         C
          B         C        941.33      12    4fc
          B         C
          B         C        935.58      12    none
          B         C
          B         C        914.33      12    2bc
          B         C
          B         C        895.58      12    6bc
                    C
                    C        767.58      12    6fc
```

IB test

Tukey's Studentized Range (HSD) Test for IB

NOTE: This test controls the Type I experimentwise error rate.

Alpha	0.05
Error Degrees of Freedom	363
Error Mean Square	0.029568
Critical Value of Studentized Range	4.50221

Comparisons significant at the 0.05 level are indicated by *.**

treatment Comparison	Difference Between Means	Simultaneous 95% Confidence Limits		
2fc - 2bc	0.09721	-0.04057	0.23500	
2fc - 4f	0.10804	-0.03051	0.24660	
2fc - 2f	0.11277	-0.02290	0.24845	
2fc - 4fc	0.12107	-0.01915	0.26129	
2fc - 4bc	0.18731	0.05164	0.32299	***
2fc - 6bc	0.20179	0.06474	0.33884	***
2fc - 6f	0.21870	0.08091	0.35648	***
2fc - none	0.22665	0.09097	0.36232	***
2fc - 6fc	0.37392	0.23455	0.51329	***
2bc - 2fc	-0.09721	-0.23500	0.04057	
2bc - 4f	0.01083	-0.11560	0.13726	
2bc - 2f	0.01556	-0.10771	0.13883	
2bc - 4fc	0.02386	-0.10439	0.15211	
2bc - 4bc	0.09010	-0.03317	0.21337	
2bc - 6bc	0.10458	-0.02020	0.22935	
2bc - 6f	0.12148	-0.00410	0.24707	
2bc - none	0.12944	0.00617	0.25270	***
2bc - 6fc	0.27671	0.14939	0.40403	***
4f - 2fc	-0.10804	-0.24660	0.03051	
4f - 2bc	-0.01083	-0.13726	0.11560	
4f - 2f	0.00473	-0.11940	0.12886	
4f - 4fc	0.01303	-0.11605	0.14211	
4f - 4bc	0.07927	-0.04486	0.20340	
4f - 6bc	0.09375	-0.03188	0.21938	
4f - 6f	0.11065	-0.01578	0.23708	
4f - none	0.11861	-0.00552	0.24274	
4f - 6fc	0.26588	0.13773	0.39403	***

The GLM Procedure

Tukey's Studentized Range (HSD) Test for IB

Comparisons significant at the 0.05 level are indicated by *.**

treatment Comparison	Difference Between Means	Simultaneous 95% Confidence Limits		
2f - 2fc	-0.11277	-0.24845	0.02290	
2f - 2bc	-0.01556	-0.13883	0.10771	
2f - 4f	-0.00473	-0.12886	0.11940	
2f - 4fc	0.00830	-0.11768	0.13428	
2f - 4bc	0.07454	-0.04636	0.19545	
2f - 6bc	0.08902	-0.03343	0.21146	
2f - 6f	0.10592	-0.01734	0.22919	
2f - none	0.11388	-0.00703	0.23478	
2f - 6fc	0.26115	0.13612	0.38618	***
4fc - 2fc	-0.12107	-0.26129	0.01915	
4fc - 2bc	-0.02386	-0.15211	0.10439	
4fc - 4f	-0.01303	-0.14211	0.11605	
4fc - 2f	-0.00830	-0.13428	0.11768	
4fc - 4bc	0.06624	-0.05974	0.19222	
4fc - 6bc	0.08072	-0.04674	0.20818	
4fc - 6f	0.09762	-0.03062	0.22587	
4fc - none	0.10558	-0.02040	0.23156	
4fc - 6fc	0.25285	0.12290	0.38280	***
4bc - 2fc	-0.18731	-0.32299	-0.05164	***
4bc - 2bc	-0.09010	-0.21337	0.03317	
4bc - 4f	-0.07927	-0.20340	0.04486	
4bc - 2f	-0.07454	-0.19545	0.04636	
4bc - 4fc	-0.06624	-0.19222	0.05974	
4bc - 6bc	0.01448	-0.10797	0.13692	
4bc - 6f	0.03138	-0.09189	0.15465	
4bc - none	0.03934	-0.08157	0.16024	
4bc - 6fc	0.18661	0.06157	0.31164	***
6bc - 2fc	-0.20179	-0.33884	-0.06474	***
6bc - 2bc	-0.10458	-0.22935	0.02020	
6bc - 4f	-0.09375	-0.21938	0.03188	
6bc - 2f	-0.08902	-0.21146	0.03343	
6bc - 4fc	-0.08072	-0.20818	0.04674	
6bc - 4bc	-0.01448	-0.13692	0.10797	
6bc - 6f	0.01691	-0.10787	0.14168	
6bc - none	0.02486	-0.09758	0.14730	
6bc - 6fc	0.17213	0.04561	0.29865	***

The GLM Procedure

Tukey's Studentized Range (HSD) Test for IB

Comparisons significant at the 0.05 level are indicated by ***.

treatment Comparison	Difference Between Means	Simultaneous 95% Confidence Limits		
6f - 2fc	-0.21870	-0.35648	-0.08091	***
6f - 2bc	-0.12148	-0.24707	0.00410	
6f - 4f	-0.11065	-0.23708	0.01578	
6f - 2f	-0.10592	-0.22919	0.01734	
6f - 4fc	-0.09762	-0.22587	0.03062	
6f - 4bc	-0.03138	-0.15465	0.09189	
6f - 6bc	-0.01691	-0.14168	0.10787	
6f - none	0.00795	-0.11531	0.13122	
6f - 6fc	0.15523	0.02791	0.28254	***
none - 2fc	-0.22665	-0.36232	-0.09097	***
none - 2bc	-0.12944	-0.25270	-0.00617	***
none - 4f	-0.11861	-0.24274	0.00552	
none - 2f	-0.11388	-0.23478	0.00703	
none - 4fc	-0.10558	-0.23156	0.02040	
none - 4bc	-0.03934	-0.16024	0.08157	
none - 6bc	-0.02486	-0.14730	0.09758	
none - 6f	-0.00795	-0.13122	0.11531	
none - 6fc	0.14727	0.02224	0.27230	***
6fc - 2fc	-0.37392	-0.51329	-0.23455	***
6fc - 2bc	-0.27671	-0.40403	-0.14939	***
6fc - 4f	-0.26588	-0.39403	-0.13773	***
6fc - 2f	-0.26115	-0.38618	-0.13612	***
6fc - 4fc	-0.25285	-0.38280	-0.12290	***
6fc - 4bc	-0.18661	-0.31164	-0.06157	***
6fc - 6bc	-0.17213	-0.29865	-0.04561	***
6fc - 6f	-0.15523	-0.28254	-0.02791	***
6fc - none	-0.14727	-0.27230	-0.02224	***

Thickness Swell Test

The GLM Procedure

Tukey's Studentized Range (HSD) Test for TS

NOTE: This test controls the Type I experimentwise error rate, but it generally has a higher Type II error rate than REGWQ.

Alpha	0.05
Error Degrees of Freedom	50
Error Mean Square	0.000135
Critical Value of Studentized Range	4.68143
Minimum Significant Difference	0.0222

Means with the same letter are not significantly different.

Tukey Grouping	Mean	N	treatment
A	0.072210	6	none
A			
A	0.061700	6	2bc
A			
A	0.061149	6	2f
A			
A	0.061016	6	2fc
A			
A	0.059963	6	4fc
A			
A	0.059676	6	4bc
A			
A	0.058760	6	6bc
A			
A	0.055812	6	6fc
A			
A	0.055669	6	4f
A			
A	0.054413	6	6f

Water Absorption test

The SAS System

The GLM Procedure

Tukey's Studentized Range (HSD) Test for WA

NOTE: This test controls the Type I experimentwise error rate, but it generally has a higher Type II error rate than REGWQ.

Alpha	0.05
Error Degrees of Freedom	50
Error Mean Square	0.000135
Critical Value of Studentized Range	4.68143
Minimum Significant Difference	0.0222

Means with the same letter are not significantly different.

Tukey Grouping	Mean	N	treatment
A	0.101014	6	6fc
A			
A	0.100432	6	none
A			
A	0.100159	6	2bc
A			
A	0.097921	6	4f
A			
A	0.095227	6	2fc
A			
A	0.093698	6	6bc
A			
A	0.093385	6	4bc
A			
A	0.087564	6	6f
A			
A	0.086018	6	2f
A			
A	0.084932	6	4fc